Molecular Design of Degradable Polyrotaxane Composed of α-Cyclodextrin Inclusion Complexes

HOJOON SHIN

Japan Advanced Institute of Science and Technology

Doctoral Dissertation

Molecular Design of Degradable Polyrotaxane Composed of α-Cyclodextrin Inclusion Complexes

HOJOON SHIN

Supervisor : Associate Professor Tatsuo Kaneko

School of Materials Science

Japan Advanced Institute of Science and Technology

March 2014

ABSTRACT

Polyrotaxanes, demonstrated as a molecular necklace composed of a polymeric chain and cyclic compounds, are interesting in terms of their structural features. A mechanism of biodegradation based on the dissociation of supramolecular structure triggered by cleavage of end groups in a cleavable polyrotaxane can give various novel designs of biodegradable polymers. By utilizing these merits of supramolecular structure, we designed and prepared polyrotaxane hydrogel based on water-soluble hydrolyzable polyrotaxane and polyamide rotaxane composed of photo-cleavable 4,4ô-diacetoamido-α-truxillic acid.

In chapter 2, a hydrolyzable polyrotaxane composed of an ester-containing poly(ethylene glycol) chain and α-cyclodextrins was prepared and showed gradual degradation into its water-soluble components in aqueous conditions, based on the dissociation of the polyrotaxane triggered by the hydrolysis of the ester groups.

In chapter 3, we designed and prepared various hydrolyzable polyrotaxane hydrogel composed of α-cyclodextrins, poly(ethylene glycol) with Mw 3K and 20K as back bone chain, and two types of crosslinker (liner and multi-arm PEG). One of the degradable polyrotaxanes was crosslinked between the internal rings with linear PEG chain and the other was crosslinked between the terminals with multi-arm PEG chain. Every hydrogels had good water content (>90%) and hydrophilic surface. The *internally*-crosslinked gels had higher compressive stress and initial modulus, while the *terminally*-crosslinked gels showed higher ultimate strain. These results imply that *terminally*-crosslinked gels were rigid and the *terminally*-crosslinked gels were flexible. In stress relaxation test, the *internally*-crosslinked gels showed unique viscoelastic behavior, in which was similar to that of topological gel. We investigated the gradual degradation of the hydrogels in terms of changes in mass and storage modulus of the gels. The *internally*-crosslinked gels degraded and disappeared in a relatively shorter period than the *terminally*-crosslinked gels. The *terminally*-crosslinked gels survived for weeks with gradual degradation that allowed us to apply the degrading gels to a preliminary cell adhesion test. In the cell adhesion test, the number, size, and morphology of NIH 3T3 cells was changed by degradation of hydrogels and change of surface chemical characteristics due to cleavage of carboxyl residue introduced to hydroxyl group in CD at the same time.

In chapter 4, we introduced a unique chemical structure, polyrotaxane, to give structural rigidity to polymer back bones using a necklace-like structure and cinnamic acid as a photo-reactive monomer to prepare a new polyamide. By utilizing this unique concept, we designed aliphatic-aromatic polyamides containing the rotaxane structure composed of 4,4ô-diacetoamido-α-truxillic acid, poly(ethylene glycol) bisamine (PEGBA) and methylated-α-cyclodextrin (Me-α-CD), and observed their thermo-mechanical performance and degradation behavior under UV-irradiation. The thermal degradation temperature of the polyamides was enhanced by inclusion complex formation with Me-α-CD, and the polyamide polyrotaxane was degraded by UV-irradiation via the photocleavage of the cyclobutane ring in 4,4ô-diacetoamido-α-truxillic acid.

Keywords : hydrogel, supramolecular structure, hydrolyzable polyrotaxane, polyamide, photocleavage

TABLE OF CONTENTS

Chapter 1

General Introduction

1 General Introduction

1-1. Supramolecular chemistry

1-1-1. Supramolecular chemistry[1-3]

Supramolecular chemistry is concerned with the study of the basic feature of molecular nitration and with their implementation in designed non-natural systems. In this chapter, introductory descriptions are presented on the basis of reviews and books.

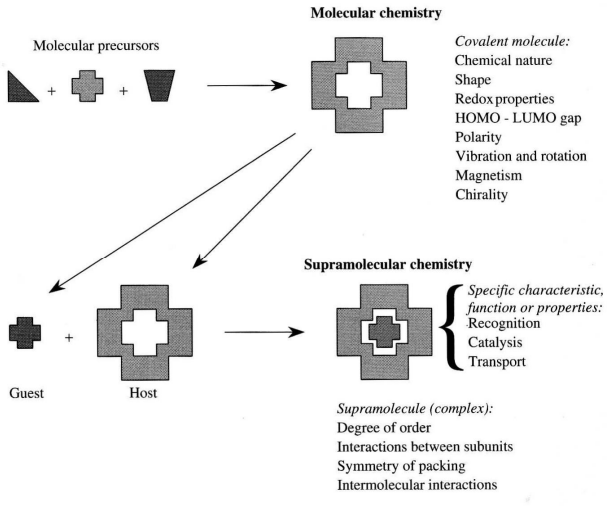

Figure 1. Comparison between the scope of molecular and supramolecular chemistry according to Lehn.

For more than150 years, molecular chemistry has developed a vast array of highly sophisticated and powerful methods for the construction of more complex molecular structure by the making or breaking of covalent bonds with atoms in a controlled and precise fashion. The time has come to do the same for non-covalent intermolecular forces. Just as there is a field of molecular chemistry based on the covalent bond, and there is a field of supramolecular chemistry, the chemistry of molecular assembles and of the intermolecular bond. It is ñchemistry beyond the molecule,ò whose objects are supramolecular entities, supramolecules processing feature as well defined as those of molecules themselves. This kind of definitions is highlighted in Figure 1, which illustrated the relationship between molecular and supramolecular chemistry in terms of both structures and function.

Such labels, while helpful, are by their nature noncomprehensive and there are many exceptions if these definitions are taken too literally. The problem may be linked to the definition of organometallic chemistry as ôthe chemistry of compounds with metal-to-carbon bondsõ. This immediately rules out Wilkinsonõs compound, $RhCl(PPh_3)_3$, for example, which is one of the most important industrial catalysts for organometallic transformations known in the filed. Indeed, it is often the objectives and thought processes of the chemist undertaking the work, as much as the work itself, which determine its field. The rapid expansion in supramolecular chemistry over the past 15 years has resulted in an enormous diversity of

chemical systems, both designed and accidentally stumbled upon, which may lay some claim, either in concept, origin or nature, to being supramolecular. In particular, workers in the filed of supramolecular photochemistry have chosen to adopt a rather different definition of a supramolecular compound as a group of molecular components that contribute properties that each component processes individually to the whole assembly (covalent or noncovalent). Thus an entirely covalent molecule comprising, for example, a chromophore (light-absorbing moiety), spacer and redox centre might be thought of as supramolecular because the chromophore and redox centre are able to absorb light, or change oxidation state, whether they form part of the supramolecule or not. Similarly, much recent work has focused on the development of self-assemble using a variety of interactions, some of which are clearly noncovalent (e.g. hydrogen bonds) and some of which process a significant covalent compound (e.g. metal-ligand interactions).

Supramolecular chemistry is an interdisciplinary field of science that covers chemical, physical, and biological features by means of intermolecular (non-covalent) binding interactions. Its roots extend into synthetic procedures for molecular construction, into biological process that all start with substrate binding and recognition, and into the mechanical properties of solids. A major feature is the range of perspectives offered by the cross fertilization of supramolecular chemical research owing to its location at the intersection

of chemistry, biology, and physics. Taking the large research field of supramolecular chemistry into account, it can be called a supramolecular science. Such wide horizons are a challenge and a stimulus to the creative imagination of the chemist.

1-1-2. Host-guest chemistry

In supramolecular chemistry, host-guest chemistry describes complexes that are composed of two or more molecules or ions held together in unique structural relationships by hydrogen bonding or by ion pairing or by van der Waals force other than those of full covalent bonds. The host component is defined as an organic molecule or ion whose binding sites converge in the complex. In 1967, Pederson reported the synthesis of crown ether (Figure 2).[4] The crown ether is a cyclic oligoether and it can selectively form an inclusion complex with a cationic ion in relation to its ring size. The cyclic molecule is called the host molecules. The guest component is defined as any molecule or ion whose binding sites diverge in the complex.

Many artificial cyclic molecules have been researched and there artificial host molecules were designed to interact with the guest molecule by the electrostatic interaction, ´-´ interaction and charge-transfer interaction.[5]

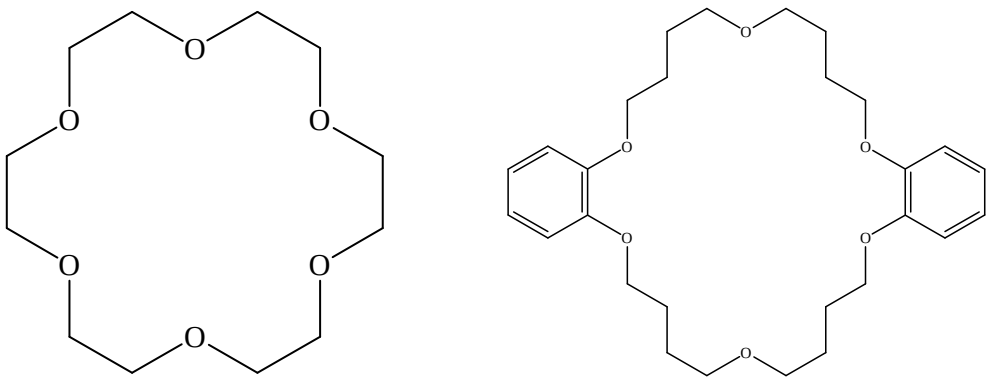

(a) (b)

Figure 2. Schematic diagram of crown ether derivatives.[4]

1-2. Polyrotaxanes

1-2-1. Cyclodextrin (CD)[6]

Cyclodextrins, as they are known today, were called "cellulosine" when first described by A. Villiers in 1891. Soon after, F. Schardinger identified the three naturally occurring cyclodextrins -Ŭ, -ɓ, and -ɔ. These compounds were therefore referred to as "Schardinger sugars". For 25 years, between 1911 and 1935, Pringsheim in Germany was the leading researcher in this area, demonstrating that cyclodextrins formed stable aqueous complexes with many other chemicals. By the mid 1970's, each of the natural cyclodextrins had been structurally and chemically characterized and many more complexes had been studied. Since the 1970s, extensive work has been conducted by Szejtli and others exploring encapsulation by cyclodextrins and their derivatives for industrial and pharmacologic applications.

Typical cyclodextrins are constituted by 6-8 glucopyranoside units (Figure 3), can be topologically represented as toroids with the larger and the smaller openings of the toroid exposing to the solvent secondary and primary hydroxyl groups respectively. Because of this arrangement, the interior of the toroids is not hydrophobic, but considerably less hydrophilic than the aqueous environment and thus able to host other hydrophobic molecules. In contrast,

the exterior is sufficiently hydrophilic to impart cyclodextrins (or their complexes) water solubility. The characteristics of the CDs are summarized in Table 1.

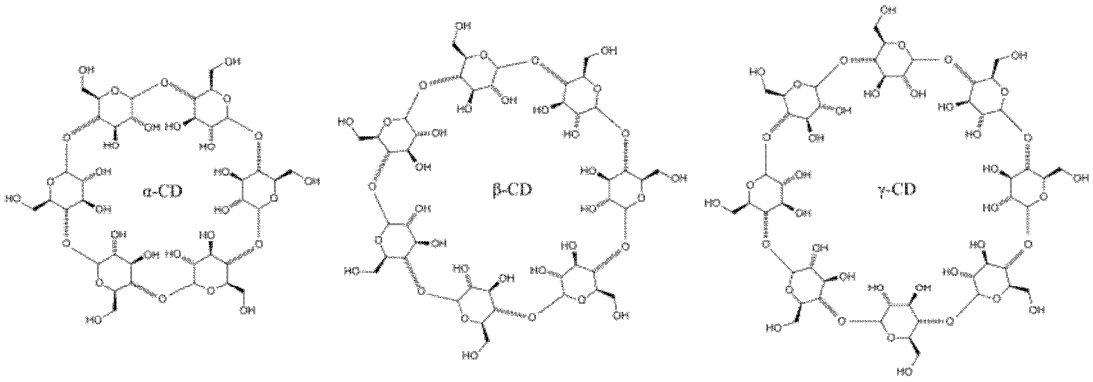

Figure 3. Schematic diagram of Ŭ-, ɓ-, ɔ-CDs

The formation of the inclusion compounds greatly modifies the physical and chemical properties of the guest molecule, mostly in terms of water solubility. This is the reason why cyclodextrins have attracted much interest in many fields, especially pharmaceutical applications: because inclusion compounds of cyclodextrins with hydrophobic molecules are able to penetrate body tissues, these can be used to release biologically active compounds under specific conditions. In most cases the mechanism of controlled degradation of such complexes is based on pH change of water solutions, leading to the cleavage of hydrogen or ionic bonds between the host and the guest molecules. Alternative means for the disruption of the complexes take advantage of heating or action of enzymes able to cleave Ŭ-1,4 linkages between glucose monomers.

Table 1. Characteristics of Ŭ-, ɓ-, ɔ-CDs

	Ŭ	ɓ	ɔ
No. of glucose units	6	7	8
Molecular weight	972	1135	1297
Solubility in water. g/L	145	18.5	232
Cavity diameter, Å	4.7-5.3	6.0-6.5	7.5-8.3
Height of torus, Å	7.9±0.1	7.9±0.1	7.9±0.1
Diameter of outer periphery, Å	14.6±0.4	15.4±0.4	17.5±0.4
Approx volume of cavity, $Å^3$	174	262	427
Crystal water, wt%	10.2	13.2-14.5	8.1-17.7
Diffusion constant at 40℃	3.44	3.22	3.00

1-2-2. Backgrounds and basic characteristics

Supramolecular assemblies of cyclic molecules and linear molecules were demonstrated in 1967.[7] The name is the rotaxane comes from the Latin words for wheel and axle. Schill and his co-workers developed a synthetic procedure strategy.[7-9] They reported that cyclic space of 24 skeletal C, O or N atoms were requested in order to provide a cavity size enough to be threaded onto a polymer chain [8)] and the relationship between ring size, linear molecular length, blocking size of terminal molecules, and the threading efficiency.[9] The application of host-guest chemistry to the synthesis of rotaxane and catenanes was studied by Sauvage et al. and Stoddart et al..[10,11]

Polyrotaxanes are polymers with a novel molecular architecture where cyclic molecules are threaded onto the polymer chain. The bulky end-groups of polyrotaxane capped linear polymer and prevent the escape of cyclic molecules from the assembly by dethreading. There are in principle many subclasses of polyrotaxanes which differ in the nature and location of the covalent and physical linkages. Since polyrotaxanes are a novel class of polymer molecular topology it is anticipated that their properties are distinct from other polymeric architectures. The distinguishing feature of polyrotaxanes is the potential for lateral and translational motion of the cyclic molecules relative to the linear chain that penetrates it.

In 1976, Ogata and co-workers studied the formation of poly(amide / rotaxanes) using the reaction of ß-cyclodextrin complexation of Ù, ý-diaminohydrocabons with diacid chlorides.[12] This paper was the first one related to synthesis and characterization of polyrotaxane. They called this polymer to ñtunnel polymerò. Tunnel polymer showed specific viscosity. The polyrotaxane were soluble in dipolar aprotic solvent while the parent polymers were not. Further, the polyrotaxane did not show melting points, in contrast to the parent backbone polymer. These characteristics were not taken into account in the case of low molecular weight rotaxanes.

Wenz and co-workers reported inclusion complexation consisting Ù-CD and poly(iminooligomethylene)s.[13-15] Inclusion complex carried out by Wenz et al. was water soluble in acidic condition. Hydrophobic interaction between cyclodextrin and oligomethylene spacer was considered to play an important role in inclusion complex.

Harada and his co-workers have reported the first different type of pseudo- and polyrotaxane based on complex formation between CDs and PEG[16-23] and then they have reported preparation of pseudo- and polyrotaxane with CDs and the various polymers, such as poly(isobutylene),[20] poly(ε-caporolactone) (PCL),[21] poly(dimethyl siloxane).[22] In these researches, they reported that the size of CD cavity and the cross-section area of the polymer chain were related to the interaction between CD cavity and the polymer chain (Figure 4).

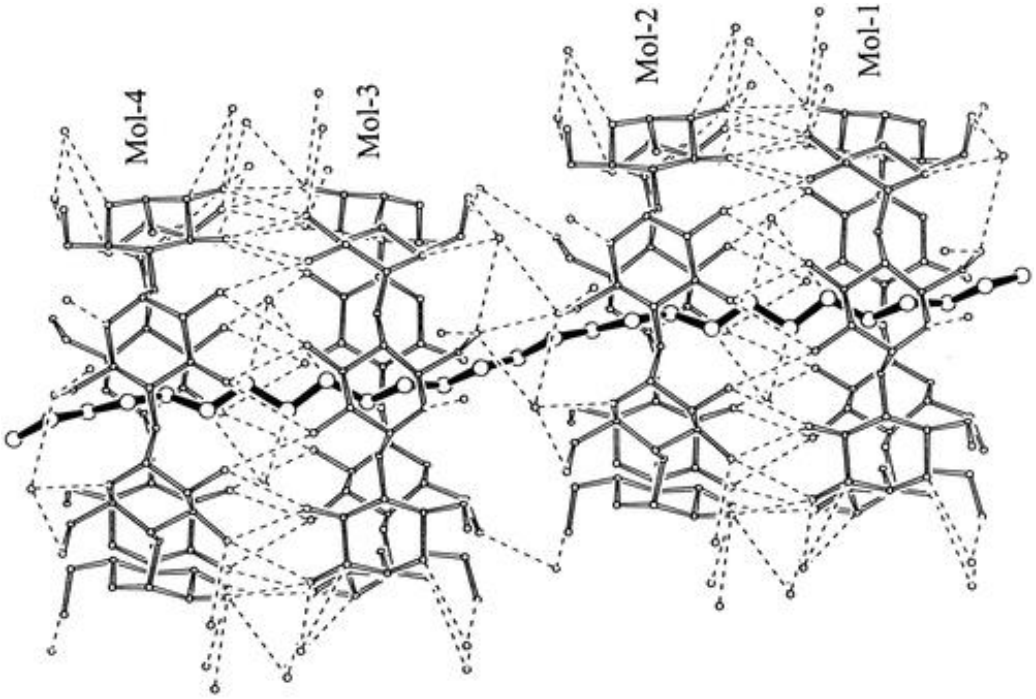

Figure 4. Crystal structure of inclusion complexes of ϐ-CDs with poly(trimethylene oxide). Intramolecular hydrogen bonds are shown as dotted lines. Solvent molecules which form direct hydrogen bonds with ϐ-CDs are as open circles with hydrogen bonds.

They confirmed that 6-cynnamoyl ϐ-CD forms a cyclic daisy-chain pseudopolyrotaxane and prepared a cyclic tri[2]-rotaxane (daisy-chain necklace) by attaching bulky stopper.[24] They reported the formation of daisy-chain pseudopolyrotaxane from the bi-functional host and guest molecules (Figure 5).[25]

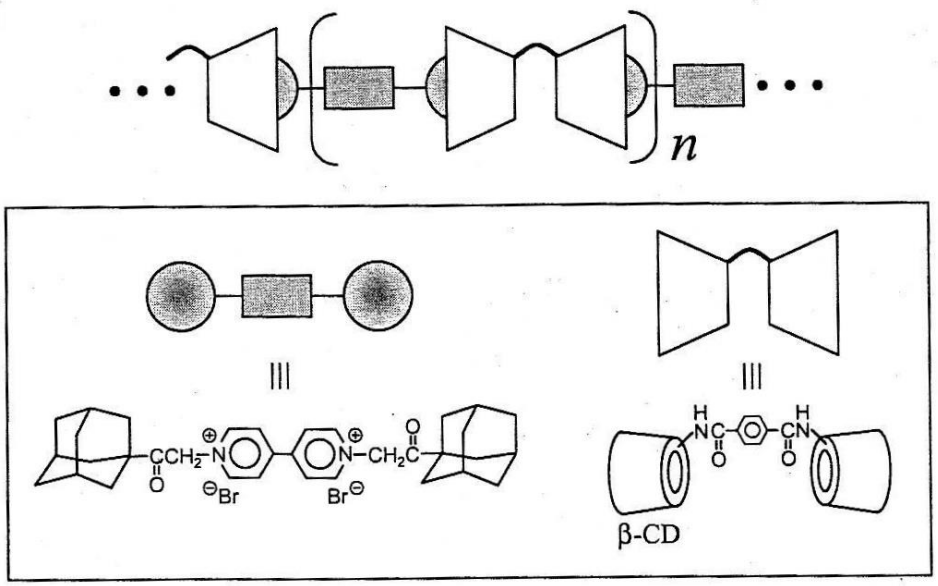

Figure 5. Supramolecular polymer consisting for bi-functional host and guest molecules.[25]

Some researchers have reported that inclusion complexation between ABA triblock copolymer and Ŭ-, ɓ-, and ɔ-CDs, respectively. Tonelli and coworker prepared Ŭ- and ɔ-CD complexes using PEG-PCL-PEG ABA triblock copolymer in order to research the behavior of isolated and segregated polymer chain. They showed that sided-by-side chains could reside in the ɔ-CD channel as only a single chain can be incorporated inside the Ŭ-CD cavity.[26]

Yui and his coworkers prepared stimuli-responsive polyrotaxane composed of Ŭ-, and ɓ-CDs and ABA triblock copolymers.[27-29] Temperature-sensitive polyrotaxane[27,28] was designed by complexation between ɓ-CDs and PEG-PPG-PEG triblock. It showed that majority of ɓ-CDs on PEG-PPG- PEG triblock copolymer moved toward the PPG segment with increasing

temperature although some β-CDs might reside on the PEG segment (Figure 6). pH-sensitive polyrotaxane[29] was prepared by utilizing α-CDs and PEI-PEG-PEI triblock copolymer. As shown in Figure 7, α-CDs in the water-soluble polyrotaxane showed pH-dependent movement along PEI and PEG block.

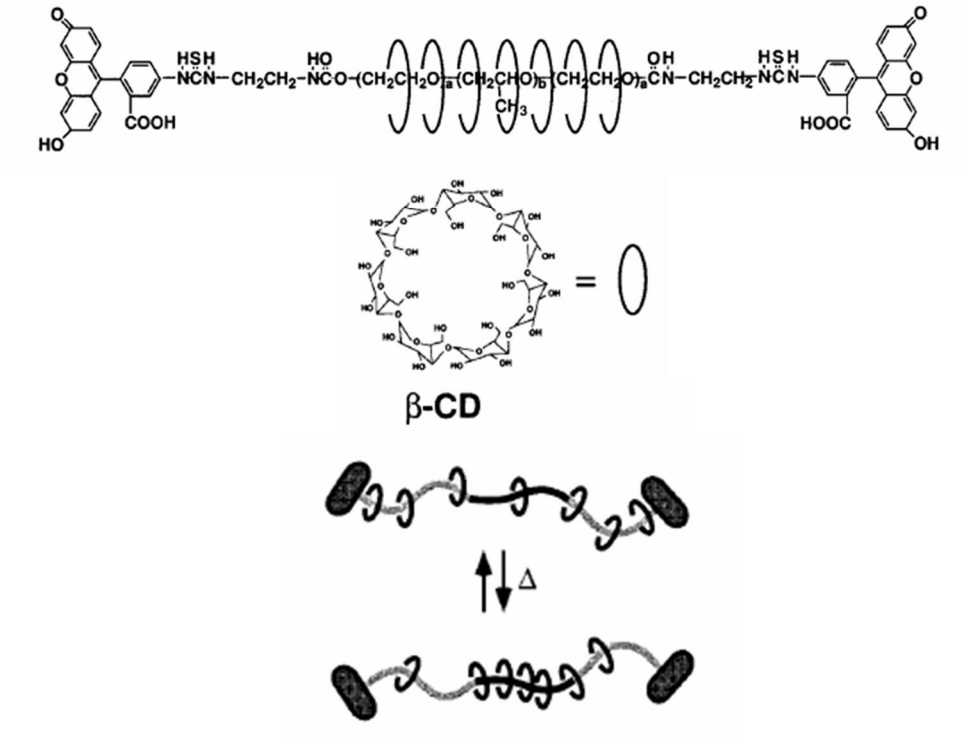

Figure 6. Schematic diagram of stimuli-responsive polyrotaxane composed of β- CDs and PEG-PPG-PEG triblock copolymer.[27]

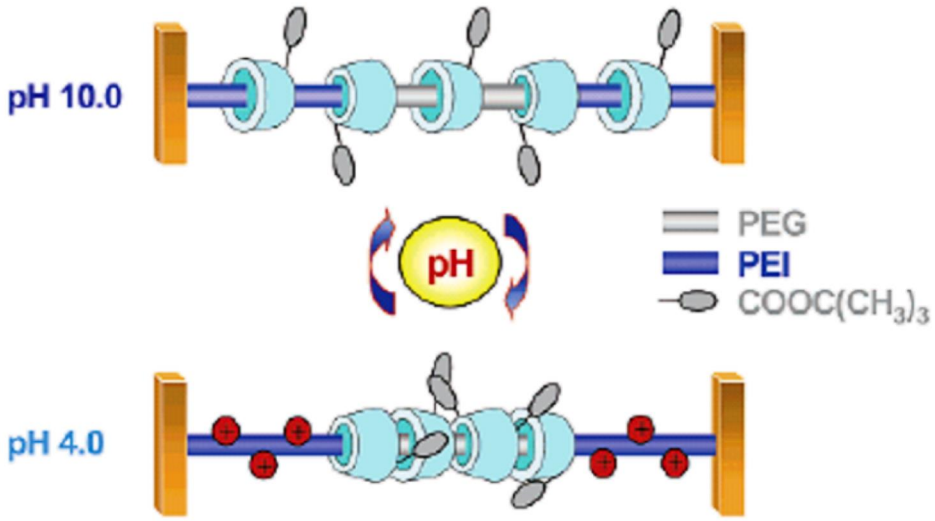

Figure 7. Schematic illustration for the mobility of macrocycles in the block-selective polyrotaxane via pH variation.[29]

1-2-3. Water-soluble polyrotaxane

The modification of CDs aims at converting them into amorphous, noncrystallizable derivatives, to provide high CD concentration in aqueous solutions that remain physically and microbiologically stable for reasonable period of time, ether as free or complex, with the simultaneous reduction of toxicity.[30] Hundreds of publications are treading the potential use of these derivatives in various drug formulations. The water-soluble modified cyclodextrins that are available in industrial quantities and are expected to have commercial pharmaceutical values are as follows:

(1) Methylated derivatives of ß-CD[31]

(2) 2-hydroxypropylated ß- and ɔ-CD[32]

(3) Branched CDs (glucosyl- and maltosyl-ß-CDs)

(4) Acetylated ß- and ɔ-CD

(5) Sulfated CDs[33]

Utilizing previous methods, some researchers have prepared water-soluble polyrotaxane by modifying CDs.

Yui and coworkers prepared some types of water-soluble polyrotaxane. They increased the solubility of polyrotaxane in aqueous solution by elimination the hydrogen bonding between the Ŭ-CDs by introducing *tert*-butoxy groups (Figure 8).[29] A carboxyethylester-polyrotaxane, introducing carboxyethylester (CEE) to OH-group of CDs, was prepared as a novel calcium chelating polymer in the field of oral drug delivery (Figure 9).[34,35]

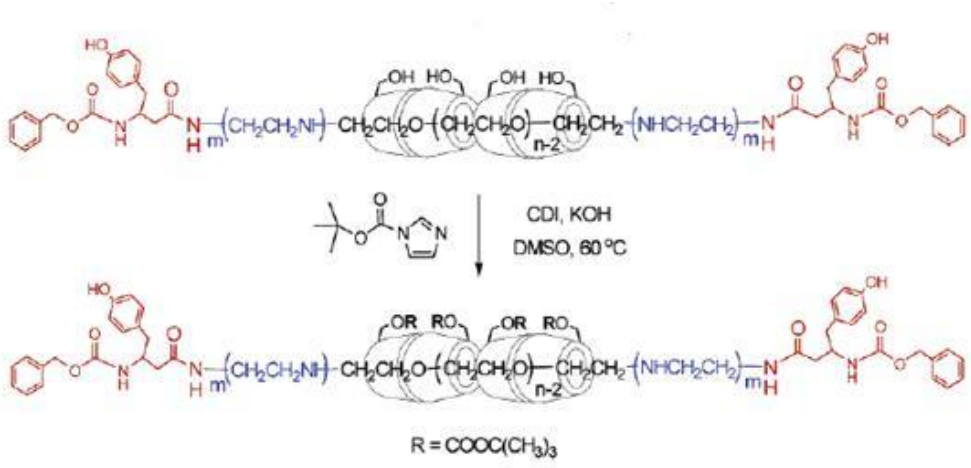

Figure 8. Butoxy-PRx-Tyr composed of PEI-PEG-PEI copolymer and Ŭ-CDs.[29]

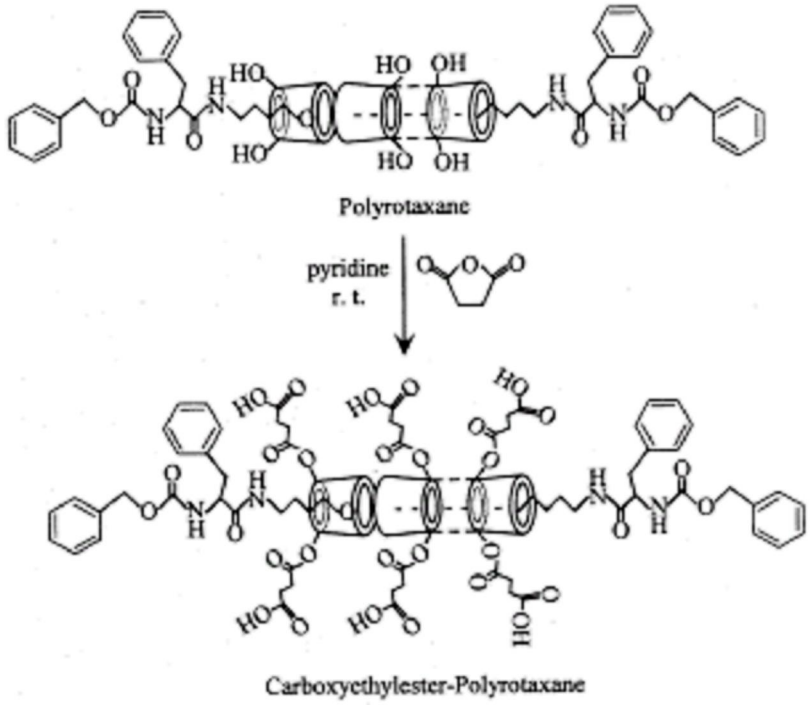

Figure 9. Carboxyethylester-polyrotxane.[34]

1-2-4. Biodegradable polyrotaxane

Since the later half of 1990s, Yui et al. have demonstrated the feasibility of the biodegradable polyrotaxanes, in which a number of Ŭ-CDs are threaded onto a linear chain capped with bulky end-groups via biodegradable linkages.[36-40] They reported the enzymatic degradable polyrotaxane as gene delivery system and hydrolyzable polyrotaxane as polymer scaffold in tissue engineering by using bio-cleavable groups (Figure 10).

Biodegradable polyrotaxane has some attractive characteristics comparing to other

biodegradable polymers, such as PGA, PLAG, PLLA and PCL. Biodegradable polyrotaxane was composed of Ŭ-CDs, backbone polymer (such as PEG), and end-capping materials via bio-cleavable groups such as SS and ester linkage. By cleavage of SS or ester linkage, supramolecular structure is dissociated and then polyrotaxane degraded perfectly. The other characteristics involve; (Ⅰ) high crystallinity due to intermolecular hydrogel bonds between hydroxyl groups of CDs; and (Ⅱ) the position of cleavable groups. In the case of PLA, the high crystallinity is based on well-arranged packing of the repeating units of ester groups. This indicates that the crystallinity region involves almost all ester groups, which reduce water intrusion. Moreover, cleavage of many ester-groups generates acidic byproduct. On the other hands, the ester or SS groups of polyrotaxane are independent of the high crystalline region. It is expected that the supramolecular dissociation may be achieved via terminal group hydrolysis due to water intrusion in polyrotaxane and stable on pH condition due to a little acidic byproduct.

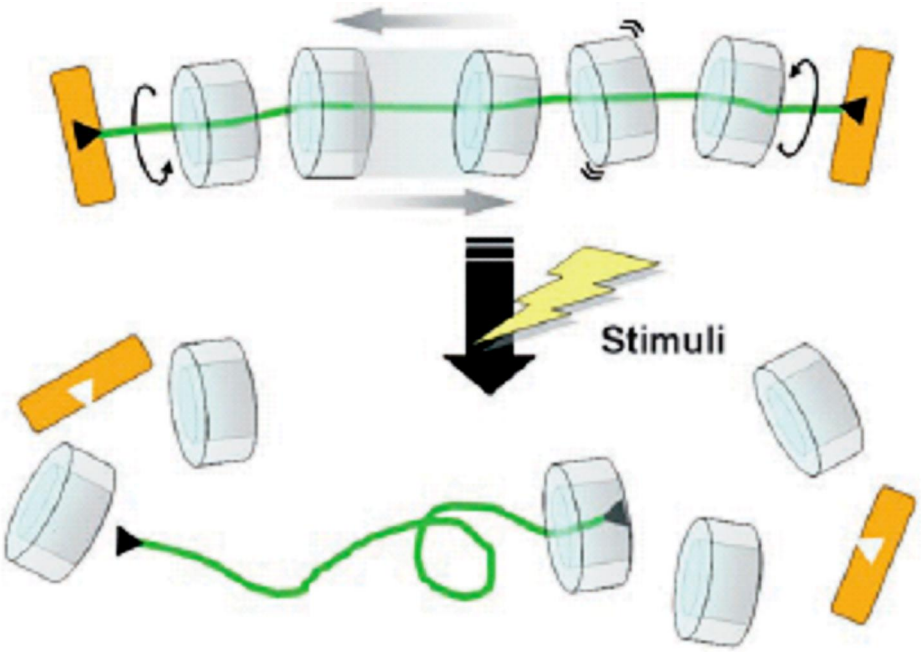

Figure 10. Characteristic image of cleavable polyrotaxane. The supramolecular structure can be dissociated by the terminal cleavage of capping groups by means of external stimuli.[40]

1-2-5. Multivalent interaction

The valency of a particle a small molecules, oligosaccharide, protein, nucleic acid, lipid or aggregate of these molecules; a membrane or organelle; a virus, bacterium, or cell is the number of separate connections of the same kind that it can form with other particles through ligand -receptor interactions. The idea that many biological systems interact through multiple simultaneous molecular contacts is familiar; it has, however, become of interactions involving multiple protein and ligands has begun to be unraveled. The possibility that multiple

simultaneous interactions have unique collective properties that are qualitatively different from properties displayed by their constituents, which interact monovalently, suggests new strategies for the design of drugs and research reagents for biochemistry and biology. Enhancing or blocking collective or multivalent interactions may benefit from strategies fundamentally different from those used in monovalent molecular interactions.[41]

Ooya and Yui et al. have reported that ligand-introduced polyrotaxane enhance multivalent interaction with complement binding protein due to both many lingnds and high mobility of ligand-introduced Ŭ-CDs (Figure 11).[35,42] They investigated how Ŭ-CDs and ligand mobility in ligand-polyrotaxane conjugates affect the multivalent interaction with a binding protein. Maltose and Concanavalin A (Con A) were selected as a ligand and a binding protein, respectively, because Con A recognizes maltose. When the threading percentage of Ŭ-CDs against the threading percentage was 38%, the highest mobility of maltosyl groups is observed. And the maltose-polyrotaxane conjugate with a highly mobile nature maintains water cluster structure. From these results, the combination of multiple copies of ligands and their supramolecular mobility along the mechanically locked structure should contribute to significant enhancement of the multivalent interaction due to a reduction of the special mismatches of binding

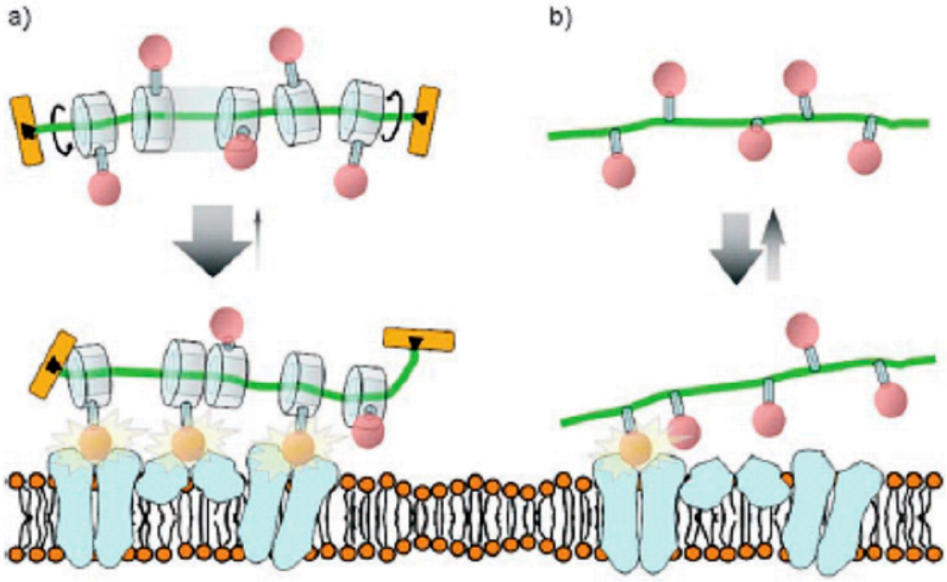

Figure 11. The effect of ñmobileò motion of the cyclic compounds in polyrotaxanes on binding receptor proteins in a multivalent manner: Image of binging/dissociating equilibrium a) between a ligandï polyrotaxane conjugate and receptor sites and b) between a ligandï immobilized-polymer and receptor sites.[40]

1-2-6. Hydrogel based on polyrotaxane.

Some researchers have reported polyrotaxane gel based on supramolecular network.[43,44] Supramolecular network is a network crosslinked by supramolecular structure.

Yui et al. prepared a polyrotaxane hydrogel crosslinked by PEG between CDs in the polyrotaxane (Figure 12 (a)).[43] This polyrotaxane hydrogel was consisted of hydrolyzable

polyrotaxane with hydrolyzable bulky end groups. Polyrotaxane dissociated in a few days by the hydrolysis of end groups. However, it takes several months to degrade the polyrotaxane hydrogel. They reported that degradation time could be controlled the molecular weigh of the crosslinker.

Ito et al. prepared polyrotaxane gel by crosslinking the CDs in polyrotaxane (Figure 12 (b)).[44] This hydrogel was called ñtopological gelò. This hydrogel was composed of large molecular weight of back bone polymer in polyrotaxane. And the number of CDs in the polyrotaxane is a little. Thus the cyclic compound can move along the polymer chain. In this gel, polymer chains are neither covalently cross-linked like chemical gel, nor do they interact like physical gel.

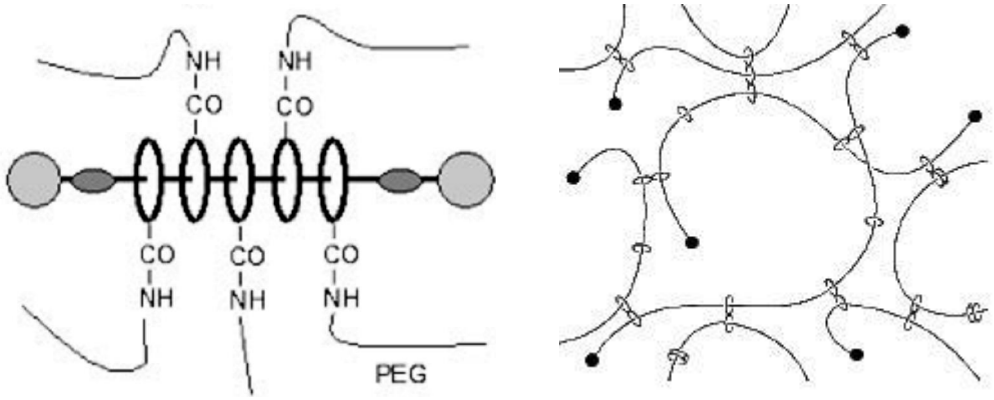

(a) (b)

Figure 12. Schematic diagram of the various polyrotaxane gels (a)[43] and (b)[44]

1-3. Aim and outline of this dissertation

The thesis deals with design, synthesis and characterization of various degradable polyrotaxanes; such as hydrolyzable hydrogel based on hydrolyzable polyrotaxane and polyamide rotaxane composed of photo-cleavable monomer. The objectives of this thesis are as follows;

I. To design and prepare hydrolyzable polyrotaxane containing ester-linkage.

II. To design and prepare two types of water-soluble hydrolyzable hydrogel containing different crosslinking system. One is crosslinked by linear PEG between OH-groups of CDs and the other is crosslinked by multi-arm PEG between terminal groups in polyrotaxane.

III. To observe the characteristics of hydrolyzable polyrotaxane hydrogels, such as mechanical properties, water content, degradation, and cell adhesion properties.

IV. To observe the thermal-mechanical performance and UV-degradation behavior of photo-reactive polyrotaxane composed of aliphatic-aromatic polyamides as back bone chain.

This dissertation consists of five chapters. Chapter 2 describes the preparation of

hydrolyzable polyrotaxanes containing ester-linkage in terminal group. Chapter 3 deals with the preparation of water-soluble polyrotaxane containing ester-linkage in end-capping molecules and two types of hydrogels with different crosslinking systems, respectively. These developed structures of polyrotaxane would affect the gel formation and properties of hydrogels. Chapter 4 shows synthesis of polyrotaxane composed of aliphatic-aromatic polyamides and their thermo-mechanical performances and UV degradation behavior.

.

Reference

1. Steed, J. W.; Atwood, J. L. Supramolecular Chemistry, John Wiley & Sons, Ltd: Chichester, 2000, 2.

2. Lehn, J. -M. *Science,* 1993, **260**, 1762.

3. Lehn, J. -M. Supramolecular chemistry, VCH, Weinhein, 1995.

4. Pederson, C. J. *J. Am. Chem. Soc*., 1967, **89**, 7017.

5. Odashima, K.; Koga, K. *Comprehensive supramolecular Chemistry*, Elsevier Science, New York, 1996, Vol.2, p143.

6. Szejtli, *J. Chem. Rev*. 1998, **98**, 1743.

7. Lipatov, Y. S.; Lipatova, T. E.; Kosyanchuk, L. F. *Adv. Polym. Sci.*, 1989, **88**, 49.

8. Harrison, I. T.; Harrison, S.; *J. Am. Chem. Soc*., 1967, **89**, 5723.

9. Agam, G.; Gravier, D.; Zikha, A. *J. Am. Chem. Soc*., 1976, **98**, 5206.

10. Dietrich-Buchecker, C. O.; Sauvage J. ï P. *Chem. Rev*., 1987, **87**, 795.

11. Anelli, P. L.; Ashoton, P. R.; Ballardini, R.; Balzani, V.; Delgado, M.; Gandolfi, M. T.; Goodnow, T. M.; Kaifer, A. E.; Philp, D.; Pietraszkiewicz, M.; Prodi, L.; Reddington, M. V.; Slawin, A. M. Z.; Spencer, N.; Stoddart, J. F.; Vicent, C.; Williams, D. J. *J. Am. Chem. Soc*. 1992. **114**, 193.

12. Ogata, N.; Sanui, K.; Wada, J. *J. Polym. Sci., Polym. Lett. Ed*. 1976, 14, 459.

13. Wens, G.; Keller, B, *Angew. Chem., Int. Ed. Engl*., 1992, **31**, 197.

14. Wens, G.; Keller, B, *Macromol. Symp*., 1994, **87**, 11.

15. Meier, L. P.; Heule, M.; Caseri, W. R.; Shelden, R. A.; Suter, U. W. *Macromolecules,* 1996, **29**, 718.

16. Harada, A.; Kamachi, M. *Macromolecules*, 1990, **23**, 2821.

17. Harada, A.; Li, J.; Kamachi, M. *Nature*, 1992, **356**, 325.

18. Harada, A.; Li, J.; Kamachi, M. *Macromolecules*, 1993, **26**, 5698.

19. Harada, A.; Okada, M.; Li, J.; Kamachi, M. *Macromolecules*, 1995, **28**, 8406.

20. Harada, A.; Suzuki, S.; Okada, M.; Kamachi, M. *Macromolecules*, 1996, **29**, 5611.

21. Kawaguchi, Y.; Nishiyama, T.; Okada, M.; Kamachi, M.; Harada, A. *Macromolecules,* 2000, **33**, 4472.

22. Okumura, H.; Okada, M.; Kawauchi, Y.; Harada, A. *Macromolecules*, 2000, **33**, 4297.

23. Kamitori, S.; Matsukaka, O.; Kondo, S.; Muraoka, S.; Okuyama, K.; Noguchi, K.; Okada, M.; Harada, A. *Macromolecules*, 2000, **33**, 1500.

24. Hoshino, T.; Miyauchi, M.; Kawaguchi, Y,; Yamaguchi, H.; Harada, A. *J. Am. Chem. Soc.* 2000, **122**, 9876.

25. Ogami, K.; Hoshino, T.; Miyauchi, M.; Kawaguchi, Y,; Harada, A. *Polym. Prep. Jpn,* 2001, **50**, 1471.

26. Lu, J.; Shin, I. D.; Nojima, S.; Tonelli, A. E. *Polymer*, 2000, **41**, 5871

27. Fujita, H.; Ooya, T.; Yui, N. *Macromolecules*, 1999, **32**, 2534.

28. Fujita, H.; Ooya, T.; Yui, N. *Macromol. Chem. Phys*. 1999, **200**, 706.

29. Choi, H. S.; Lee, S. C.; Yamamoto, K.; Yui, N. *Macromolecules*, 2005, **38**, 9878.

30. Szente, L.; Szejtli, J. *Adv. Drug Deliv. Rev*., 1999, **36**, 17.

31. Takeo, K.; Kuge, T. *Starch / Starke*, 1976, **287**, 226.

32. Pitha, J,; Szabo, L.; Fales, H. *Carbohydr. Res*., 1987, **168**, 191.

33. Folkman, J.; Weisz, P.; Joullie, M. *Scinece*, 1989, **243**, 1490.

34. Ooya, T.; Eguchi, M.; Ozaki, A.; Yui, N. *Int. J. Pharmaceutics*, 2002, **242**, 47.

35. Ooya, T.; Eguchi, M.; Yui, N. *J. Am. Chem. Soc*., 2003, **125**, 13016.

36. Watanabe, J.; Ooya, T.; Yui, N. *J. Biomater. Sci. Polym. Ed*., 1999, **10**, 1275.

37. Watanabe, J.; Ooya, T.; Yui, N. J. *Chem. Lett.*, 1998, 1031

38. Ooya, T.; Yui, N. *J. Control. Release*, 1999, **58**, 251.

39. Yamashita, A.; Yui, N.; Ooya, T.; Kano, A.; Maruyama, A.; Akita, A.; Kogure, K.; Harashima, H. *Nature Protocols*, 2006, **1**, 2861.

40. Yui, N.; Ooya, T. *Chem. Eur. J.* 2006, **12**, 6730.

41. Mammen, M.; Choi, S. K.; Whitesides, G. N. *Angew. Chem. Int. Ed*. 1998. **37**, 2755.

42. Ooya, T.; Utsunomiya, H.; Eguchi, M.; Yui, N. *Bioconjug. Chem*. 2005, **16**, 62.

43. Ichi, T.; Watanabe, J.; Ooya, T.; Yui, N. *Biomacromolecules,* 2001**, 2**, 204.

44. Okumura, Y.; Ito, K. *Adv. Mater.,* 2001, **13**, 485.

Chapter 2

Preparation of Hydrolyzable polyrotaxane Containing Ester Linkages

Published in Chemistry Letters, 37, 2008, pp988-989

2 Preparation of Hydrolyzable Polyrotaxane Containing Ester Linkages

2-1. Introduction

In the last several decades, biodegradable polymers have been studied as implantable materials for cell growth and tissue engineering.[1] These materials must satisfy various requirements such as sufficient mechanical strength, non-toxicity, and bioinertness before and after degradation for clinical use in a living body. In order to design and construct biodegradable materials,[2] some attention should be paid to the fact that the material has to have the potential to degrade perfectly in appropriate conditions, and that undesirable decomposition has to be avoided during the preparation and purification. It is of course necessary to purify the materials aimed at a clinical use in a living body. In this context, our approach for the design of biodegradable materials based on the structural features of polyrotaxanes, and especially on their dissociation, is promising. Stimuli-responsive biodegradable polyrotaxanes as shown in Scheme 1 would provide quite a new model as a mode of biodegradation.[3] Degradation based on the dissociation of polyrotaxanes, that is, the transformation of the supramolecular materials with a high molecular weight into water-

soluble and bioinert components would be favorable in terms of effective degradation, low toxicity, and biocompatibility in a living body.

A polyrotaxane composed of a PEG chain containing ester groups at both ends and α-cyclodextrins (α-CDs) was designed and prepared as a candidate for biodegradable polymers, in which the ester group(s) would be expected to hydrolyze to trigger the following dissociation in response to pH. Thus, a successful preparation of the ester-containing polyrotaxane in spite of the potential of degradation[4] and its hydrolysis behavior were demonstrated.

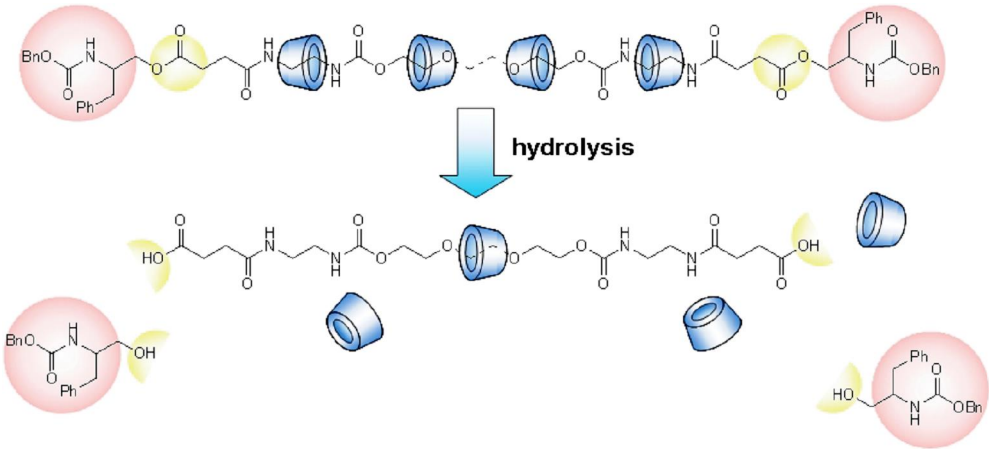

Scheme 1. Biodegradation based on dissociation of polyrotaxane triggered by stimuli-responsive cleavage of biodegradable linkages.

2-2. Experimental section

2-2-1. Materials

Polyethylene Glycol 4,000 (averaged molecular weight; approximate 3,000), Tetraborate pH standard solution adjusted to pH 9.18 (028-03205), and Phosphate pH standard solution adjusted to pH 6.86 (025-03195) were purchased from Wako Pure Chemical Industries, Ltd.

2-2-2. Preparation of polyrotaxane 1 and 4

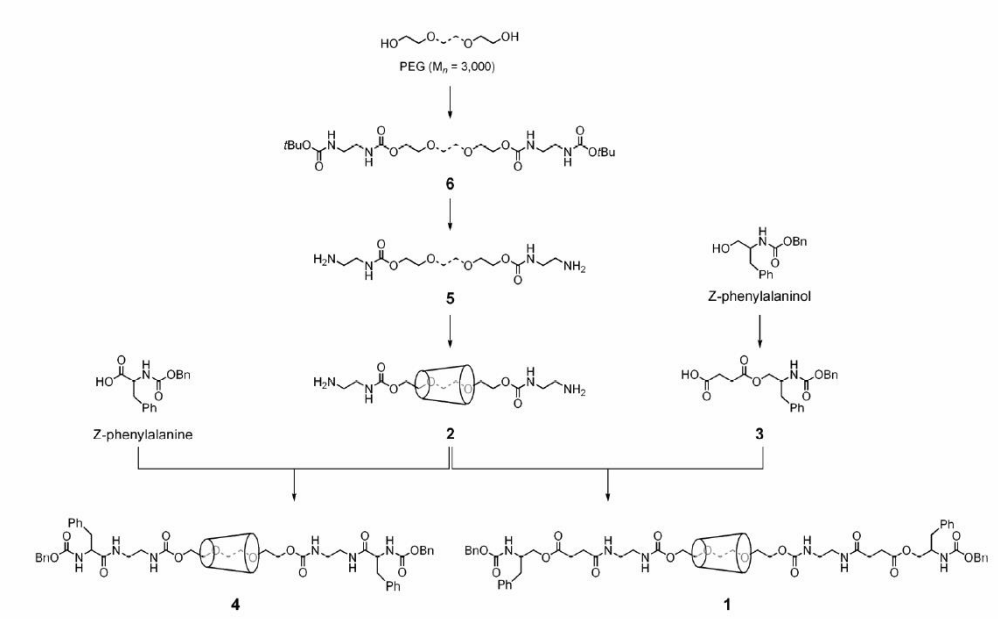

Scheme 2. Preparation of hydrolyzable polyrotaxane **1** and chemical structure of ester-free polyrotaxane **4**

2. Preparation of Hydrolyzable Polyrotaxane Containing Ester Linkages

*Preparation of **3***

To a solution of Z-phenylalaninol (3.0 g, 11 mmol) in pyridine (36 mL) were added succinic anhydride (1.5 g, 15 mmol) and 4-dimethylaminopyridine (0.65 g, 5.3 mmol). The mixture was stirred at room temperature for 18 hrs. After evaporation of the solvent in vacuo, the residue was diluted with AcOEt and 1N HCl aq., and extracted with AcOEt. The organic layer was washed with water, brine, and dried over $MgSO_4$. The crude product was purified by column chromatography on silica gel (AcOEt / CH_2Cl_2, 2:3) to give **3** (3.0 g) as a white solid in 74% yield.

Data of **3**

mp 126-127 °C; ^{1}H NMR (300 MHz, DMSO-d_6) δ/ppm 12.5-12.0 (1H, br. s, -(C=O)OH), 7.44 - 7.12 (10H, m, ArH), 4.96 (2H, s, -OCH_2Ph), 4.12-3.98 (1H, m, -CH(CH2Ph)NH-), 3.98-3.82 (2H, m, -OCHHCH(CH2Ph)NH-), 2.81 (1H, dd, *J* = 4.2, 13.2 Hz), 2.67 (1H, dd, *J* = 8.4, 13.2 Hz), 2.54-2.43 (4H, br, -CH_2CH_2-); ^{13}C NMR (75 MHz, DMSO-d_6) ŭ/ppm 173.6 (-C(=O)OH), 172.1 (-CH_2C(=O)OCH_2-), 155.9 (-NC(=O)O-), 138.4, 137.4, 129.3, 128.5, 128.4, 127.9, 127.7, 126.4 (C_{Ar}×8), 65.5, 65.3 (-OCH2-, -OCH_2-), 51.5 (-CH(CH_2Ph)NH-), 36.8 (-CH(CH_2Ph)NH-), 28.9, 28.8 (-CH_2CH_2-); IR (KBr) 3246 (-(C=O)NH-), 1741 (-CH2(C=O)OCH2-), 1715 (-(C=O)OH), 1662 (-N(C=O)O-) cm^{-1}; ESI-MS m/z 386 ([M+H]+, BP); ESI-HR-MS Calcd. for $C_{21}H_{23}NO_6Na$ 408.1418, Found 408.1410.

2. Preparation of Hydrolyzable Polyrotaxane Containing Ester Linkages

Preparation of PEG bis[2-(N-tert-buthoxycarbonyl)-aminoethylcarbamate] ***6***

To a solution of *N*,*N*ô-carbonyldiimidazole (21.0 g, 130 mmol) in CH_2Cl_2 (130 mL) was added a solution of PEG (20.0 g, 6.7 mmol) in CH_2Cl_2 (70 mL) at room temperature, and then the mixture was stirred for 60 hrs. After quenching the reaction by addition of water (150 mL), the organic layer was separated, and dried over $MgSO_4$. After removal of a solid by filtration, the filtrate was evaporated to some extent. Addition of Et_2O into the remaining solution gave PEG bis(*N*-imidazolecarboxylate) (21.0g) as a white solid in 99% yield. ^{1}H NMR (300 MHz, $CDCl_3$) δ/ppm 8.168 (2H, s, -(C=O)NC<u>H</u>N-), 7.451 (2H, s, -(C=O)NC<u>H</u>=CHN-), 7.076 (2H, s, -(C=O)NCH=C<u>H</u>N-), 4.60-4.55 (4H, m, -PEG-OCH_2CH_2O(C=O)-), 3.87-3.81 (4H, m, -O<u>CH_2</u>CH_2O(C=O)-), 3.92-3.38 (256H, m, -O<u>CH_2</u><u>CH_2</u>O-).

To a solution of *N*-(*tert*-buthoxycarbonyl)ethylenediamine[1] (0.18 g, 1.2 mmol) in CH_2Cl_2 (4 mL) was added a solution of PEG bis(*N*-imidazolecarboxylate) (0.57 g, 0.19 mmol) in CH_2Cl_2 (6 mL) over 30 min by using an additional funnel. After stirring at room temperature for 24 hrs, the mixture was poured into water, and then separated. The organic layer was washed with brine, and dried over $MgSO_4$. The crude product was purified by reprecipitation from CH_2Cl_2/Et_2O to give **6** (0.49 g) as a white solid in 79% yield.

Data of **6**

mp 41-43 °C; ^{1}H NMR (300 MHz, $CDCl_3$) δ/ppm 5.36-5.26 (2H, br. s, -O(C=O)N<u>H</u>CH_2-),

5.09-4.95 (2H, br. s, -HN(C=O)O-), 4.21 (4H, t, *J* = 4.4 Hz, -(C=O)OCH$_2$-), 3.91-3.82 (272H, m, -OCH$_2$CH$_2$O-), 3.33-3.16 (8H, br. s, -NHCH$_2$CH$_2$NH-), 1.44 (18H, s, -(C=O)OC(CH$_3$)$_3$); ^{13}C NMR (75 MHz, $CDCl_3$) δ/ppm 156.2, 156.7 (-(C=O)NH-), 79.2 (-OC(CH$_3$)$_3$), 76.6-70.4 (-CH$_2$CH$_2$O-), 69.4 (-CH$_2$CH$_2$O-CH$_2$CH$_2$O(C=O)N-), 63.9 (-CH$_2$CH$_2$O-CH$_2$CH$_2$O(C=O)N-), 28.3 (-OC(CH$_3$)$_3$).; IR (KBr) 3339 (NH), 2885 (CH), 1709 (N(C=O)O) cm^{-1}.

Preparation of PEG bis(2-aminoethylcarbamate) ***5***

A solution of **6** (14g, 4.2 mmol) in TFA/CH_2Cl_2 (10 mL/40 mL) was stirred at room temperature for 13 hrs. After removal of the volatiles by evaporation, the residue was dissolved in CH_2Cl_2 and 0.5 N NaOH aq.. The organic layer was separated, and dried over $MgSO_4$. The crude product was purified by reprecipitation from CH_2Cl_2/Et_2O to give **5** (11 g) in 84% yield as a white solid.

Data of **5**

mp 47-49 °C; ^{1}H NMR (300 MHz, $CDCl_3$) δ/ppm 5.33-5.20 (2H, br. s, -(C=O)NHCH$_2$-), 4.22 (4H, t, *J* = 4.5 Hz, -(C=O)OCH$_2$-), 3.91-3.83 (272H, m, -OCH$_2$CH$_2$O-), 3.23 (4H, dt, *J* = 5.7, 6.0 Hz, -CH$_2$(C=O)NHCH$_2$-), 2.82 (4H, t, *J* = 5.7 Hz, -CH$_2$NH$_2$); ^{13}C NMR (75 MHz, $CDCl_3$) δ/ppm 156.6 (-(C=O)NH-), 71.8-70.5 (-CH$_2$CH$_2$-), 69.5 (-(C=O)OCH$_2$CH$_2$-), 63.9 (-(C=O)OCH$_2$CH$_2$-), 41.7, 43.7 (-CH$_2$CH$_2$NH$_2$); IR (KBr) 3379 (NH), 2885 (CH), 1714

(N(C=O)O) cm^{-1}.

*Preparation of pseudopolyrotaxane **2***

To a solution saturated with Ŭ-CD (8.7 g, 9.0 mmol) in water (60 mL) was added **5** (0.78 g, 0.25 mmol) at room temperature. After stirring for 24 hrs, centrifugation of the mixture gave an inclusion complex (4.2 g) as a white paste, followed by freeze-drying. The ratio of Ŭ-CD to PEG in the inclusion complex was determined by ^{1}H NMR in D_2O containing approximate 1wt% NaOD to be ca. 24/1.

*Preparation of ester-containing polyrotaxane **1***

To a solution of **3** (2.0 g, 5.2 mmol) and N-hydroxysuccinimide (0.65 g, 5.7 mmol) in THF (12 mL) was added a solution of *N,N'*-dicyclohexylcarbodiimide (1.0 g, 4.9 mmol) in THF (7.8 mL) at 0 ℃ over 30 min.[2] The mixture was stirred at room temperature for 20 hrs. After removal of precipitates by filtration, the filtrate was added into cold hexane to give succinimidyl succinate (2.3 g) as a white solid in 92%.

To a suspension of **2** (10.0 g containing 0.99 g, 0.31 mmol of **5**) in DMF (30 mL) was added the succinimidyl succinate (3.15 g, 6.2 mmol), and the mixture was stirred for 60 hrs at room temperature. After dilution with DMF (80 mL), centrifugation of the reaction mixture

gave a white solid. The crude product was washed with acetone, and dried in vacuo. The solid was dissolved in DMSO, and precipitated in acidic water and then dialyzed against acidic water, DMSO for 2 days with a cellulose tubing (MWCO = 3,500) and then freeze-dried to give **1** (1.85 g) as a white powder in 32% yield. The number of CD molecules in **1** was calculated to be ca. 18.

Data of **1**

mp > 278 °C (decomp.); ^{1}H NMR (300MHz, DMSO-d_6) δ/ppm 7.41-7.12 (br., Ar-H), 5.89-5.60 (br. s, OH^2, CD), 5.60-5.35 (br. s, OH^3, CD), 5.01-4.64 (br. s, H^1, CD), 4.64-4.30 (br. s, OH^6, CD), 3.99-3.68 (br. s, H^3, H^5, H^6, H$^{6\delta}$, CD), 3.60-3.42 (br. s, -CH$_2$-, PEG), 3.43-3.27 (br. m, H^4, H^2, CD) (Figure 1a).; ^{1}H NMR (300MHz, D2O containing approximate 1wt% NaOD) δ/ppm 7.34-7.14 (m, Ar-H), 4.84 (105H, d, J = 3.3 Hz), 3.86-3.63 (m, 420H, H^3, H^5, H^6, H$^{6\delta}$, CD), 3.55 (s, 272H, -CH$_2$-, PEG), 3.44-3.26 (m, 120H, H^4, H^2, CD), 3.19-3.03 (m, -NCH$_2$CH$_2$N-), 2.31-2.27 (br. s, -C(=O)CH$_2$CH$_2$C(=O)-); IR (KBr) 3357 (OH, CD), 2923 (CH, CD), 1697 (C=O), 1647 (OH, CD) cm^{-1}.

*Preparation of ester-free polyrotaxane **4***

To a suspension of **2** (1.6 g containing 0.19 g, 0.060 mmol of **5**) in DMF (10 mL) was added Z-phenylalanine succinimidyl ester (0.95 g, 2.4 mmol), and the mixture was stirred for

72 hrs at room temperature. After dilution with DMF, centrifugation of the reaction mixture gave a white solid. The crude product was washed with acetone, and dried in vacuo. The solid was dissolved in DMSO, and precipitated in acidic water and then dialyzed against water, DMSO with a cellulose tubing (MWCO = 3,500) and then freeze-dried to give **4** (0.61 g) as a white powder in 51% yield. The number of CD molecules in **4** was calculated to be ca. 17.

Data of **4**

mp > 277 °C (decomp.); ^{1}H NMR (300MHz, D_2O containing approximate 1wt% NaOD) ŭ/ppm 7.36-7.05 (m., Ar-H), 5.0-4.8 (br. m, H^1, CD), 4.0-3.6 (br. m, H^3, H^5, H^6, $H^{6ô}$, CD), 3.6-3.5 (br. s, -CH_2-, PEG), 3.5-3.2 (br. m, H^2, H^4, CD) (Figure S3b).; ^{1}H NMR (300MHz, DMSO-d_6) δ/ppm 7.36-7.18 (br. m, Ar-H), 5.90-5.59 (br. s, OH^2, CD), 5.59-5.33 (br. s, OH^3, CD), 4.88-4.71 (br. s, H^1, CD), 4.57-4.32 (br. s, OH^6, CD), 4.05-2.94 (br. s, $H^{2\text{-}6,6ô}$, CD), 3.51 (br. s, -CH_2-, PEG) (Figure S3c).; IR (KBr) 3366 (OH, CD), 2925 (CH, CD), 1700 (C=O), 1648 (OH, CD) cm^{-1}.

2-2-3. Hydrolysis of polyrotaxane 1, 4, and pseudopolyrotaxane 2

To a tetraborate/phosphate pH standard solution adjusted to pH 9.18/6.86 (2 mL) was added respectively 1.5 mg of polyrotaxane **1** which had been freeze-dried until just before the

use. The suspension was applied to the transmittance measurement at 500 nm with stirring at room temperature. Each of pseudopolyrotaxane **2** and ester-free polyrotaxane **4** was examined in the same manner as that for **1**.

2-3. Results and discussion

The hydrolyzable polyrotaxane **1** was prepared by capping a pseudopolyrotaxane **2** with an ester-containing bulky N-benzyloxycarbonyl (Z-) phenylalanine-based succinic acid derivative **3** in DMF as shown in Scheme 2. The pseudopolyrotaxane **2** was obtained by mixing a PEG chain **5** attached to amino groups at both ends with α-CD in water, followed by lyophilization according to a method reported by Harada et al.[5] The bulky capping molecule **3** was derived from a commercially available Z-phenylalaninol by treatment with succinic anhydride in pyridine containing a catalytic dimethylaminopyridine, and then employed as a succinimidyl succinate just before the capping reaction by condensation with **2**. Reprecipitation and dialysis using DMSO and acidic water (pH 3.2)[9] allowed **1** to be isolated without decomposition, which was confirmed by ^{1}H NMR and GPC measurements. The ester-free polyrotaxane **4** was also prepared as a reference by capping the pseudopolyrotaxane **2** with Z-phenylalanine in a similar manner to that used for **1**.

According to Figure 1a, notable broadening signals were observed for CD protons in **1**, which is characteristic of CD based polyrotaxanes in DMSO-d_6.[5] Aromatic protons assigned to capping moieties in **1** were also detected. Figure 1b shows sharp signals as is observed for common pseudopolyrotaxanes without any terminal bulky groups implying the dissociation of **2** in DMSO-d_6 into the respective components α-CD and PEG. These observations clearly indicate that the polyrotaxane **1** was successfully prepared and isolated in pure form (Figure 1-3).[6] This was also confirmed by GPC measurements for **1**, **2**, and **4** eluted with DMSO, in which a shorter retention time (40 min) for the polyrotaxanes **1** and **4** was observed than for the α-CD (50 min) accompanied with the dissociation of pseudopolyrotaxane **2** in DMSO (Figure 1).

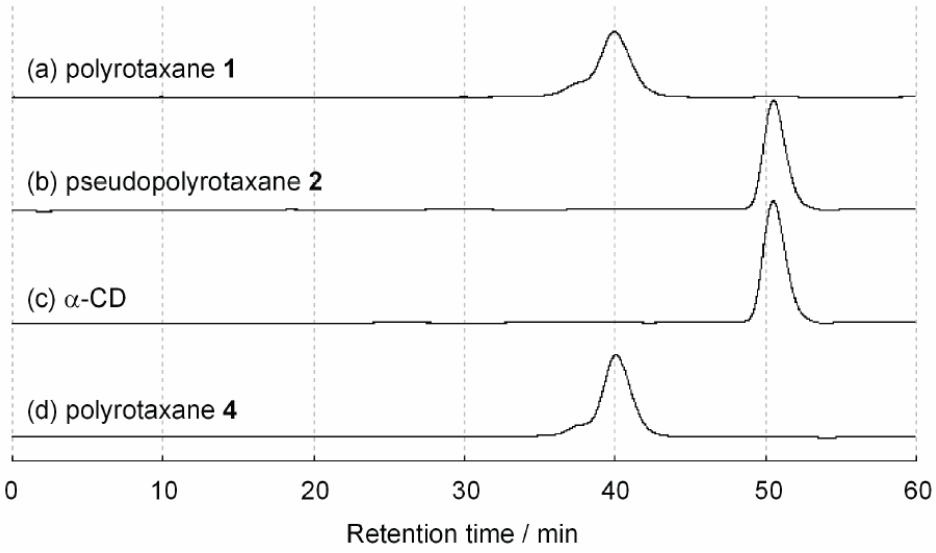

Figure 1. GPC profiles for (a) polyrotaxane **1**, (b) pseudopolyrotaxane **2**, (c) Ŭ-CD, and (d) polyrotaxane **4** (DMSO, flow rate = 0.4 mL/min, RI).

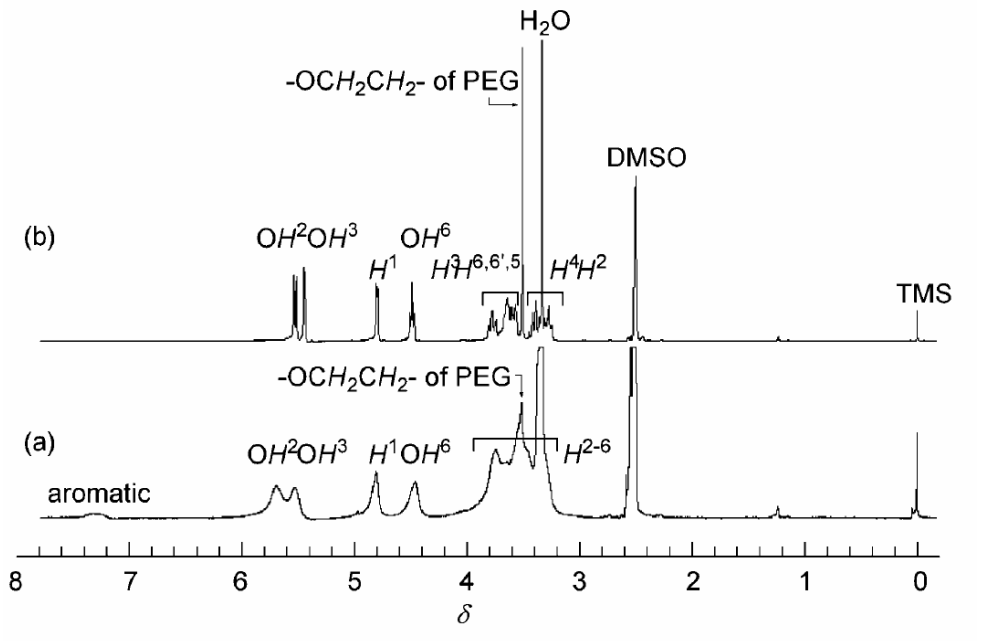

Figure 2. ^{1}H NMR spectra (300 MHz) of (a) polyrotaxane **1** and (b) pseudopolyrotaxane **2** in DMSO-d_6 at room temperature.

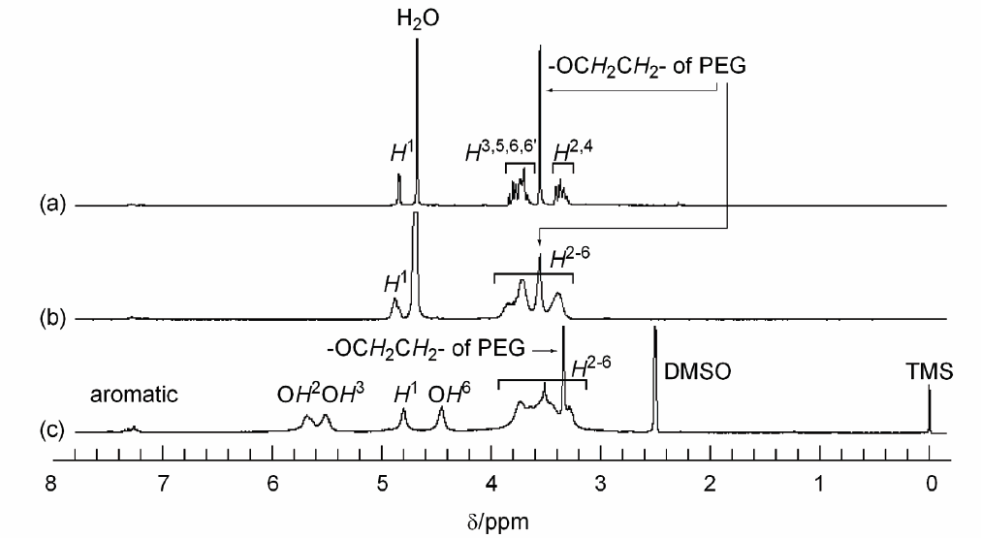

Figure 3. ^{1}H NMR spectra (300 MHz) of (a) polyrotaxane **1**, (b) polyrotaxane **4** in D_2O containing approximate 1wt% NaOD and (c) polyrotaxane **4** in DMSO-d_6 at room temperature.

2. Preparation of Hydrolyzable Polyrotaxane Containing Ester Linkages

The hydrolysis property of the ester-containing polyrotaxane **1** was investigated by monitoring the time change in the transmittance by comparison with that for the pseudopolyrotaxane **2** and the ester-free polyrotaxane **4**. It is difficult to estimate exactly the amount of cleaved ester linkages from the change in transmittance because the cleavage of both ester linkages is not required for triggering the dissociation. Each sample was suspended in a tetraborate pH standard solution adjusted to a pH of 9.18. A gradual increase in the transmittance at 500 nm from the baseline for **1** indicates qualitatively[7] that the water-insoluble **1** was gradually reduced by hydrolysis to produce water-soluble component(s), whereas an instantaneous change from a turbid suspension to a clear solution for **2** showed the dissociation of the inclusion complex. Any change in the transmittance for the ester-free polyrotaxane **4** was not found during the observation (Figure 4a). In order to obtain further information on water-soluble component(s) in each suspension, several clear upper portions were collected at an arbitrary time for GPC measurements. The signals detected by RI for each portion collected from the suspension of **1** and **2** had the same retention time, indicating that at least one of the water-soluble components is α-CD (Figure 5). The concentration of the PEG component in the portion was too low to be detected by RI on GPC measurements.[8] On the other hand, the portions collected from the suspension of **4** did not contain any water-soluble components, which means that it was intact under the conditions in accordance with

the result of the transmittance measurements. These observations demonstrate that the ester-containing polyrotaxane **1** was hydrolyzed to produce its water-soluble components.

Hydrolysis under almost neutral conditions (pH 6.86) was also examined through transmittance measurement (Figure 4b). It then took much more time for the ester-containing polyrotaxane **1** to initiate hydrolysis than under basic conditions (pH 9.18), to reach only 10% even after 13 days.

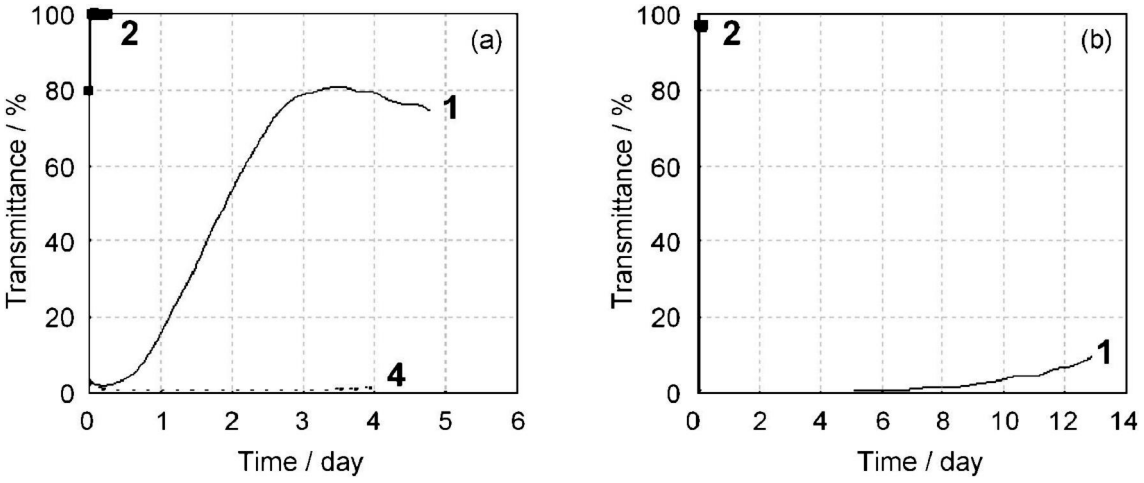

Figure 4. Continuous changes in transmittance of suspensions for **1** (thin line), **2** (bold line), and **4** (dashed line) at (a) pH 9.18 and **1** (thin line), and **2** (bold line) at (b) pH 6.86 at room temperature.

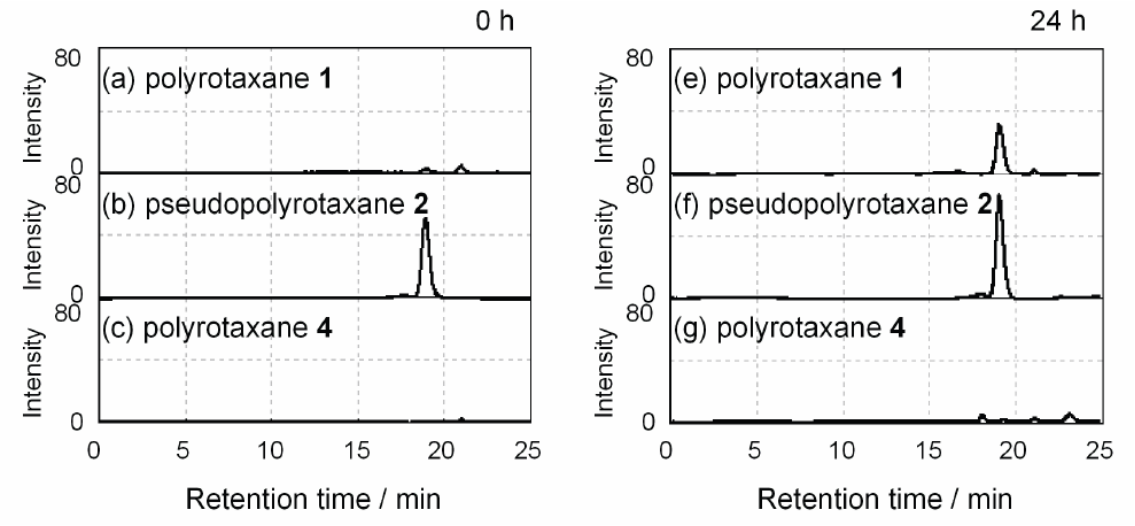

Figure 5. GPC profiles for clear upper portions collected from suspensions of a) **1**, b) **2** and c) **4** at 0 h, and e) **1**, f) **2** and g) **4** at 24 h in water adjusted to pH 9.18 (tetraborate pH standard solution adjusted to pH 9.18, flow rate = 1 mL/min, RI).

2-4. Conclusion

In conclusion, we demonstrated the design and preparation of the hydrolyzable polyrotaxane **1** composed of an ester-containing PEG chain and α-CDs. The hydrolysis of **1** into its water-soluble components under aqueous conditions adjusted to both a basic and almost neutral pH was confirmed by monitoring continuous changes in transmittance and by GPC measurements of clear upper portions collected from suspensions. We are now studying the design of hydrogels based on hydrolysable polyrotaxanes. It is easily conceivable that the

dissociation of polyrotaxanes in hydrogel form into its components upon degradation of labile linkage(s) such as the ester group will be suitable for biocompatible materials such as scaffolds for tissue engineering.

References and Notes

1. a) Langer, R.; Tirrel, D. A. *Nature*, 2004, **428**, 487. b) Rezwan, K.; Chen, Q. Z.; Blaker, J. J.; Boccaccini, A. R. *Biomaterials*, 2006, **27**, 3413. c) Furth, M. E.; Atala, A.; Dyke, M. E. V. *Biomaterials,* 2007, **28**, 5068.

2. Aliphatic polyesters such as poly(lactic acid), and poly-(glycolic acid) have been widely investigated to develop biomaterials which undergo hydrolysis for degradation. Recent reviews: a) Tokiwa, Y.; Jarerat, A.; *Biotechnol. Lett*., 2004, **26**, 771. b) Tsuji, H. *Macromol. Biosci*., 2005, **5**, 569. c) Tokiwa, Y.; Calabia, B. P.; *Appl. Microbiol. Biotechnol*., 2006, **72**, 244. d) Chitkara, D.; Shikanov, A.; Kumar, N.; Domb, A. J. *Macromol. Biosci*., 2006, **6**, 977.

3. Yui, N.; Ooya, T. *Chem.- Eur. J*., 2006, **12**, 6730.

4. A labile bond such as ester linkage was introduced prospectively into a capping agent not a CD-based pseudopolyrotaxane[5] which is commonly prepared in water. Another

estercontaining polyrotaxane **1'** had been designed in previous reports such as the following a) and b), however, the preparation and isolation of desired polyrotaxane **1'** could not be achieved sufficiently due to the lack of attention to the potential of degradation. a) Watanabe, J.; Ooya, T.; Yui, N. *Chem. Lett*., 1998, 1031. b) Watanabe, J.; Ooya, T.; Yui, N. *J. Biomater. Sci. Polym. Ed*., 1999, **10**, 1275.

5. Harada, A.; Li, J.; Kamachi, M. *Nature,* 1992, **356**, 325.

6. The number of threading α-CD molecules in the obtained polyrotaxane **1** was calculated from the ratio of peak integrations for both C(1) protons in CD and methylene protons in PEG in the NMR spectrum measured in D_2O containing approximately 1wt% NaOD to be ca. 18 (See Figure 3).

7. A quantitative understanding for the dissociation of polyrotaxane is difficult because some inclusion complexes can be soluble in water when the number of threading α-CD molecules is small.

8. A PEG component in the clear upper portion was detectable by TLC on silica gel significantly. Also, after evaporation of the portion, the remaining solid was suspended in CH_2Cl_2. It was confirmed by ^1H NMR that the CH_2Cl_2 layer contained the PEG component.

9. See the supporting information.

Supporting Information

*Preparation of polyrotaxane **1'** containing ester-linkage in back-bone polymer*

In order to obtain another ester-containing polyrotaxane,[1] analogous PEG chain **5'** attached to amino groups at both ends is also available as shown in Scheme S1, however, it should be dealt with much more attention in water. Preparation of an inclusion complex **2'** by mixing the PEG chain **5'** and Ŭ-CD in water adjusted to pH 5-10 can be competitive to decomposition due to hydrolysis and/or aminolysis. It was found that the above competition upon inclusion complexation was avoided by the adjustment of the solution to pH 3.2, in which the amine groups was thought to be fully-protonated (Figure S1, Table S1). The following capping reaction of the pseudopolyrotaxane **2'** with Z-phenylalanine succinimidyl ester **2** in DMF was allowed to proceed by the gradual addition of triethylamine to neutralize. Eventually reprecipitation from DMSO/water gave the ester-containing polyrotaxane **1'** (yield 45%).

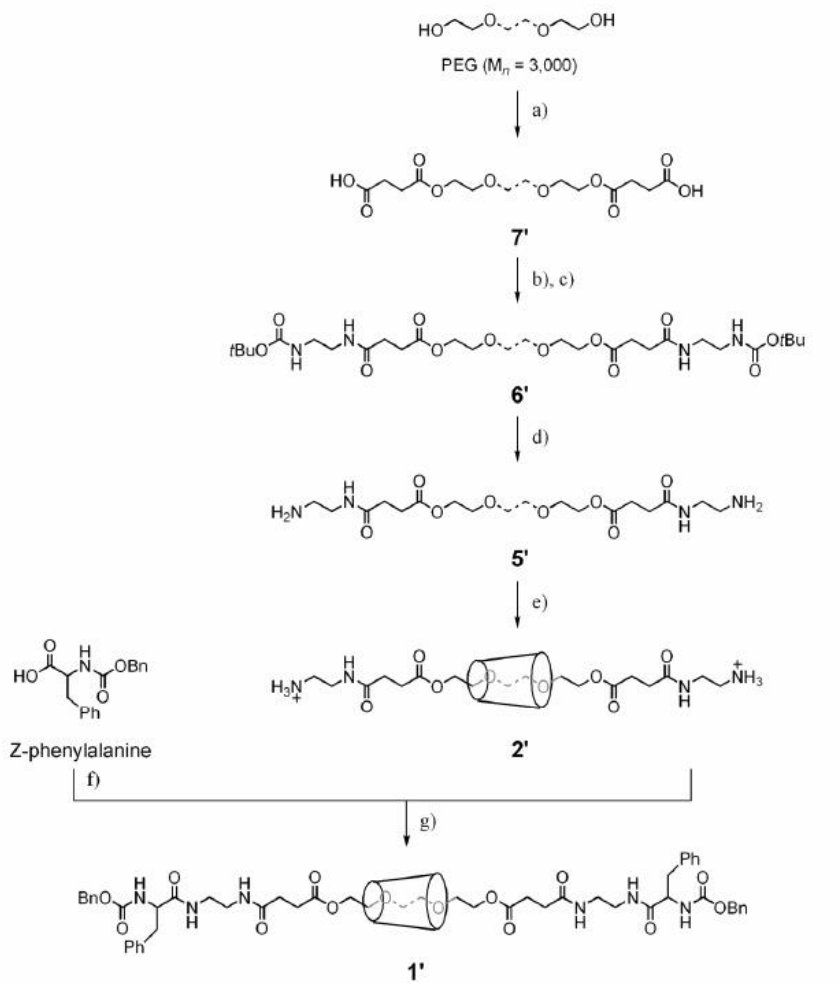

Scheme S1. Preparation of polyrotaxane **1'**. Reagents and conditions; a) succinic anhydride, toluene (77%); b) *N*-hydroxysuccinimide, DCC, THF (82%); c) (*N*-tert-buthoxycarbonyl)ethylenediamine, CH_2Cl_2 (86%); d) TFA, CH_2Cl_2 (92%); e) Ŭ-CD, water (pH = 3.2); f) *N*-hydroxysuccinimide, DCC, THF; g) Et_3N, DMF (45%).

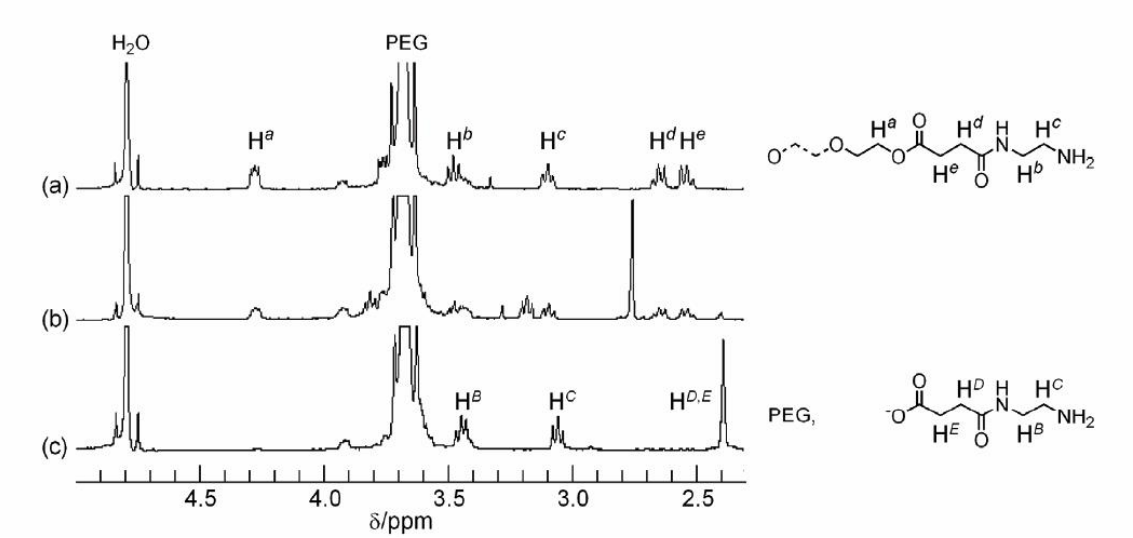

Figure S1. ^{1}H NMR spectra (300 MHz) of an ester-containing PEG bis(amine) **5'** dissolved for 24 hrs in D_2O adjusted to a) an acidic (pH 3.2), b) a neutral (pH 7.0), and c) a basic (pH 10.0) conditions, respectively.

Table S1. Changes in survival rate of the ester group in **5'** and pH in respective aqueous conditions.

Time (h)		0	0.5	24
Survival rate (pH)	acidic	1.0 (3.2)	> 0.9	> 0.9 (3.2)
	neutral	1.0 (7.0)	0.8	0.3 (6.8)
	basic	1.0 (10.0)	0	0 (8.5)

Reference

1. a) Watanabe, J.; Ooya, T.; Yui, N. *Chem. Lett*. 1998, 1031. b) Watanabe, J.; Ooya, T.; Yui, N.; *J. Biomater. Sci. Polym. Edn.*, 1999, **10**, 1275, where the preparation and isolation of desired polyrotaxane **1'** could not be achieved sufficiently due to the lack of attention to the degradation of intermediate **5'** which underwent hydrolysis in water without any careful adjustment of pH. And also it was difficult to confirm whether the pseudopolyrotaxane **1'** composed of the labile intermediate **5'** and Ŭ-CD still contained ester linkage(s) or not before the capping reaction.

Chapter 3

Molecular Design of Degradable Polyrotaxane Hydrogels for Tissue Engineering

3 Molecular Design of Degradable Polyrotaxane Hydrogels for Tissue Engineering

3-1. Introduction

During the past decade, many researchers have developed and investigated synthetic degradable biomaterials for drug delivery application, using micro- / nanoparticular system, and implant application, such as scaffold, for tissue engineering of various organs and tissue.[1-4] Poly(lactic acid) (PLA), poly(glycolic acid) (PGA), and their copolymer poly(lactic-co-glycolic acid) (PLGA), polycaprolactone (PCL), polydioxanone (PDS), and poly(trimethylene carbonate) were the degradable polymers to be utilized to various surgical implantable materials and drug delivery service.[2,5,6] PLGA has been shown the various rate of degradation speed depending on a variety of parameters including the GA/LA ratio and molecular weight. Especially, the popularity of PLGA is attributed in their approval by FDA for use in human.[6]

Polyrotaxane is a molecule in which a number of cyclic molecules are threaded on a long-chained polymer capped with a bulky group at both terminals,[7,8] and a promising candidate to design degradable materials thanks to a supramolecular feature of leading to dissociation upon

cleavage of a bond in the main chain in response to external stimuli.[9,10] In addition to the degradable feature, chemical and physical properties of a polyrotaxane molecule are modulated by lots of structural parameters such as residual appendage to the cyclic component, molecular weight of the main chain, and so on.[11-13] Materials based on polyrotaxanes[14] as well as a polyrotaxane molecule itself are fascinating because further modulation is available, for instance, on the construction of materials by crosslinking, giving a chance to select a crosslinking manner as a parameter. In fact, the slide-ring gel, which has a network structure crosslinked at the cyclic component of a polyrotaxane forming a movable crosslink point, should be representative of polyrotaxane-based materials.[15] We envisaged that not only materials property but also degrading behavior would vary on the crosslinking method if the materials are based on a degradable polyrotaxane. Thus we designed two types of degradable polyrotaxane hydrogels with different crosslink method. One of the two has crosslink points at the cyclic component, and the other has crosslink points at the terminals. Both were based on a degradable polyrotaxane composed of modified α-cyclodextrin (α-CD), poly(ethylene glycol) (PEG), and Z-phenylalanine and Z-tyrosine as capping moieties containing ester linkages, and were crosslinked with a ditopic or tetratopic crosslinker (Scheme 1). The polyrotaxanes in the crosslinked materials would degrade on the cleavage of ester linkages and result in degradation of the materials (Figure 1). During the degradation,

the crosslinked materials would undergo modulation of chemical and physical properties. The degradable materials, of course, should be obtained with avoiding undesired decompositions during the preparation. Here we demonstrated a successful preparation of degradable polyrotaxane hydrogels, and degradation behavior of the crosslinked materials by monitoring changes in mass and storage modulus during the duration. For some hydrogels with relatively longer periods of duration, we attempted a preliminary cell adhesion test on the degrading materials. Details of the above mentioned demonstration are described below.

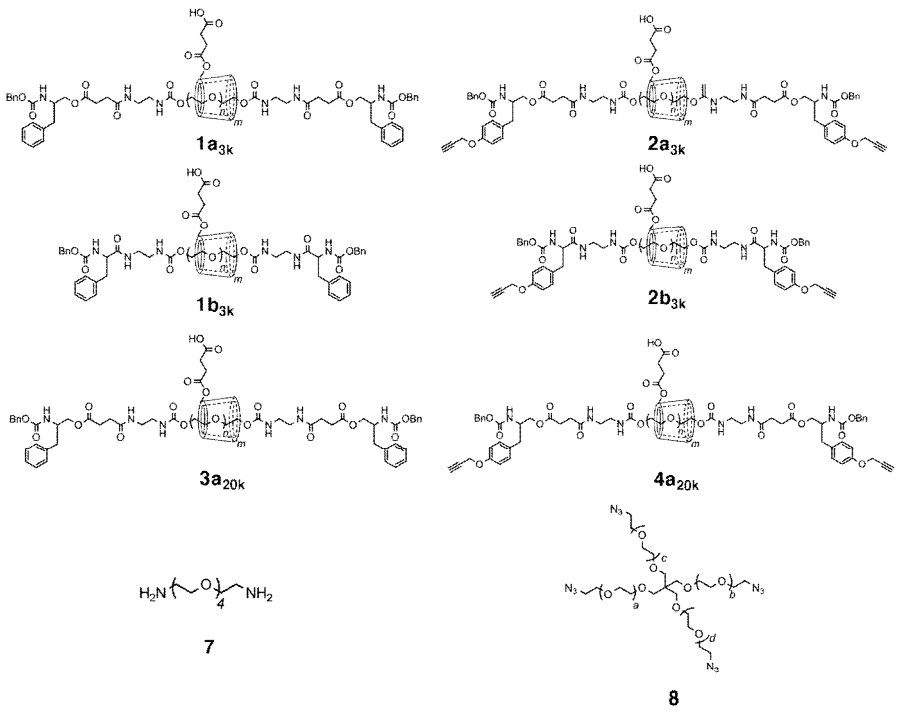

Scheme 1. Chemical structures of degradable polyrotaxanes **1**-**4** and crosslinkers **7** and **8.**

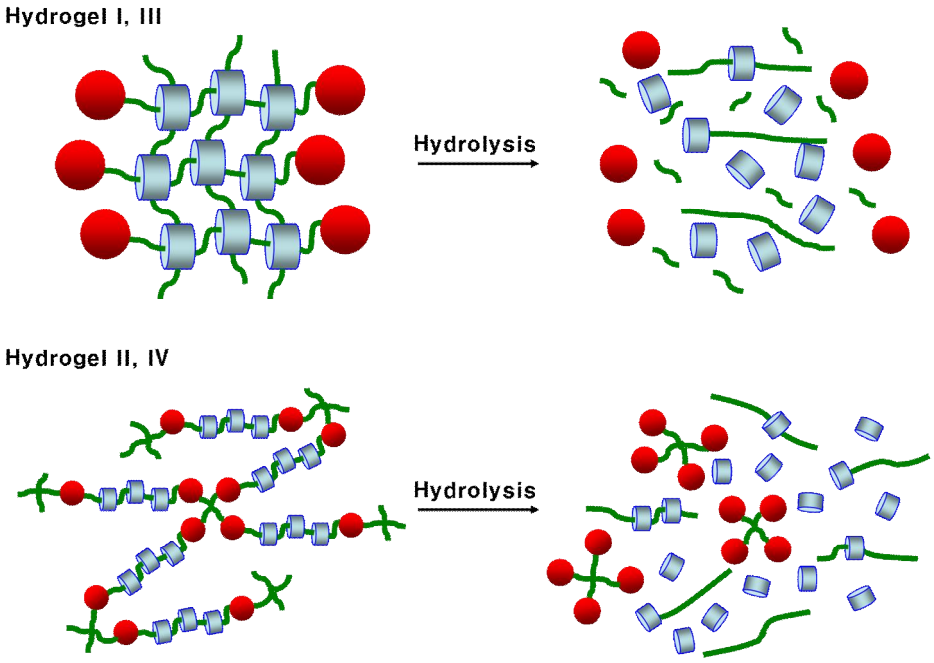

Figure 1. Schematic illustration for degradation of hydrogels based on degradable polyrotaxanes triggered by ester cleavage.

3-2. Experimental section

3-2-1. Materials

Poly(ethylene glycol) 4000 (PEG, average molecular weight 3000) and poly(ethylene glycol) 20000 (M_r; 16000-24000) were purchased from Wako Pure Chemicals Industries, Ltd. (Osaka, Japan) and Fluka Chemie AG (Buchs, Switzerland), and were used as starting materials for preparing PEG bis(2-aminoethylcarbamate)s (PEGBAs $\mathbf{9}_{3k}$[9] and $\mathbf{9}_{20k}$). Capping molecules **5** and **6** were derived from Z-phenylalanine and Z-tyrosine. Ditopic and tetratopic crosslinkers **7** and **8** were prepared according to literature.[16,17] Abbreviations for some reagents (Scheme 2 and 3) are as follows: CDI (carbonyldiimidazole), HOBt (1-hydroxybenzotriazole), DCC (*N*,*N*'-dicyclohexylcarbodiimide), HOSu (*N*-hydroxysuccinimide), DMT-MM (4-(4,6-dimethoxy-l,3,5-triazin-2-yl)-4-methylmorpholinium chloride).

3-2-2. Preparation of polyrotaxanes hydrogels I-IV

(a) Preparation of pseudopolyrotaxanes $\mathbf{9}_{3k}{}^{9}{}_{/20k}$

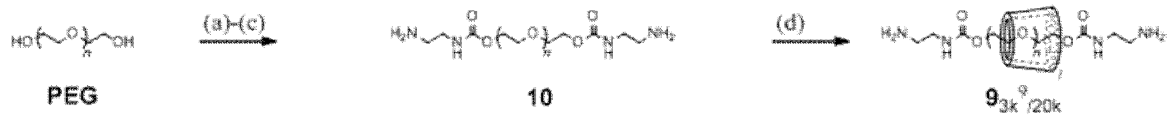

PEG (M_n = 3000/20000) — **10** — $\mathbf{9}_{3k}{}^{9}{}_{/20k}$

(b) Preparation of capping reagents **5** and **6**.[9]

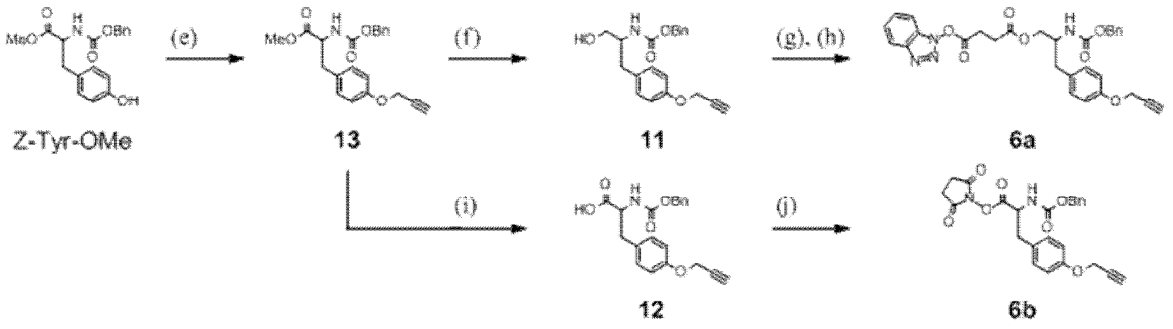

Z-Tyr-OMe — **13** — **11** — **6a**

12 — **6b**

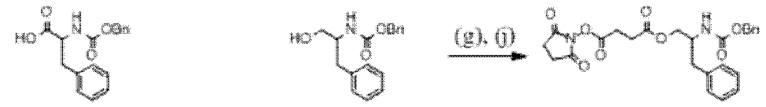

Z-Phe-OH — Z-pheylalaninol — **5a**[9]

5b[9]

(c) Preparation of crosslinkers **7**[16] and **8**[17].

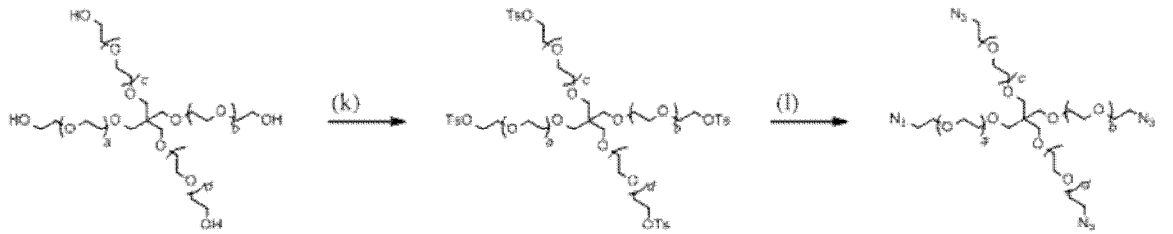

Pentaerythritol ethoxylate ($a + b + c + d$ = 15) — **14**[17] — **8**[17]

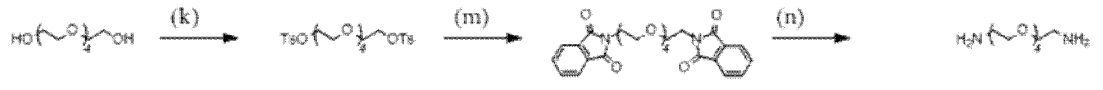

Tetraethylene glycol — **16**[16] — **15**[16] — **7**[16]

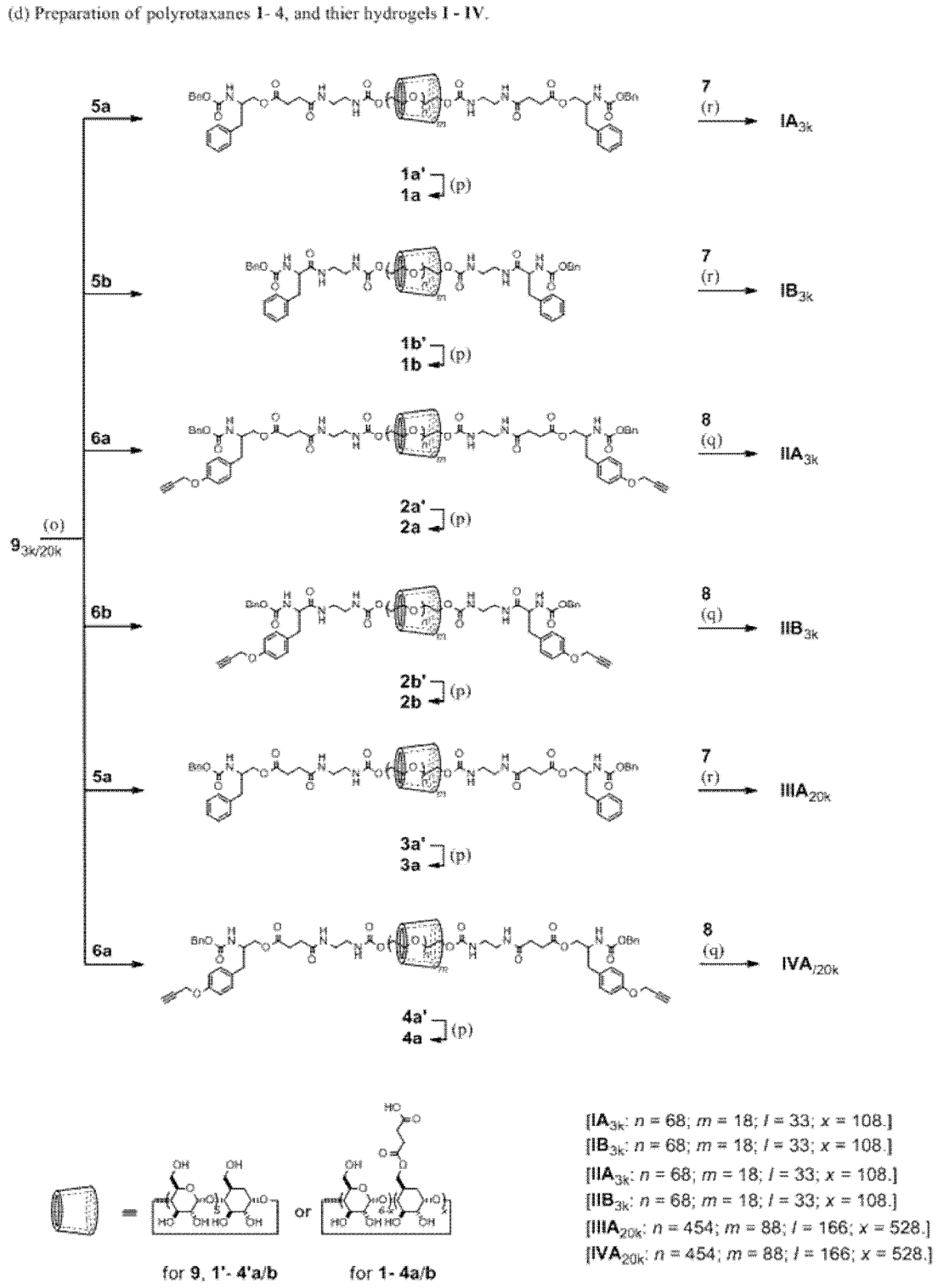

Scheme 2. Preparation of polyrotaxane hydrogels **I** ï **IV** ; Reagents. (a) CDI, CH_2Cl_2 (85 % for PEG_{3k}, 99 % for PEG_{20k}); (b) *N*-Boc-ethylenediamine, CH_2Cl_2 (87 % for PEG_{3k}, 87 % for

PEG_{20k}); (c) TFA, CH_2Cl_2 (89 % for PEG_{3k}, 95 % for PEG_{20k}); (d) α-CD, water, (9_{3k} : 91 %; 9_{20k} : 79 %); (e) Propargyl bromide, K_2CO_3, 2-butanoe (85 %); (f) $NaBH_4$, THF (84 %); (g) Succinic anhydride, DMAP, pyridine (6a : 88 %; 5a : 91%); (h) HOBt, DCC, THF (97%); (i) LiOH, THF, water (90%); (j) HOSu, DCC, THF (6b : 87%; 5a : 79%; 5b : 70%); (k) TsCl, Et_3N, CH_2Cl_2 (14 : 78%; 16 : 87%); (l) NaN_3, EtOH (76%); (m) Potassium phthalimide, DMF (90%); (n) H_2NNH_2, EtOH (91%); (o) DMF ($1a'_{3k}$: 36%; $1b'_{3k}$: 50%, $2a'_{3k}$: 46%; $2b'_{3k}$: 36%; $3a'_{20k}$: 54%; $4a'_{20k}$: 42%); (p) Succinic anhydride, pyridine ($1a_{3k}$: 74%; $1b_{3k}$: 82%; $2a_{3k}$: 68%; $2b_{3k}$: 87%; $3a_{20k}$: 68%; $4a_{20k}$: 79%); (q) 8, $CuSO_4$, (+)-ascorbic acid, 01.M phosphate buffer solution (pH = 7.0) containing 1v/v% DMSO; (r) 7, DMT-MM,[39,40] 01.M phosphate buffer solution (pH = 7.0).

*Preparation of **13***

To a solution of Z-Tyr-OMe (5.00 g, 15.18 mmol) and K_2CO_3 (2.10 g 15.18 mmol) in 2-butanone (50 mL) was added propargyl bromide (1.80 g, 15.18 mmol), the mixture was refluxed for 15 hrs. After removal of a solid by filtration, the solvent was evaporated. The residue was diluted with diethylether and water, and extracted with diethylether. The organic layer was dried over $MgSO_4$. Chromatographic separation on SiO_2 (ethyl acetate/hexane = 1:1) gave **13** (4.7 g) as a white solid at 85% yield. ^{1}H NMR (300 MHz, DMSO-d_6) δ / ppm

7.77 (1H, d, *J*=9 Hz), 7.36-7.20 (5H, m), 7.13 (2H, d, *J* = 8.7 Hz), 6.84 (2H, d, *J* = 8.4 Hz), 4.93 (2H, s), 4,71 (2H, d, *J* = 2.7 Hz), 4.43-4.10 (1H, m), 3.58 (3H, s), 3.29 (1H, s), 2.93 (1H, dd, *J* = 9, 19.2 Hz), 2.76 (1H, dd, *J* = 3.3, 24 Hz).

*Preparation of **11***

To an ice-cooled solution of **13** (10.41 g, 28.34 mmol) in THF/MeOH (1:1, 210 mL) was added $NaBH_4$ (2.14 g, 56.68 mmol), the mixture was stirred for 40 min at room temperature. To the reaction mixture was added 1% HCl aq. (200 mL) at 0 °C, the solution was further stirred for 1 hr at the temperature. After removal of the solvent by evaporation, the residue was diluted with ethyl acetate and water, and extracted with ethyl acetate. The organic layer was dried over $MgSO_4$. Chromatographic separation on SiO_2 (ethyl acetate/hexane = 2:1) gave **11** (7.69 g) as a white solid at 84% yield. ^{1}H NMR (300 MHz, $CDCl_3$) δ / ppm 7.39-7.25 (5H, m), 7.10 (2H, d, *J* = 8.1 Hz), 6.88 (2H, d, *J* = 8.1 Hz), 5.11 (1H, d, *J* = 7.8 Hz), 5.05 (2H, s), 4.64 (2H, d, *J* = 2.4 Hz), 3.87 (1H, s), 3.63 (1H, dd, *J* = 7.8, 14.4 Hz), 3.52 (1H, dd, *J* = 6.3, 15 Hz), 2.77 (2H, d, *J* = 7.2 Hz), 2.50 (1H, ddd, *J* = 1.5, 2.4, 5.7 Hz).

*Preparation of **6a***

To a solution of **11** (6.51 g, 19.39 mmol) in pyridine (65 mL) were added succinic

anhydride (1.98 g, 19.78 mmol) and 4-(dimethylamino)pyridine (DMAP, 2.41 g, 19.78 mmol), the mixture was stirred for 36 hrs at room temperature. After removal of the solvent by evaporation, the residue was diluted with ethyl acetate and 0.5N HCl aq., and extracted with ethyl acetate. The organic layer was washed with DW, brine, and then dried over $MgSO_4$. After removal of a solid by filtration, the filtrate was evaporated and then purified by column chromatography on SiO_2 (ethyl acetate : CH_2Cl_2 = 2 : 1) to give an acid (7.56 g) as a white solid at 88% yield. ^{1}H NMR (300 MHz, $CDCl_3$) δ / ppm 7.39-7.27 (5H, m), 7.07 (2H, d, *J* = 6.3 Hz), 6.87 (2H, d, *J* = 8.1 Hz), 5.05 (2H, s), 4.94 (1H, d, *J* = 8.1 Hz), 4.63 (2H, d, *J* = 2.4 Hz), 4.10 (2H, d, *J* = 8.4 Hz), 4.07-3.87 (1H, m), 2.76 (2H, t, *J* = 4.8 Hz), 2.70-2.51 (4H, br), 2.48 (1H, t, *J* = 2.1 Hz).

To a solution of the acid (3.93 g, 8.93 mmol) and 1-hydroxybenzotriazole (HOBT, 1.38 g, 9.02 mmol) in THF (53 mL) was added *N*,*N*-dicyclohexylcarbodiimide (DCC, 1.86 g, 9.02 mmol), the mixture was stirred for 24 hrs at room temperature. After removal of a solid by filtration, the filtrate was concentrated, dissolved into THF / acetone (3 : 1), and precipitated into cold hexane to give **6a** (4.37 g) as a white solid at 97% yield. ^{1}H NMR (300 MHz, $CDCl_3$) δ / ppm 8.31 (1H, d, *J* = 8.1 Hz), 7.97 (1H, d, *J* = 8.4 Hz), 7.69 (1H, t, *J* = 7.5 Hz), 7.53 (1H, t, *J* = 7.5 Hz), 7.36-7.27 (5H, m), 7.11 (2H, d, *J* = 8.1 Hz), 6.88 (2H, d, *J* = 8.4 Hz),

5.10 (2H, d, *J* = 8.4 Hz), 5.05 (1H, s), 4.65 (2H, d, *J* = 2.1 Hz), 4.26-3.93 (3H, m), 3.43 (2H, dd, *J* = 1.2, 12.6 Hz), 2.88-2.73 (4H, m), 2.52 (1H, t, *J* = 2.4 Hz).

*Preparation of **12***

A mixture of **13** (5.14 g, 13.99 mmol) and LiOH (1.34 g 55.96 mmol) was dissolved in THF / DW (1:1, 51 mL), and stirred for 22 hrs at room temperature, and then concentrated. The residue was dissolved in 0.5M $NaHCO_3$ aq, and extracted with ethyl acetate. The organic layer was dried over $MgSO_4$. The crude product was purified by reprecipitation from CH_2Cl_2/hexane to give **12** (4.46 g) as a white solid at 90% yield. ^{1}H NMR (300 MHz, DMSO-d_6) δ / ppm 7.39-7.26 (5H, m), 7.06 (2H, d, *J* = 7.8 Hz), 6.78 (2H, d, *J* = 9 Hz), 4.94 (2H, dd, *J* = 12.6, 12.9 Hz), 4.70 (2H, d, *J* = 2.4 Hz), 3.52 (1H, t, *J* = 2.4 Hz), 3.05 (1H, d, *J* = 11.4 Hz), 2.81 (1H, dd, *J* = 6, 21 Hz).

*Preparation of **6b***

To a solution of **12** (2.70 g, 8.09 mmol) and HOSu (0.93 g, 8.09 mmol) in THF (20 mL) was added a solution of DCC (1.67 g, 8.09 mmol), the mixture was stirred for 24 hrs at room temperature. The reaction mixture was cooled, filtered, and the filtrate was precipitated into cold hexane to give **6b** (3.19 g) as a white solid at 87% yield. ^{1}H NMR (300 MHz, $CDCl_3$) δ /

ppm 7.41-7.28 (5H, m), 7.19 (2H, d, *J* = 8.7 Hz), 6.90 (2H, d, *J* = 9 Hz), 5.10 (2H, d, *J* = 6.9 Hz), 5.06-4.95 (1H, m) 4.66 (2H, d, *J* = 2.4 Hz), 4.62-4.48 (1H, br), 3.31-3.13 (2H, m), 2.85 (4H, s), 2.51 (1H, t, *J* = 2.4 Hz).

Preparation of ***14***[17]

To a solution of pentaerythritol ethoxylate (2.01 g, 2.54 mmol) and Et_3N (1.34 mL, 10.26 mmol) in CH_2Cl_2 (20 mL) was added *p*-toluenesulfonyl chloride (TsCl, 1.96 g, 10.26 mmol), and the mixture was stirred for 48 hrs at room temperature, and then 1N HCl aq. or water was added. The organic layer was separated, and dried over $MgSO_4$. Chromatographic separation on SiO_2 (MeOH/CH_2Cl_2 = 1:9) gave **14** (2.91 g) as a colorless oil at 78% yield. ^{1}H NMR (300 MHz, $CDCl_3$) δ / ppm 7.79 (8H, *J* = 8.1 Hz). 7.34 (8H, d, *J* = 8.1 Hz), 4.15 (8H, t, *J* = 4.8 Hz), 3.68 (8H, t, *J* = 4.8 Hz), 3.65-3.32 (68H, m), 2.44 (12H, s).

Preparation of ***8***[17]

A mixture of **14** (9.00 g, 6.36 mmol), NaN_3 (3.31 g, 50.9 mmol), and EtOH (120 mL) was refluxed for 18 hrs. After removal of a solid by filtration, the filtrate was evaporated, and dissolved in CH_2Cl_2. The solution was washed with water, and dried over $MgSO_4$. The organic layer was dried to give **8** (4.35 g) as a colorless oil at 76% yield. ^{1}H NMR (300 MHz,

$CDCl_3$) δ / ppm 3.66-3.36 (76H, m), 3.34 (8H, t, *J* = 4.8 Hz); ^{13}C NMR (75 MHz, $CDCl_3$) δ/ppm 77.1, 77.0, 96.9, 76.4, 57.1

Preparation of ***16***[16]

To a solution of tetraethylene glycol (12.40 g, 61.98 mmol) and Et_3N (34.6 mL, 247.92 mmol) in CH_2Cl_2 (300 mL) was added TsCl (47.26 g, 247.92 mmol), and the mixture was stirred for 5 hrs at room temperature, and then DW was added. The organic layer was separated, and dried over $MgSO_4$. Chromatographic separation on SiO_2 (MeOH/CH_2Cl_2 = 5:95) gave **16** (22.53 g) as a colorless oil at 87% yield. ^1H NMR (300 MHz, $CDCl_3$) δ / ppm 7.78 (4H, d, *J* = 8.4 Hz), 7.34 (4H, d, *J* = 8.1 Hz), 4.15 (4H, t, *J* = 4.2 Hz), 3.66 (4H, t, *J* = 5.1 Hz), 3.55 (8H, s), 2.43 (6H, s); ^{13}C NMR (75 MHz, $CDCl_3$) δ/ppm 145, 133.1, 130, 128.1, 70.8, 69.5, 68.8, 21.8.

Preparation of ***15***[16]

A mixture of **16** (13.99 g, 27.83 mmol), potassium phthalimide (30.93 g, 166.98 mmol), and DMF (280 mL) was stirred at 60 °C for 6 hrs, and the solvent was removed by evaporation. The residue was dissolved in CH_2Cl_2, washed with 0.5N $NaHCO_3$ aq., DW and brine, and dried over $MgSO_4$. The organic layer was concentrated and purified by column

chromatography ($MeOH/CH_2Cl_2$ = 5:95) to give **15** (11.45 g) as a colorless oil at 90% yield. ^1H NMR (300 MHz, $CDCl_3$) δ / ppm 7.80 (4H, dd, *J* = 2.4, 8.7 Hz), 7.67 (4H, dd, *J* = 2.7, 8.4 Hz), 3.84 (4H, t, *J* = 6 Hz), 3.67 (4H, t, *J* = 6.3 Hz), 3.51 (8H, m); ^{13}C NMR (75 MHz, $CDCl_3$) δ/ppm 168.5, 134.6, 132.5, 123.9, 70.9, 70.4, 68.2, 37.6.

Preparation of ***7***[16]

A mixture of **15** (4.00 g, 8.84 mmol), hydrazine hydrate (9.28 g, 88.4 mmol), and EtOH (200 mL) was refluxed for 12 hrs, and concentrated. The resiue was dissolved in CH_2Cl_2, the resulting precipitates were removed by filtration. The filtrate was extracted with DW and concentrated to give **7** (1.55 g) as a curde oil at 91% yield. ^1H NMR (300 MHz, D_2O) δ / ppm 3.52 (8H, s), 3.39 (4H, t, *J* = 5.4 Hz), 2.61 (4H, t, *J* = 5.4 Hz); ^{13}C NMR (75 MHz, $CDCl_3$) δ/ppm 72.7, 69.9, 69.6, 41.1.

Preparation of pseudopolyrotaxanes $\boldsymbol{9}_{3k}{}^{9}{}_{/20k}$

A mixture of α-CD (17.00 mmol), $PEG\text{-}BA_{3k/20k}$ (0.47 mmol for 3k and 0.075mmol for 20k), and water ([α-CD] = 149 mM) was stirred for 24 hrs at room temperature. The resulting precipitates were collected by centrifugation, and washed with water, and then freeze-dried to give pseudopolyrotaxanes $\boldsymbol{9}_{3k/20k}$ as a white solid at 91% yield for 3k and 79% yield for 20k.

The ratio of α-CD to PEG-$BA_{3k/20k}$ (*l*) in $\mathbf{9}_{3k/20k}$ was determined to be 33 / 166 by ^{1}H NMR measured in D_2O containing 1wt% NaOD.

A typical spectral data is as follows ($\mathbf{9}_{3k}$); ^{1}H NMR (300 MHz, D_2O, signal for H_2O was set as 4.7 ppm) δ / ppm 4.90 (198H, d, *J* = 3.3 Hz), 3.89-3.63 (792H, m), 3.58 (272H, s), 3.50-3.35 (396H, m).

*General procedure for the preparation of precursor polyrotaxanes **1'-4'***

A mixture of pseudopolyrotaxane $\mathbf{9}_{3k/20k}$ (0.31 mmol), **5**/**6** (6.2 mmol), and DMF ([**9**] = 10 mM for 3k and 1.5 mM for 20k) was stirred at room temperature for 3 days. The suspension was collected by centrifugation, and washed with DMF and acetone. The resulting solid was dissolved in DMSO, and the solution was added to water adjusted to a pH of 3.2 to give a solid. The solid was dialyzed in water (pH 3.2) for 3 days, and the resulting solid was collected by centrifugation, and freeze-dried to give polyrotaxanes **1'-4'** as a white solid at 36-54% yield. The number of α-CD molecules (*m*) in the polyrotaxane was determined by ^{1}H NMR measured in D_2O containing 1wt% NaOD.

A typical spectral data is as follows ($\mathbf{1a'}_{3k}$); ^{1}H NMR (300 MHz, D_2O containing 1wt% NaOD, signal for H_2O was set as 4.7 ppm) δ / ppm 7.36-7.26 (10H, m), 7.15 (4H, d, *J* = 7.8

Hz), 6.87 (4H, d, *J* = 7.8 Hz), 4.82 (108H, d, *J* = 3 Hz), 3.84-3.62 (432H, m), 3.55 (272H, s), 3.42-3.25 (216H, m).

*General procedure for the preparation of polyrotaxanes **1-4***

To a solution of polyrotaxane **1'-4'** (0.10 mmol) in pyridine ([**1'**/**2'**] = 2 mM and [**3'**/**4'**] = 0.37 mM) was added succinic anhydride (18 equiv. of α-CD), the mixture was stirred at room temperature for 24 hrs, and then poured into diethylether to give a solid. The solid was collected by filtration, and then dialyzed in water (pH 3.2) for 3days. The resulting solid was collected by centrifugation, and freeze-dried to give polyrotaxanes **1**-**4** as a white solid in 68-87% yield. The number of carboxyl groups (*x*) appended to an α-CD molecule was determined by ^{1}H NMR measured in D_2O containing 1wt% NaOD.

A typical spectral data is as follows (**1a**$_{3k}$); ^{1}H NMR δ / ppm (300 MHz, D_2O containing 1wt% NaOD, signal for H_2O was set as 4.7 ppm) 7.34-7.24 (10H, m), 7.17 (4H, d, *J* = 9 Hz), 6.90 (4H, d, *J* = 9 Hz), 4.86 (108H, d, *J* = 3 Hz), 3.87-3.65 (432H, m), 3.56 (272H, s), 3.46-3.51 (216H, m), 2.26 (432H, s).

*Preparation of hydrogels **IA**$_{3k}$, **IB**$_{3k}$ and **IIIA**$_{20k}$ for the internal crosslink*

To a 0.1M phosphate buffer solution (PBS) (pH 7.0, 11 mL for **1a**/**b** or 50 mL for **3a**) of **1a**/**b** (0.015 mmol) or **3a** (0.030 mmol) were added DMT-MM (2.16 mmol) and **7** (0.54 mmol). Portions of the mixture were poured into a Teflon mold (diameter / thickness 15 mm / 10 mm for a compressive stress-strain test; 10 mm / 5 mm for a degradation test), which was set in a shaking apparatus (60 rpm) with maintaining at 37 °C for 24 hrs. The resulting gel was rinsed by immersion in DMSO and mixture of 0.1M PBS (pH 7.0) for periods of 2 and 5 days, respectively. The time when the purification was completed is defined as t = 0 in the degradation. The dry weight of a hydrogel was measured after dialysis in acidic water (pH 3.2) for 2 days to remove salts.

Preparation of hydrogels ***IIA***$_{3k}$, ***IIB***$_{3k}$ *and* ***IVA***$_{20k}$ *for the terminal crosslink*

To a 0.1M PBS (pH 7.0) of **2a**/**b** (0.015 mmol) or **4a** (0.015 mmol) (11 mL for **2a**/**b** or 50 mL for **4a**) were added a solution of **8** (0.0075 mmol) in DMSO (0.06 mL for **2a**/**b** or **4a**) and a 0.1M PBS (pH 7.0) of $CuSO_4 \cdot 5H_2O$ (0.012 mmol) and ascorbic acid (0.012 mmol) (0.3 mL for **2a**/**b** or **4a**) in a Teflon mold (diameter / thickness 15 mm / 10 mm for a compressive stress-strain test; 10 mm / 5 mm for a degradation test). The mixture was set in a shaking apparatus (60 rpm) with maintaining at 37 °C for 24 hrs. The resulting gel was rinsed by immersion in DMSO and 0.1M PBS (pH 7.0) for periods of 1 and 5 days, respectively. The

time when the purification was completed is defined as $t = 0$ in the degradation test and cell adhesion test. The dry weight of a hydrogel was measured after dialysis in acidic water (pH 3.2) for 2 days to remove salts.

3-2-3. Measurement

3-2-3-1. Water content

The pre-weight (W_d) dry hydrogels were immersed into a 0.1M PBS (pH 7.0) and left to reach equilibrium swelling for 48hrs at 37 °C. The swollen hydrogels were removed from PBS, whipped with filter paper gently, and weighted as soon as possible (W_s). Water content (%) was defined according to the following equation: Water content (%) = $(W_s - W_d) / W_s \times 100$, where W_d and W_s represent the dry and swollen mass of samples.

3-2-3-2. Static contact angle using air-bubble (in wet condition)[42]

Contact angles (θ) were measured by using the static captive bubble method. Hydrogels (t=0) attached to slide-glass were inverted in the pure water at a room temperature. Air bubble was injected (5-10 $\mu\ell$) from a syringe onto the hydrogels surface water. At least 10

measurement of bubble were averaged to obtain angle (θ') on the surface of hydrogels. Contact angles were calculated by 180 - θ'.

3-2-3-3. Compression test

The mechanical property of the hydrogels was characterized in terms of a compressive stress-strain measurement through a uni-axial and unconfined compression test using Microload System (R & B Co. Ltd., Daejeon, Korea). The unconfined compression test was performed in a 0.1 M PBS (pH 7.0) at 37 ℃ to maintain the sample hydration. Prior to the compression test, the samples were preconditioned for 20 cycles at 3% strain, put in the fluid bath, and then loaded by an upper jig fitted with a 1 kg load cell. After confirming their full swelling, the samples were compressed at a rate of 1 mm/min until their fracture. Load - displacement data were recorded at 2 Hz and converted into the strain-stress curves.

3-2-3-4. Stress relaxation test

IB$_{3k}$ and **IIB**$_{3k}$ were immersed in 0.1M PBS (pH 7.0) in a chamber at 37℃ and cyclic compressive load at a rate of 3% strain / sec (20 times) applied as precondition. After samples swelled fully in buffer, compressive load applied at a rate of 100% strain / min and held at 10, 20, 30 and 40%.

3-2-3-5. Curve fitting of stress relaxation curve [41]

The governing standard linear solid (SLS) equation is displayed in equation (1) and solved for the case of a constant strain ε_0, yielding a mathematical description of stress relaxation. In order to adjust model descriptors to experiment data (time-stress curve), Equation (4) was calculated.

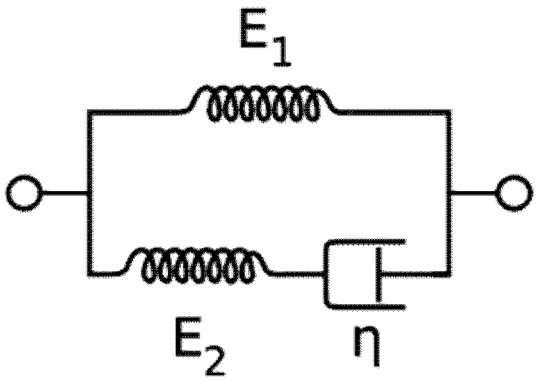

Standard linear solid (SLS) model

$$\frac{d\sigma}{dt}+\frac{1}{\tau}\sigma=\left[E_1+E_2\right]\frac{d\varepsilon}{dt}+\frac{E_1}{\tau}\varepsilon \qquad (1)$$

$$\frac{\sigma(t)}{\varepsilon_0}=G(t)=E_1+E_2e^{-t/\tau} \qquad (2)$$

$$\sigma(t)=\varepsilon_0E_1+\varepsilon_0E_2e^{-t/\tau} \qquad (3)$$

$$\sigma(t)=A+Be^{-t/\tau} \qquad (4)$$

$$\tau=\frac{\eta}{E_2}$$

where A, B, τ are constant determined by suing experimental data. Experimental data were used to determine constant A, B, and Ű from equation (4). Linear regression was performed using SPSS to generate model function for each sample. High Pearsonôs correlation ($R > 0.95$) between the modeled responses and experimental data supports the choice of viscoelastic theory and particularly the SLS model to describe stress relaxation behavior.

3-2-3-6. Changes in mass and storage modules upon degradation

Degradation of the hydrogels was examined at 37 °C in a 0.1M PBS (pH 7.0). The samples were immersed into a 50 mL of PBS, which was renewed every two weeks. Degrading samples were harvested, freeze-dried for 2 days, and then weighed (M_d). Harvested samples were gently wiped with tissue paper to remove attached water droplet and weighed (W_s). Mass loss (%) was defined according to the following equation:

$$\text{Mass loss (\%)} = [1 - (M_0 - M_d) / M_0] \times 100$$

where M_o and M_d represent the dry mass of the samples before and after the degradation test, respectively.

The storage modulus of the hydrogels was determined through a dynamic viscoelastic measurement using Rheosol-G3000 (UBM Co., Ltd, Kyoto, Japan) with parallel plate

geometry. The samples were fully swollen in a 0.1 M PBS (pH 7.0) at 37 °C and subjected to a condition of frequency sweep with the range of 0.07-10 Hz at 37 °C.

3-2-3-7. Quantification of the amount of fibronectin adhered on the hydrogel

Three hydrogel samples were immersed in a 0.1M PBS (pH 7.4) at room temperature for 3 hrs after the duration time was 0, 2 or 4 weeks for **IIA**$_{3k}$ and **IIB**$_{3k}$, and 0, 3 or 7 days for **IVA**$_{20k}$. After the 3-hour-immersion, each sample was then immersed in a human fibronectin (FN) solution (5 μg/mL in PBS, Sigma-aldrich, Inc., MO, USA) at 37 °C for 1 hr to coat, and which was gently washed with PBS. The FN-coated hydrogels were further immersed in 1% SDS solution and sonicated for 30 minutes to detach excess of FN on the surface of FN-coated gels. The quantity of FN adhered on each surface of the hydrogels was determined using a Micro BCA^{TM} protein assay kit (Thermo Fisher Scientific Inc., Waltham, MA, USA) by a spectrophotometer (570 nm) (Multiskan FC, Thermo Fisher Scientific Inc., Waltham, MA, USA).

3-2-3-8. Quantification of the amount and size of cells adhered on the hydrogel

Three types of hydrogels (**IIA**$_{3k.}$, **IIB**$_{3k}$ and **IVA**$_{20k}$) were immersed in a serum-free Dulbeccoûs modified Eagleûs medium (DMEM) containing penicillin and streptomycin at

room temperature for 3 hrs as pre-wetting when the duration time was 0, 2 or 4 weeks for **IIA**$_{3k}$ and **IIB**$_{3k}$, and 0, 3 or 7 days for **IVA**$_{20k}$. After the immersion, each sample was then immersed in a FN solution (5 μg/mL/ in PBS) at 37 °C for 1 hr to be coated, and which was placed into a stainless steel ring to prevent loss of cells during cell seeding. NIH 3T3 cells were seeded on upper side of the hydrogels at a density of 1.1×10^5 cells/cm^2 and cultivated in DMEM containing 10% fetal bovine serum (FBS) for 12 hrs under a humidified 5% CO_2 atmosphere at 37 °C. After removing the medium, cells on the hydrogel surface were stained with Cell-TrackerÊ Green fluorescent probe (Molecular Probes, Inc., Oregon, USA) in the serum-free medium at 37 °C for 45 minutes, and then loosely adherent cells were removed by washing with PBS. Cells were fixed with 3.7% formaldehyde in PBS. Cell morphology on hydrogels was visualized and imaged by an Olympus FluoViewÊ FV1000 confocal scanning laser microscope (Olympus Optical, Tokyo, Japan). The number and size of cells were quantified by using Image J software (National Institutes of Health, Maryland, USA) from the image of confocal microscope.

3-3. Results and discussion

3-3-1. Design and preparation of ester-containing polyrotaxanes 1-4 for gelation

Preparation of degradable polyrotaxane hydrogels consists of the following three parts: preparation of precursor polyrotaxanes (**1'-4'**), solubilization of **1'-4'** in water (**1-4**), and gelation of **1-4** (**I-IV**). The precursor polyrotaxanes **1a'**[9] and **2a'** were successfully prepared by endcapping of a pseudpolyrotaxane (α-CD$_l$·PEGBA **9**$_{3k}$ (l = 33)) with ester-containing capping molecules **5a** and **6a**, respectively (Scheme 2), because preinstalled ester linkages in the main chain undergo undesired hydrolysis during preparation of intermediates[9] and caused very difficulty to prepare pure polyrotaxanes well and very low yield.[18,19] The ester-containing capping molecules **5a** and **6a** were derived from Z-phenylalanine for the *internal* crosslink and Z-tyrosine for the *terminal* crosslink, respectively (Scheme 2), according to our previous report.[9] The precursor polyrotaxanes **1a'** and **2a'** were characterized by gel permeation chromatography (Figure 2) and NMR spectroscopy (Figure 3), showing that **1a'** and **2a'** were purified enough to determine the number of α-CD in the polyrotaxane (m = 18 for **1a'** and **2a'**). The precursor polyrotaxanes **1a'** and **2a'** were so insoluble in water[20-25] that a carboxylic residue was attached to α-CD in **1a'** and **2a'** to attain water solubility (x = 108 for

1a and **2a**). The *internal* crosslink utilized the carboxyl group in a condensation reaction of **1a** with a ditopic amine **7** upon galation of **1a** to give a hydrogel $\mathbf{IA}_{3k}$ (Scheme 3). The *terminal* crosslink was achieved through a 1,3-dipolar addition reaction[26,27] between an alkyne tethered to the tyrosine in **2a** and a tetratopic azide **8** upon gelation of **2a** to give a hydrogel $\mathbf{IIA}_{3k}$ (Scheme 3). Reference polyrotaxanes **1b** and **2b**, which do not have any ester linkages in the main chain, were prepared using similar end-capping reactions of α-$CD_l \cdot \mathbf{9}_{3k}$ (l = 33) with ester-not-containing capping molecules **5b** and **6b**, and were crosslinked to give hydrogels $\mathbf{IB}_{3k}$ (*internal*) and $\mathbf{IIB}_{3k}$ (*terminal*), respectively (Scheme 2). Degradable polyrotaxanes with higher molecular weight **3a** and **4a** (average n = 454, m = 88, x = 528 for **3a** and **4a**) were also obtained by the similar method employing a pseudopolyrotaxane (see supporting information) α-CD_l·PEGBA $\mathbf{9}_{20k}$ (l = 166) and capping molecules **5a** and **6a**, and were crosslinked to give hydrogels $\mathbf{IIIA}_{20k}$ (*internal*) and $\mathbf{IVA}_{20k}$ (*terminal*) (Scheme 3).

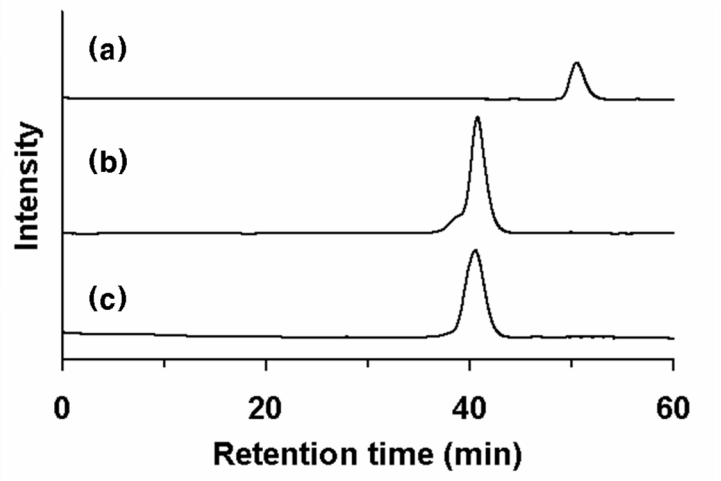

Figure 2. GPC profiles of (a) $\mathbf{9}_{3k}$, (b) $\mathbf{1a}'_{3k}$, and (c) $\mathbf{1b}'_{3k}$, eluted with DMSO containing 0.1M $NaNO_3$ with 0.3mL/min flow rate at 313K, detected by RI. (Column : TSKgel G-5000HHR + TSKgel G-3000HHR).

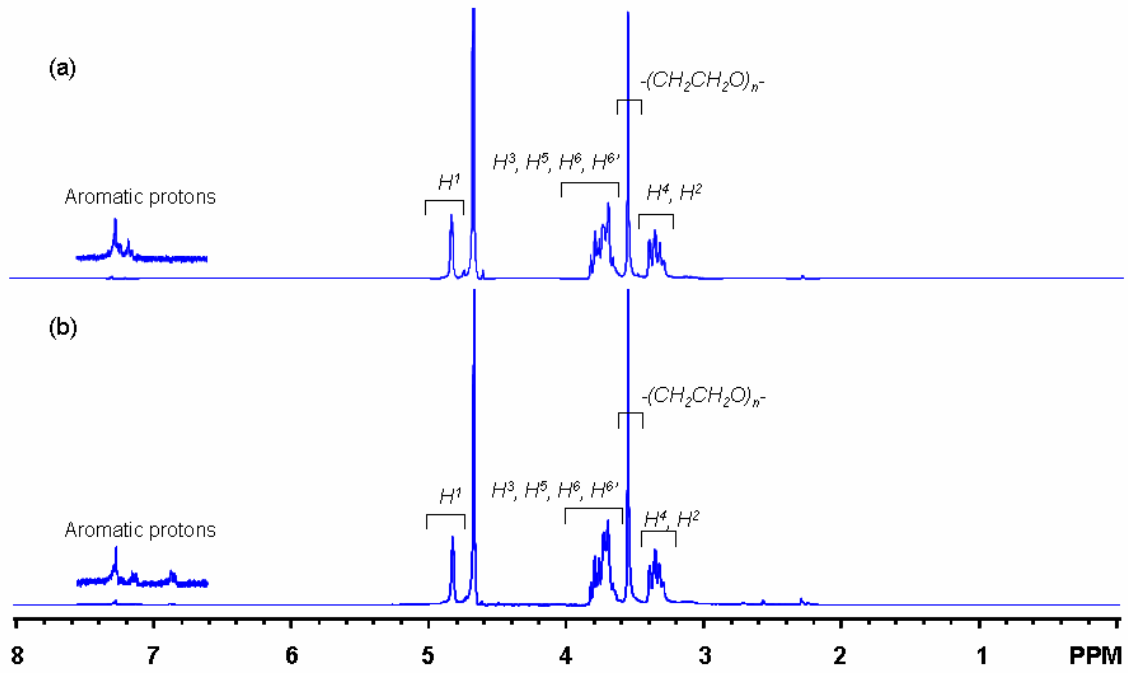

Figure 3. ^{1}H NMR spectra (300MHz) (a) $\mathbf{1a}'_{3k}$, and (b) $\mathbf{2a}'_{3k}$ measured in D_2O containing 1wt% NaOD.

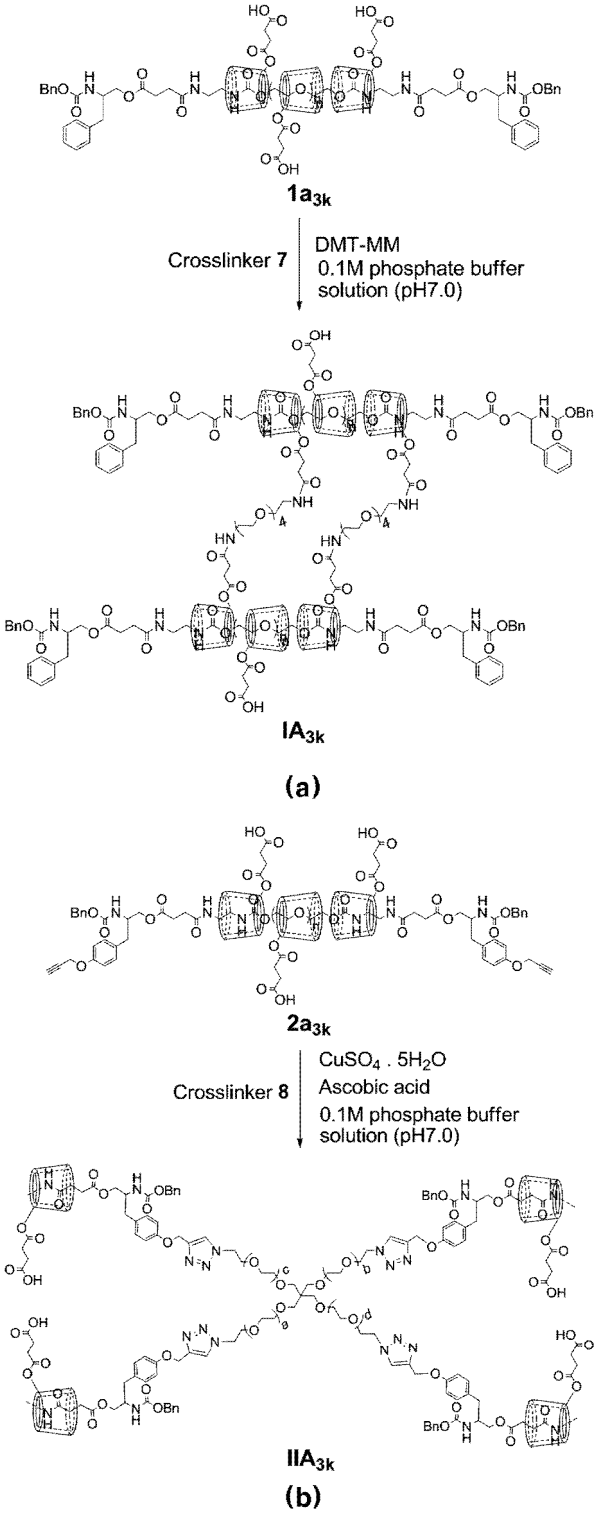

Scheme 3. Gelation of polyrotaxanes, (a) the *internal* crosslink and (b) the *terminal* crosslink.

3-3-2. Design and preparation of degradable hydrogels I-IV

The *internal* crosslink was carried out for gelation of **1** through a condensation reaction with the ditopic amine **7** in PBS adjusted to a pH of 7. Although we know the ester linkages in these polyrotaxanes are more stable against the hydrolysis in lower-pH-solutions,[9] in such solutions the carboxylic residue did not act as the solubilizing group due to neutralization and the amine decreased reactivity due to protonation. Four equivalents of the amine to one molecule of α-CD in **1** were aimed to crosslink the polyrotaxanes intermolecularly, and 73/82% weight of the total amount of **1a**/**b** and **7** was found in a solid obtained by drying after purification. For the polyrotaxane **3** with higher molecular weight, the similar treatment resulted in a hydrogel that gave a solid with 74% weight of the total amount of **3** and **7** by drying after purification. Crosslink reactions at the terminals of **2** or **4** with the tetratopic azide **8** were also performed in PBS adjusted to pH 7, in which equi-molar amounts of the alkyne and azide groups were feed, and gave hydrogels (81/87% weight for **2a**/**b** and **8**, and 76% weight for **4** and **8** in respective solids after purification and drying). Details of gelation conditions are summarized in Table 1.

Water contents and contact angle of hydrogels were summarized in Table 2. Hydrogel **I-IV** composed of water-soluble polyrotaxane showed very high water content (> 90%). Water

content of hydrogel **II** was superior to that of hydrogel **I** and hydrogel **III** and **IV** composed of PEGBA 20K as back bone chain also showed higher water content than that of **I** and **II** composed of PEGBA 3K. These results represent that low crosslink density by means of long back bone chain or fewer crosslink points formed large cavity in gel network, in which could absorb more water in gel network.

We measured static contact angle utilizing air-bubble because surface of hydrogel absorbs drop-water easily. Contact angles of hydrogel **I-IV** was 21 - 43° and this results represented that surface of polyrotaxane hydrogel **I-IV** had hydrophilicity, in which might have an good influence on adhesion of cell and protein on hydrogel surface.

Table 1**.** Gelation conditions.

Hydrogel	PRx		Crosslinker		$CuSO_4 \cdot 5H_2O$ Ascorbic acid	DMT-MM	0.1M phosphate buffer
	Comp.	Eq. mol	Comp.	Eq. mol	Eq. mol	Eq. mol	mM
IA_{3k}	**$1a_{3k}$**	1	**7**	36		144	1.36
IB_{3k}	**$1b_{3k}$**	1	**7**	36		144	1.36
IIA_{3k}	**$2a_{3k}$**	1	**8**	0.5	0.8		1.36
IIB_{3k}	**$2b_{3k}$**	1	**8**	0.5	0.8		1.36
$IIIA_{20k}$	**$3a_{20k}$**	1	**7**	176		704	0.3
IVA_{20k}	**$4a_{20k}$**	1	**8**	0.5	0.8		0.3

Table 2**.** Water content and static contact angle.

Hydrogels	Water content (%)	Contact angle (°)
IA_{3k}	90	32
IB_{3k}	92	43
IIA_{3k}	95	21
IIB_{3k}	95	34
$IIIA_{20k}$	96	36
IVA_{20k}	97	20

3-3-3. Mechanical properties of degradable hydrogels I-IV

We carried out compressive test and stress relaxation test in order to observe mechanical stability and viscoelastic characteristics of hydrogels **I-IV**. Different cross-linking system allowed outstanding different mechanical properties.

Comparing the profiles of compressive stress-strain curves for the *internally*-crosslinked hydrogels $\mathbf{IA}_{3k}$ and $\mathbf{IB}_{3k}$ indicated that degradation of $\mathbf{IA}_{3k}$ had already proceeded to some extent during the purification (Figure 4). This was also the case for the *terminally*-crosslinked hydrogels $\mathbf{IIA}_{3k}$ and $\mathbf{IIB}_{3k}$ (Figure 4). Degradation of the hydrogel $\mathbf{IA}_{3k}$ with the *internal* crosslink would be triggered by dual cleavage of two ester linkages embedded in the main chain and the residual succinic moiety at α-CD (Figure 1). The hydrogel $\mathbf{IIA}_{3k}$ with the *terminal* crosslink would degrade only by cleavage of the ester linkage in the main chain, and the residual ester groups in **2a** would have no responsibility for the degradation at all (Figure 1). *Internally*-crosslinked hydrogels $\mathbf{IA}_{3k}$, $\mathbf{IB}_{3k}$ and $\mathbf{IIIA}_{\mathbf{20k}}$ showed higher ultimate compressive stress and initial modulus than those of *terminally*-crosslinked hydrogels $\mathbf{IIA}_{3k}$ $\mathbf{IIB}_{3k}$ and $\mathbf{IVA}_{\mathbf{20k}}$**.** On the contrary to this, ultimate strain of *terminally*-crosslinked hydrogels was superior to *internally*-crosslinked hydrogels (Figure 4 and Table 3). These results represented that dense gel network in *internally*-crosslinked hydrogel allowed higher

mechanical stability and reduced flexibility of gel structure comparing with the *terminally*-crosslinked hydrogels.

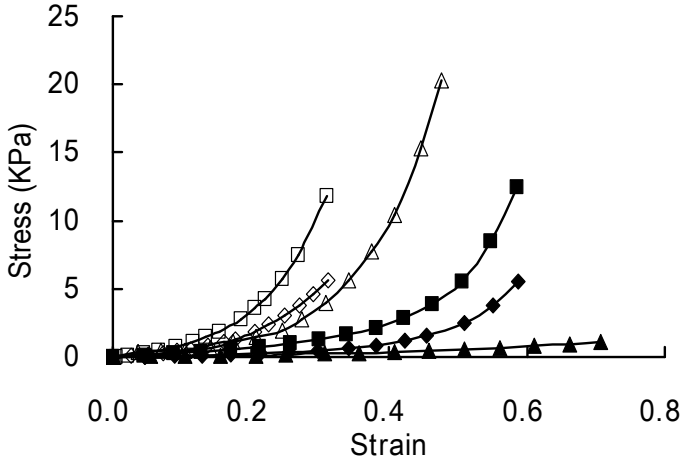

Figure 4. Stress - strain curves of *internal* crosslink hydrogels and *terminal* crosslink hydrogels. ◇ : **IA_{3k}**, □ : **IB_{3k}**, △ : **$IIIA_{20k}$**, ◆ : **IIA_{3k}**, ■ : **IIB_{3k}**, ▼ : **IVA_{20k}**

Table 3. Results of compressive test.

	Ultimate compressive strain	Ultimate compressive stress (kPa)	Initial modulus (kPa)	Modulus before fracture (kPa)
IA_{3k}	0.30±0.01	5.77±0.17	4.60±0.42	46.40±3.56
IB_{3k}	0.31±0.01	11.69±0.56	8.58±1.02	89.78±10.73
IIA_{3k}	0.57±0.04	5.23±0.39	0.79±0.19	36.20±5.04
IIB_{3k}	0.57±0.01	10.97±0.29	2.34±0.59	90.26±5.64
$IIIA_{20k}$	0.49±0.01	21.79±1.31	4.70±0.76	182.81±12.22
IVA_{20k}	0.70±0.03	1.18±0.04	0.69±0.09	3.82±0.29

Results of stress relaxation of hydrogel I-IV were represented to Figure 5 and Table 4. In stress relaxation test, *internally*-crosslinked hydrogel showed very unique phenomenon. Equilibrium stress of *internally*-crosslinked hydrogel was lower that of *terminally*-crosslinked hydrogels although instantaneous stress of *internally*-crosslinked hydrogels was higher than that of *terminally*-crosslinked hydrogel. Relative relaxation and relaxation time of *internally*-crosslinked hydrogel were higher and faster than those of *terminally*-crosslinked hydrogel, respectively. This phenomenon represents that network structure of *internally*-crosslinked hydrogel could reduce stress transferred to inside via polymer chain. This unique viscoelastic behavior was very similar to that of topological gel reported by Kohzo Ito and his co-works.[12,13,15] Topological gel composed of PEG chain with large molecular weigh and α-CD was topologically interlocked by figure-of-eight cross-links. These cross-links could be movable on the back bone chain freely to equalize the tension of the threaded polymer chains like pulleys. Therefore, stress might be equalized in the gel.[15] The fast relaxation time of *internally*-crosslinked hydrogel might result from equalization of internal stress via movable crosslink point in gel network.

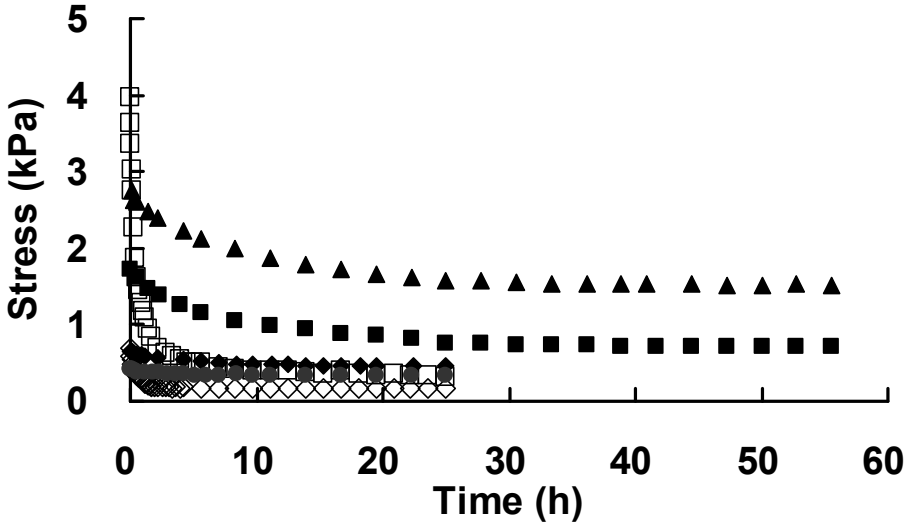

Figure 5. Stress relaxation curves of **IB$_{3k}$** and **IIB$_{3k}$** at various strain. ◇ : **IB$_{3k}$** (10%), □ : **IB$_{3k}$** (20%), ● : **IIB$_{3k}$** (10%),◆ : **IIB$_{3k}$** (20%), ■ : **IIB$_{3k}$** (30%), ▼ : **IIB$_{3k}$** (40%).

Table 4. Stress relaxation of **IA_{3k}** - **IVA_{20k}**.

	Strain (%)	Instantaneous stress (kPa)	Equilibrium stress (kPa)	Relaxed stress (kPa)	Relative relaxation (%)	Relaxation time (h) *
IA_{3k}	10	0.84	0.37	0.47	56	1.3
	20	2.08	0.57	1.51	72	1.7
IIA_{3k}	10	0.23	0.17	0.07	29	4.4
	20	0.40	0.24	0.16	39	10.8
	30	0.68	0.35	0.33	49	14.0
	40	1.28	0.79	0.49	38	23.9
IB_{3k}	10	0.69	0.17	0.51	75	3.6
	20	3.98	0.40	3.57	90	10.3
IIB_{3k}	10	0.43	0.34	0.09	20	11.4
	20	0.65	0.46	0.19	30	24.4
	30	1.72	0.72	1.00	58	40.0
	40	2.76	1.53	1.24	45	40.3
$IIIA_{20k}$	10	-	-	-	-	-
	20	0.55	0.40	0.15	27	9.4
	30	3.15	0.33	2.82	90	22.7
	40	8.94	0.38	8.57	96	28.1
IVA_{20k}	-	-	-	-	-	-

* Calculated by SLS equation (1)

3-3-4. Degradation behavior of hydrogels I-IV

Degradation was investigated by monitoring changes in mass and storage modulus of the hydrogels immersed in a 0.1M PBS at 37 °C. Hydrogels **IIB**$_{3k}$, which have no ester linkages in the back bone chain but have a number of ester linkages in the residue of the polyrotaxanes, showed 30% mass loss due to cleavage of the residual esters (Figure 6). During the 30% mass loss, the *terminally*-crosslinked **IIB**$_{3k}$ had maintained the storage modulus (~10^3 Pa), while the storage modulus for the *internally*-crosslinked **IB**$_{3k}$ was reduced gradually (Figure 7) because gel network was cleaved by cleavage of crosslink point connected with CDs in polyrotaxane. Interesting point is that both hydrogels maintained good water content (>90%) even though the polyrotaxanes lost the water-solubilizing group on CD. We found a remarkable difference in the rate of degradation for the *internal* (**IA**$_{3k}$ and **IIIA**$_{20k}$) and *terminal* (**IIA**$_{3k}$ and **IVA**$_{20k}$) systems. The former showed a relatively rapid mass loss (50% loss, t = 5 and 7 days for **IA**$_{3k}$ and **IIIA**$_{20k}$) and the latter showed a gradual mass loss over a longer period (50% loss, t = 26 and 12 days for **IIA**$_{3k}$ and **IVA**$_{20k}$) (Figure 6). Continuous monitoring of the storage modulus of the hydrogels **IA**$_{3k}$, **IIA**$_{3k}$, **IIIA**$_{20k}$, and **IVA**$_{20k}$ showed gradual decreases for both systems. In the *internal*-crosslink system, relatively larger amounts of α-CD and cross-linker molecules feed in a gelation reaction of the polyrotaxane and the

crosslinker led to higher storage modulus for **IIIA**$_{20k}$ than for **IA**$_{3k}$ over the duration (Table 1 and Figure 7). In the *terminal*-crosslink system, a relatively lower ratio of the terminals in a polyrotaxane allowed the storage modulus of **IVA**$_{20k}$ to reach faster <10 Pa than **IIA**$_{3k}$ (35 days for **IIA**$_{3k}$ and 21 days for **IVA**$_{20k}$) (Table 1 and Figure 7). Differences in erosion should come from the crosslinking method. The longer period of erosion for the *terminally*-crosslinked gels would be suitable for a preliminary cell adhesion test, described below.

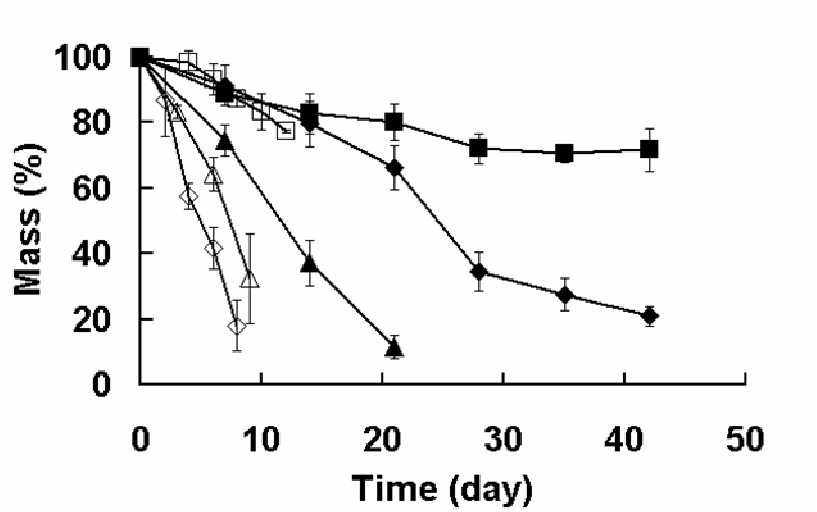

Figure 6. Changes in mass of hydrogels **IA**$_{3k}$ (◇), **IB**$_{3k}$ (Ǐ), **IIA**$_{3k}$ (◆), **IIB**$_{3k}$ (ƴ), **IIIA**$_{20k}$ (△), and **IVA**$_{20k}$ (ƶ).

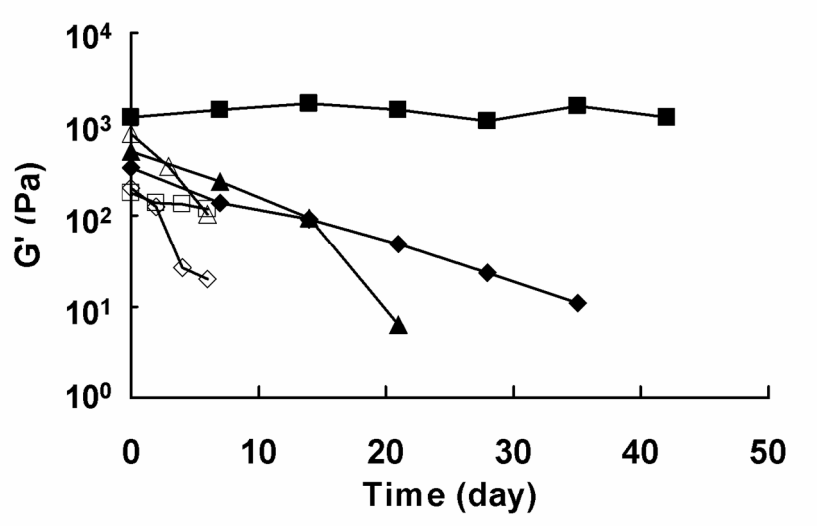

Figure 7. Changes in storage modulus of hydrogels **IA**$_{3k}$ (◇), **IB**$_{3k}$ (Ǐ), **IIA**$_{3k}$ (◆), **IIB**$_{3k}$ (y), **IIIA**$_{20k}$ (△), and **IVA**$_{20k}$ (z), measured at a frequency of 1 Hz.

3-3-5. Cell adhesion on hydrogels I-IV

Cell adhesion on a hydrogel surface is influenced by many factors, such as chemical and mechanical characteristics of a polymer surface,[28-30] cell adhesion proteins,[31-34] and so on. Some researchers have reported that mechanical stability and protein adhesion on a surface play important roles in cell adhesion at early stages of cell culture.[35-36] Fibronectin (FN), one component of extracellular matrices, is important for cell adhesion and growth by means of binding to integrin α5β1 via its cell binding domain.[32,33] A preliminary test for cell adhesion onto the *terminally*-crosslinked hydrogels **IIA**/**B**$_{3k}$ and **IVA**$_{20k}$ on degradation was carried out

using NHI3T3 cells in terms of the number, size, and morphology of adhered cells. Prior to seeding, we coated FN on surface of hydrogel and measured amount of adherent FN (Figure 8). Amount of FN adhered on **II**B_{3k} was higher than other hydrogels and amount of FN decreased and then increased at 14 and 28 days, respectively, while amount of FN adhered on **II**A_{3k} decreased. This result might imply that stability of hydrogel played an important role in protein adhesion on hydrogel surface. We also focused on increase of FN amount adhered on **II**B_{3k} at 28 days. Amount of FN on **II**B_{3k} increased at 28 days although mechanical stability of **II**B_{3k} did not change (Figure 7 and 8). Most of carboxyl residue in of **II**B_{3k} were cleaved at 28 days (Figure 6), in which might cause change of chemical condition of hydrogel surface and have influence on FN adhesion on hydrogels. Lee et al. reported that the ability of FN to enhance cellular attachment was dependent on the conditions of its adsorption to the surface with different functional group (OH, COOH, NH_2 and CH_3)[43], in which could explain the change of FN amount adhered on hydrogel **II** and **IV** due to chemical condition of surface.

Some researchers have reported that cell attachment and spreading depended on compatibility with surface and carboxylic acid groups on surface had a negative effect on cell adhesion.[37,38] In this research, we observed different cell morphology on each hydrogel during degradation. In **II**B_{3k}, cell spreading and increase of cell adhesion were observed continuously during degradation. We assumed that loss of carboxyl residue and stable substratum enhanced

cell adhesion and spreading. However, **IIA**$_{3k}$ and **IV**$_{20k}$ showed different phenomenon. Cell spreading and increase of cell adhesion in **IIA**$_{3k}$ at 14 days was observed, but spherical cell and decrease of cell number and size were observed at 28 days. This phenomenon explains that positive influence by means of loss of carboxyl residue and negative influence owing to collapse of hydrogel might affect cell adhesion and spreading in **IIA**$_{3k}$ at the same time. So that reason, in this cellular experiment, change of chemical characteristics by decreasing carboxyl residue upregulated cell biocompatibility on surface of hydrogels at early degradation. However, exceeding collapse of hydrogel structure by means of degradation had more negative influence on cell adhesion and spreading. As same reason, the cellular behavior on **IV**$_{20k}$, showing continuous decreasing cell adhesion and spherical cell morphology, also came from very fast degradation of hydrogels. This phenomenon implies that cell morphology adhered on polyrotaxane hydrogel was affected by two parameters, change of surface chemical condition by means of loss of carboxyl residue and mechanical stability of hydrogels at the same time (Figure 10).

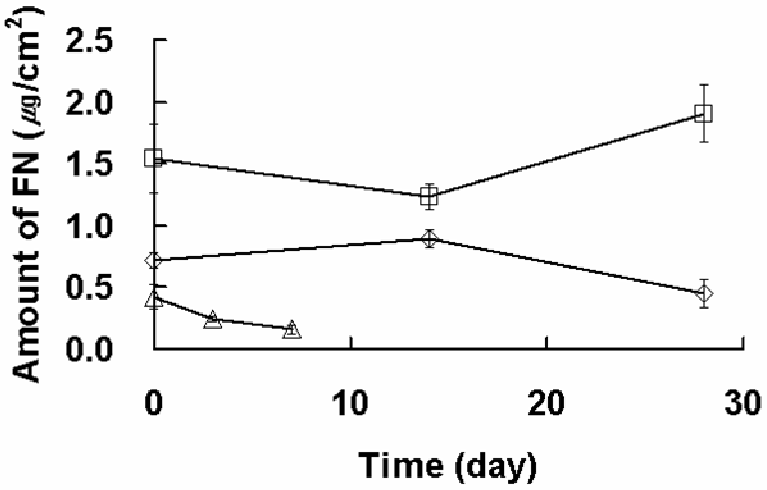

Figure 8. Amount of FN adhered on a surface of hydrogels **IIA**$_{3k}$ (◇), **IIB**$_{3k}$ (□), and **IVA**$_{20k}$ (△).

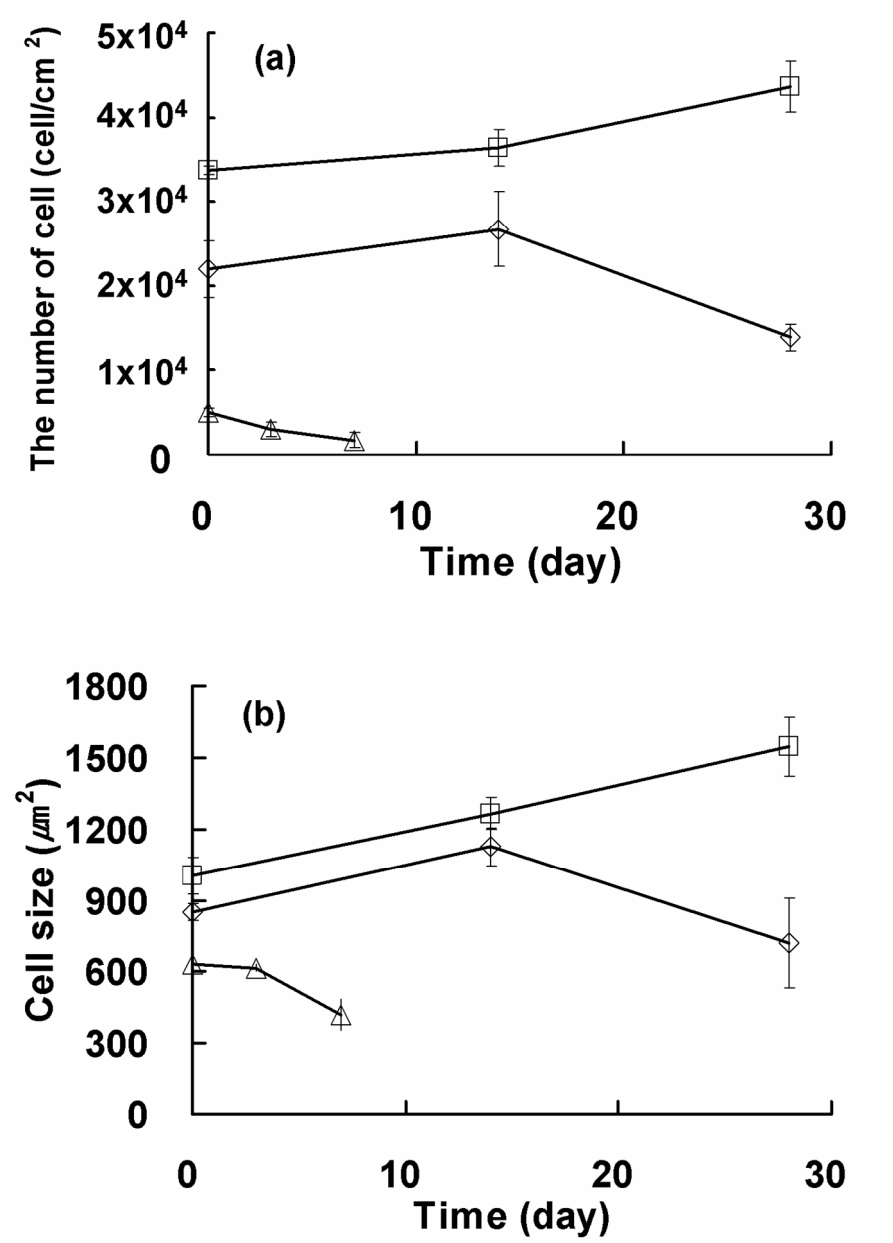

Figure 9**.** (a) Number and (b) size of adhered cells on a surface of FN-coated hydrogels **IIA**$_{3k}$ (◇), **IIB**$_{3k}$ (□), and **IVA**$_{20k}$ (△).

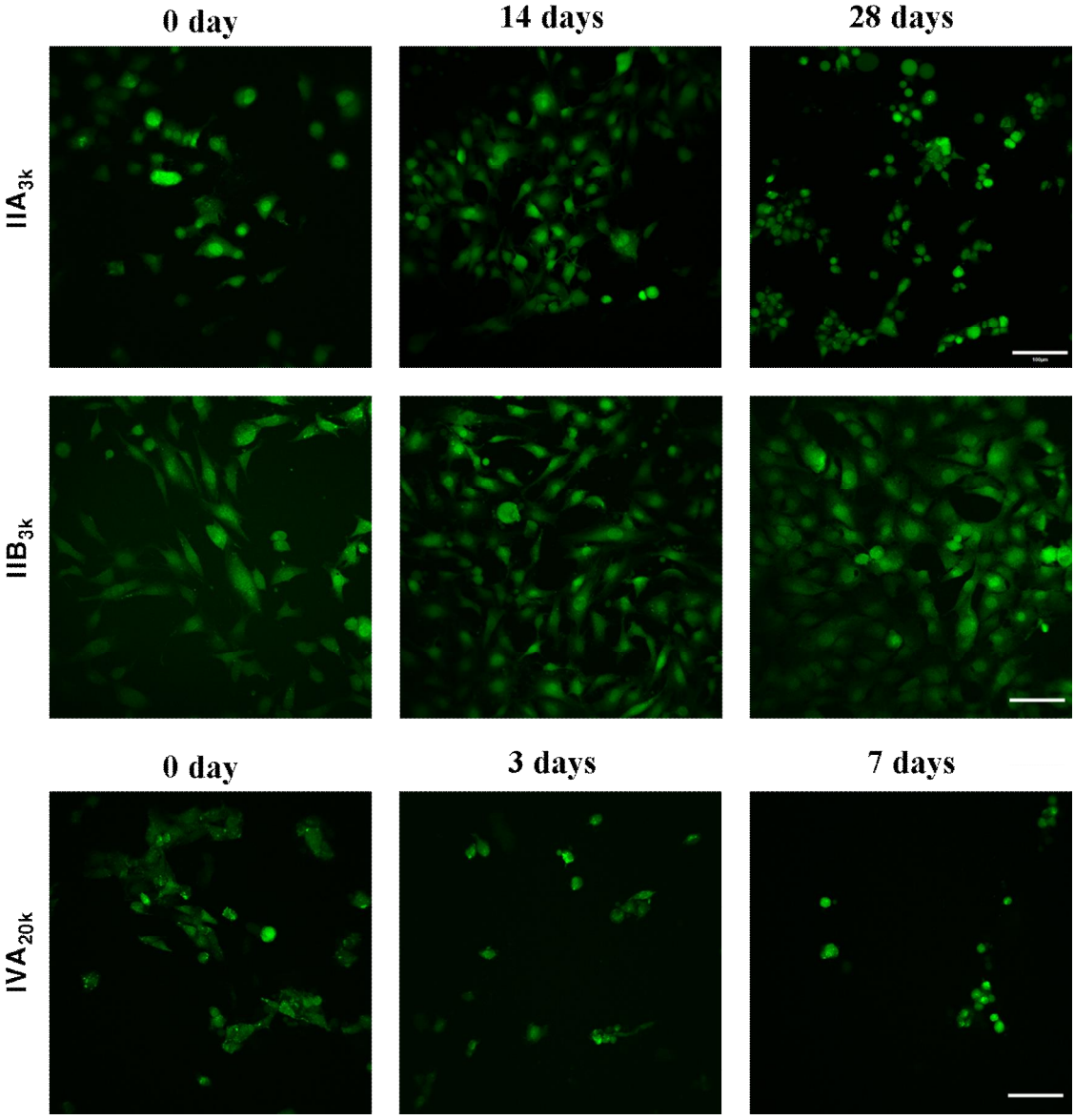

Figure 10. Confocal microscopy images of cells adhered on surface of hydrogels during degradation (scale bar : 100 ㎛).

3-4. Conclusion

We prepared series of polyrotaxanes containing ester linkages in the main chain to trigger the supramolecular dissociation in water by means of hydrolysis of the esters. A modified procedure successfully reduced a chance to cleave unfortunately such labile linkages in the course of preparation using an ester-free pseudopolyrotaxane and ester-containing capping molecules. Crosslinking of the hydrolyzable polyrotaxanes was carried out in two ways, one was a crosslinking between intermolecular cyclic components (*internal* crosslink) and the other was a crosslinking between the terminals of the polyrotaxanes (*terminal* crosslink). Hydrogel **I**-**IV** showed high water content (>90%) and hydrophilic surface. The *internally*-crosslinked gels had higher compressive stress and initial modulus, while the *terminally*-crosslinked gels showed higher ultimate strain. Viscoelastic behavior of *internally*-crosslinked hydrogels was very different from that of *terminally*-crosslinked hydrogels and similar to that of topological gel. The *terminally*-crosslinked hydrogels were more stable during degradation than the *internally*-crosslinked hydrogels in PBS. These degradations accompanied decrease in the storage modulus, and showed various degradation profiles, which were modulated by the crosslinking manners and molecular weights of the polyrotaxanes. A preliminary cell adhesion test using NIH3T3 cells onto the *terminally*-crosslinked hydrogels demonstrated

cellular responses by means of decrease in storage modulus and change of surface chemical characteristics of hydrogels. These results could provide a possibility to develop polyrotaxane-based hydrogel systems as biodegradable materials for tissue engineering, such as implantable scaffold and drug delivery system, since polyrotaxanes are allowed to be designed uniquely by modulating lots of structural parameters, such as various crosslinking methods, combinations of polyrotaxane component, and molecular weight of the backbone polymer.

Acknowledgments. We thank Professor Jung-woog Shin (Inje University, Gimhae, Korea) for his help and comments in the measurement of mechanical properties.

Reference

1. Langer, R.; Vacanti, J. P. *Science*, 1993, **260**, 920.

2. Passl, W. J. *Prog. Polym. Sci.*, 1989, **14**, 629.

3. Barrows, T. H. *Clin. Mater.*, 1986, **1**, 233.

4. Nuttelman, C. R.; Henry, S. M.; Anseth, K. S. *Biomaterials*, 2002, **23**, 3617.

5. Vainionpaa, S.; Rokkanen, P.; Tormala, P. *Prog. Polym. Sci.*, 1989, **14**, 69.

6. Nair, L. S.; Laurencin, C. T. *Prog. Polym. Sci*., 2007, **32**, 762.

7. Harada, A.; Li, J.; Kamachi, M. *Nature*, 1992, **356**, 325.

8. Wenz, G.; Han, B.; Müller, A. *Chem. Rev*., 2006, **106**, 782.

9. Katoono, R.; Fukuda, S.; Shin, H.; Yui, N. *Chem*. *Lett*., 2008, **37**, 988.

10. Ooya, T.; Yui, N. *J. Control. Release*., 1999, **58**, 251.

11. Arai, T.; Hayashi, M.; Takagi, N.; Takata, T. *Macromolecules*, 2009, **42**, 1881.

12. Araki, J.; Ito, K. *J. Polym. Sci.: Part A. Polym. Chem*., 2006, **44**, 6312.

13. Kakaoka, T.; Kidowaki, M.; Zhao, C.; Minamikawa, H.; Shimizu, T.; Ito, K. *J. Phys. Chem. B*, 2006, **110**, 24377.

14. Loethen, S.; Kim, J.; Thompson D. H. *Polym. Rev*., 2007,**47**, 383.

15. Okumura, Y.; Ito, K. *Adv. Mater.*, 2001, **13**, 485.

16. Numata, M.; Koumoto, K.; Mizu, M.; Sakurai, K.; Shinkai, S. *Org*. *Biomol*. *Chem*., 2005, **3**, 2255.

17. Kobayashi, Y.; Katoono, R.; Yamaguchi, M.; Yui, N. *Polym. J*., 2011, **43**, 893.

18. Watanabe, J.; Ooya, T.; Yui, N. *Chem*. *Lett*., 1998, 1031.

19. Watanabe, J.; Ooya, T.; Yui, N. *J. Biomater. Sci. Polym. Edn*., 1999, **10**, 1275.

20. Harada, A.; Kamachi, M. *Macromolecules*, 1990, **23**, 2821.

21. Harada, A.; Li, J.; Kamachi, M. *Macromolecules*, 1993, **26**, 5698.

22. Harada, A.; Kamachi, M. *J. Chem. Soc., Chem. Commun*., 1990, 1322.

23. Harada, A.; Okada, M.; Li, L.; Kamachi, M. *Macromolecules*, 1995, **28**, 8406.

24. Harada, A.; Li, J.; Suzuki, S.; Kamachi, M. *Macromolecules*, 1993, **26**, 5267.

25. Harada, A.; Li, J.; Kamachi, M. *Nature*, 1992, **356**, 325.

26. Rostovtsev, V. V.; Green, L. G.; Fokin, V. V.; Sharpless, K. B. *Angew. Chem. Int. Ed*., 2002, **41**, 2596.

27. Rodionov, V. O.; Fokin, V. V.; Finn, M. G. *Angew. Chem. Int. Ed*., 2005, **44**, 2210.

28. Keselowsky, B. G.; Collard, D. M.; Garcia, A. J. *J. Biomed. Mater. Res. A*, 2003, **66,** 247.

29. Engler, A. J.; Sen, S.; Sweeney, H. L.; Discher, D. E. *Cell*, 2006, **25**, 677.

30. Gunn, J. W.; Turner, S. D.; Mann, B. K. *J. Biomed. Mater. Res. A*, 2005, **72**, 91.

31. Boudreau, N. J.; Jones, P. L. *Biochem. J*., 1999, **339**, 481.

32. Wittmer, C. R.; Phelps, J. A.; Saltzman, W. M.; Vam Tassel, P. R. *Biomaterials*, 2007, **28**, 851.

33. Garcia, A. J.; Boettiger, D. *Biomaterials*, 1999, **20**, 2427.

34. Mao, Y.; Schwarzbauer, J. E. *Matrix Biol*., 2005, **24,** 389.

35. Schmedlen, R. H.; Masters, K. S.; West, J. L. *Biomaterials*, 2002, **23**, 4325.

36. Huang, S.; Ingber, D. E. *Nat. Cell Biol*., 1999, **1**, 131.

37. Lee, J. H.; Lee, J. W.; Khang, G.; Lee, H. B. *Biomaterials*, 1997, **18**, 351.

38. Ma, Z.; Gao, C.; Gong, Y.; Shen, J. *Biomaterials*, 2003, **24**, 3725.

39. Kunishima, M.; Kawachi, C.; Iwasaki, F.; Terao, K.; Tani, S. *Tetrahedron Lett*., 1999, **40**, 5327.

40. Kunishima, M.; Kawachi, C.; Morita, J.; Terao, K.; Iwasaki, F.; Tani, S. *Tetrahedron*, 1999, **55**, 13159.

41. Shazly, T. M.; Artzi, N.; Boehning, F,; Edelman, E. R. *Biomaterials*, 2008, **29**, 4584.

42. Dahlgren, C.; Elwing, H.; Magnusson, K.E. *Colloids Surf*., 1986, **17**, 295.

43. Lee, M.H.; Ducheyne, P.; Lynch, L.; Boetiger, D.; Composto R.J *Biomaterials,* 2006, **27**, 1907.

Chapter 4

Synthesis of Photo-degradable Polyamide Rotaxanes from Cinnamate Photodimer and α-Cyclodextrin

4 Synthesis of Photo-degradable Polyamide Rotaxanes from Cinnamate Photodimer and α-Cyclodextrin

4-1. Introduction

Molecular design to give rigidity to a polymer back bone is an important concept to increase the thermal stability of polymers, as many researchers have designed aromatic high-performance polymers.[1] Here, we introduced a unique chemical structure to give structural rigidity to a polymer back bone not by using an aromatic component, but a necklace-like structure. Supramolecules have been studied as promising candidates for the construction of novel molecular architectures. Polyrotaxanes, which can be visualized as a molecular necklace composed of a polymeric chain and cyclic compounds, are interesting in terms of their structural features.[2-4] Cyclic compounds in a polyrotaxane structure are allowed to slide and rotate along a polymeric chain since the components are mechanically interlocked each other. Stimuli-responsive polyrotaxanes permit the design of various novel and smart polymeric materials, such as biosensors[5], hydrogels[6], scaffolds for tissue engineering[7], and carriers for drug delivery release[8,9]. Moreover, some researchers have reported that a number

of CDs threaded onto the back bone enabled the regulation of thermo-mechanical performance by means of flexibility and crystalline structural changes.[10,11]

Cinnamic acid has been utilized as a photo-reactive monomer which showed photoreactions such as [2+2] cycloaddition[12] and *trans / cis* isomerization[13,14] to control the mechanical performance[15-17] and nanostructures[18] in the corresponding photo-polymers. Cinnamic acid formed a photodimer of truxillic acid after irradiation with ultraviolet (UV) light at a wavelength range above 260 nm, and the cyclobutane ring of truxillic acid is reversible to the original cinnamic acid under deep-UV light with a wavelength range below 260 nm.[12,19]

By utilizing the unique concept described above, we designed aliphatic-aromatic polyamides containing the rotaxane structure composed of 4,4'-diacetoamido-α-truxillic acid, poly(ethylene glycol) bisamine (PEGBA) and methylated-α-cyclodextrin (Me-α-CD). We focused on observing the thermo-mechanical performance of these new polyamides and their degradation behavior via the photocleavage of 4,4'-diacetoamido-α-truxillic acid under UV irradiation.

4-2. Experimental section

4-2-1. Materials

4-aminocinnamic acid (4-ACA) as photo-monomer was purchased from Tokyo Chemical Industry Co., Ltd. (Tokyo, Japan). Poly (ethylene glycol) bis (3-aminopropyl) terminated (PEGBA, molecular weight 1500) and anhydrous dimethylformamide (DMF) were purchased from Sigma-Aldrich Inc. (MI, USA). α-cyclodextrin (α-CD) was purchased from Wako Pure Chemicals Industries Ltd. (Osaka. Japan). Sodium hydride and iodomethane for preparation of Me-α-CD were purchased from Tokyo Chemical Industry Co. Ltd. (Tokyo, Japan). Triphenylphosphite (TPP) and anhydrous pyridine as condensation agents were purchased from Junsei Chemical Co., Ltd. (Tokyo, Japan) and Wako Pure Chemicals Industries Ltd. (Osaka. Japan). Anhydrous dimethylacetamide (DMAc), hexane, methanol, acetic anhydride, and dichloromethane were purchased from Kanto Chemical Co., Ltd. (Tokyo, Japan).

4. ***Synthesis of Photo-degradable Polyamide Rotaxanes from Cinnamate Photodimer and α-Cyclodextrin***

4-2-2. Synthesis of polymer

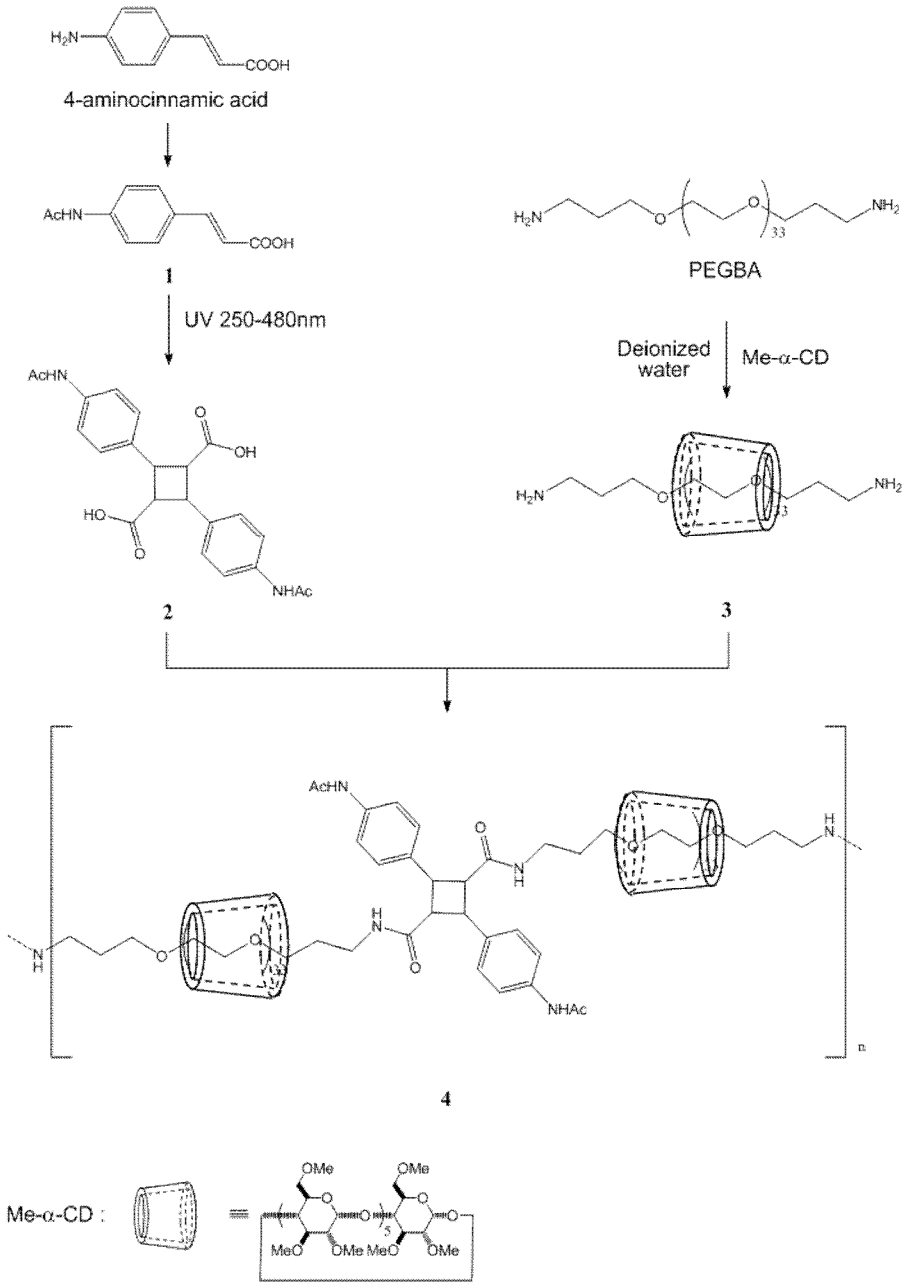

Scheme 1. Synthetic route of aliphatic-aromatic polyamides containing cyclodextrin

4. ***Synthesis of Photo-degradable Polyamide Rotaxanes from Cinnamate Photodimer and α-Cyclodextrin***

*Preparation of N-acetyl-4-aminocinnamic acid **1***

4-aminocinnamic acid (4-ACA; 2.47 g, 15.13 mmol) was dissolved in 30 ml of methanol, and acetic anhydride (5.40 g, 52.98 mmol) was then added dropwise with slow stirring under a nitrogen atmosphere at room temperature. After the complete addition of the acetic anhydride, the mixture was stirred for 23 hrs. The precipitate was filtered, washed with methanol, and then dried under reduced pressure to give **1** as a yellow powder at 79 % yield. ^{1}H NMR (400 MHz, DMSO-d_6) δ / ppm 12.63 - 12.02 (1H, br, s), 10.13 (1H, s), 7.61 (4H, s), 7.52 (1H, d, J = 16 Hz), 6.40 (1H, d, J = 16 Hz), 2.05 (3H, s); ^{13}C NMR (100 MHz, DMSO-d_6) δ / ppm 168, 167, 143, 141, 128, 118, 117, 24; MALDI-TOF $[M+Na]^+$ m / z : Calcd. for $C_{11}H_{11}NO_3Na$ 228.07, Found 228.0.

*Preparation of 4,4'-diacetoamido-α-truxillic acid **2***

The photochemical [2+2] cycloaddition of the cinnamoyl group in **1** was utilized to form the cyclobutane structure. **1** (1.00 g, 4.87 mmol) was dispersed in hexane (10 ml), and then the photoreaction was carried out with UV irradiation using a mercury lamp (250-480 nm, light intensity: 70 mW / cm^2)[13] with stirring for 24 hrs. After UV-irradiation, the product was washed with methanol, and then dried under reduced pressure to give **2** as a yellow powder at 95% yield. ^{1}H NMR (400 MHz, DMSO-d_6) δ / ppm 12.4 - 11.8 (2H, br, s), 9.91 (2H, s), 7.51

(4H, d, *J* = 8 Hz), 7.26 (4H, d, *J* = 8 Hz), 4.20 (2H, dd, *J* = 4, 20 Hz), 3.74 (2H, dd, *J* = 4, 20 Hz), 2.03 (6H, s); ^{13}C NMR (100 MHz, DMSO-d_6) δ / ppm 172, 168, 137, 133, 127, 118, 46, 40, 23; MALDI-TOF $[M+Na]^+$ m / z : Calcd. for $C_{22}H_{22}N_2O_6Na$ 433.14, Found 433.2.

Preparation of methylated α-CD (Me-α-CD) [20-22]

α-CD (1.01 g, 1.03 mmol) in anhydrous DMF (40 ml) was treated with sodium hydride (0.62 g, 25.92 mmol, 1.4 equiv to the OH groups of CD) for 2 hrs under a nitrogen atmosphere at room temperature. Next, iodomethane (3.68 g, 25.92 mmol) was added dropwise to the solution with stirring for 24 hrs at room temperature. Methanol was then added to decompose the excess hydride, and the solvent was evaporated and dried under reduced pressure for 36 hrs. After washing with hexane, the product was dissolved in dichloromethane (100 ml), and then washed with deionized water, concentrated, and dried under reduced pressure. The crude product was purified by recrystallization in hexane. The residual oil in the product was removed by hexane and then dried to give Me-α-CD as a white powder at 43 % yield. ^{1}H NMR (400 MHz, DMSO-d_6) δ / ppm 4.95 (6H, d, *J* = 4 Hz), 3.80 - 3.68 (12H, m), 3.52 (6H, d, *J* = 9.6 Hz), 3.47 (18H, s), 3.41 (6H, t, *J* = 8.8 Hz), 3.36 (18H, s), 3.21 (18H, s), 3.01 (6H, dd, *J* = 12, 4 Hz); ^{13}C NMR (100 MHz, DMSO-d_6) δ / ppm 98, 81.7, 81.5, 81, 71, 70, 60, 58, 57; MALDI-TOF $[M+Na]^+$ m / z : Calcd. for $C_{54}H_{96}O_{30}Na$ 1247.59,

Found 1247.7.

Synthesis of ***4***

The inclusion complex (pseudopolyrotaxane) **3** of PEGBA and Me-α-CD was formed in deionized water at various molar compositions ([Me-α-CD] / [PEGBA] = 0, 1, 3, 6, 13). PEGBA and Me-α-CD were dissolved in deionized water (140 mg/mL) at 60 ℃ for 24 hrs, and then freeze-dried. **3** and **2** were dissolved in anhydrous dimethylacetamide (DMAc, 133mM) and then triphenylphosphite (TPP, 5 equimolar to PEGBA) and anhydrous pyridine (5 equimolar to PEGBA) as condensation agents[23] were added to the mother solution. The reaction mixtures ([Me-α-CD] / [PEGBA] = 0, 1, 3, 6, 13) were heated in an oil bath until 100 ℃ at a heating rate of 10 ℃ / 10 min under a nitrogen atmosphere with stirring for 1, 2, 3, 4 and 5 days, respectively. After cooling, DMSO (10 ml) was added into the reaction solution and then dialyzed with a dialysis membrane (MWCO: 25 kDa) in methanol for 5 days. The products were dried under reduced pressure at 80 ℃ for 24 hrs to give **4**. ^{1}H NMR (400 MHz, DMSO-d_6) δ / ppm 10.02 - 9.74 (2H, m), 7.66 (2H, s), 7.46 (4H, d *J* = 8.4), 7.14 (4H, d *J* = 8.4), 4.95 (0.82H, s). 4.16 (2H, t, *J* = 8.8 Hz), 3.66 (2H, t, *J* = 8.8 Hz), 3.61 - 3.38 (132H, m), 3.35 (2.46H, s), 3.32 (4H, t, *J* = 2.8 Hz), 3.22 (2.46H, s), 3.02 (4H, t, *J* = 5.6 Hz), 1.99 (6H, s), 1.22 (4H, s)

4-2-3. Measurement

^{1}H NMR and ^{13}C NMR spectra were recorded on a Burker DRX 500 NMR instrument (400.13 MHz for ^{1}H NMR) using DMSO-d_6 (internal reference 2.50 ppm) as a solvent at room temperature. The molecular weight of **4** was determined using gel permeation chromatography (Shodex GPC-101 with a connection column system of 803 and 807). The chromatogram was calibrated with polystyrene standards. Dimethylformamide was utilized as the eluent at a flow rate of 0.5 mL / min. The thermal properties were analyzed by differential scanning calorimetry (DSC; EXSTAR 6100, Seiko Instruments Inc.) and thermogravimetric analysis (TGA; SSC/5200 SII, Seiko Instruments Inc.). The DSC thermograms covered a temperature range from -100 to 250 ℃ at a scanning rate of 10 ℃ / min under a nitrogen atmosphere. The TGA was carried out at a heating rate of 10 ℃ / min under a nitrogen atmosphere.

4-2-4. UV degradation

4e dissolved in DMSO was irradiated with a UV lamp (light intensity: 2.5 mW / cm^2, λ = 254 nm; xenon light source, MAX-303, Asahi Spectra Inc.) in the open air for 6 days. The

degradation of **4e** with increasing UV exposure time was observed by ^{1}H NMR and GPC analysis.

4-3. Results and discussion

4-3-1. Synthesis and Characterization of Polyamides 4

The synthesis protocol for the aliphatic-aromatic polyamides is shown in Scheme 1. 4-aminocinnamic acid (4-ACA) was utilized as a base compound in order to prepare photodimer **2**. The amine group of 4-ACA was protected by acetic anhydride to inhibit side reactions during the polymerization. **2** was prepared by using photonic [2+2] cycloaddition between the vinylene groups of cinnamic acid via UV irradiation in the solid state. The [2+2] cycloaddition was confirmed by ^{1}H NMR analysis (Figure 1). The new signal from the cyclobutane ring was observed at 4.20 and 3.74 ppm, and the signal from the aromatic group in **1** was shifted from 7.61 ppm to 7.51 and 7.26 ppm. All of the hydroxyl groups in α-CD were methylated by iodomethane in order to prevent the reaction of the CD hydroxyls with the **2** carboxyls during the polyamide polymerization. In addition, the CD methylation should prevent hydrogen bonding between the hydroxyl groups in CD after rotaxanation. The

inter/intra-molecular interactions were enhanced by the structural effects of polyrotaxane to form crystalline complexes and to affect their thermo-mechanical properties.

Polymerizations of the photodimer **2** with diaminated pseudopolyrotaxane **3** were carried out via polyamide reactions using triphenylphosphite/pyridine as condensation agents. In this synthetic stage, we focused on controlling the CD composition in the inclusion complex and removing free Me-α-CDs liberating from the PEG backbone. In order to control the composition of the inclusion complex, polymerizations were performed while changing the CD concentration from 133 mM to 1.73 M in solvent, i.e. the amount of Me-α-CDs in **3** increased from 0.067 mmol to 0.871 mmol. As a result, we synthesized **4** with various CD compositions (Table 1). The structure of **4** was confirmed by NMR analyses. In the ^{1}H NMR spectrum, the signals from the PEG-BA, **2** and C (1) H in Me-α-CD were detected, and the molar ratio of each component was summarized in Table 1. The signal from the amide bond between PEG-BA and **2** also appeared at 7.66 ppm.

4. ***Synthesis of Photo-degradable Polyamide Rotaxanes from Cinnamate Photodimer and α-Cyclodextrin***

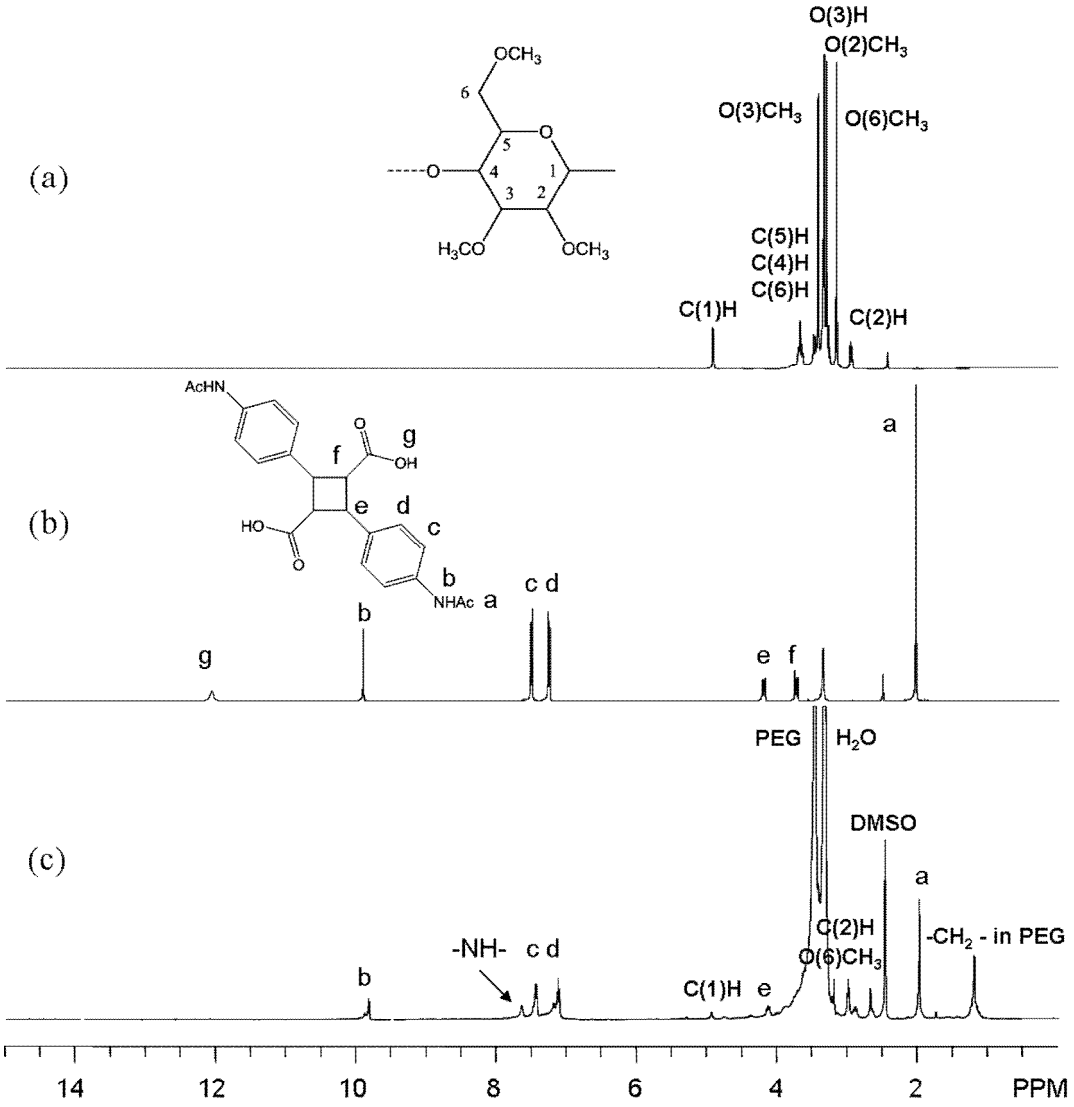

Figure 1. ^{1}H NMR spectra of: (a) Me-α-CD, (b) **2**, and (c) **4** (400 MHz, DMDO-d_6)

4. ***Synthesis of Photo-degradable Polyamide Rotaxanes from Cinnamate Photodimer and α-Cyclodextrin***

Table1. Basic characterization of aliphatic-aromatic polyamide 4 containing cyclodextrin

Name	Molar composition [Me-α-CD] / [PEGBA]		M_w [b] (g / mol)	PI	Yield (%) [c]
	Feed	Found [a]			
4a	0	0 (-)	2.64×10^4	1.21	42
4b	1	0.018 (1.8%)	2.82×10^4	1.18	46
4c	3	0.030 (1.0%)	1.91×10^4	1.21	49
4d	6	0.064 (1.1%)	1.97×10^4	1.18	31
4e	13	0.137 (1.1%)	1.74×10^4	1.18	47

[a] Determined by ^{1}H NMR analysis. The rotaxanation degree of CD to the amount of CD used in the feed is shown in parenthesis; [b] Determined by GPC analysis; [c] Based on the amount of PEGBA and **2**

4. Synthesis of Photo-degradable Polyamide Rotaxanes from Cinnamate Photodimer and α-Cyclodextrin

The rotaxanation and purification were also confirmed by GPC, in which just one peak around an elution time of 37-38 min for **4a** and **4e** was observed (Figure 2). A mixture of **4a** and Me-α-CD whose composition was adjusted to be the same as **4e** was applied to the GPC in order to confirm the removal of the Me-α-CD from **4e**. Chromatogram (a) showed two independent peaks around 37.0 and 44.5 min. Since the peaks at 37.0 min were clearly assigned to polyamide **4a**, since the shape and elution time were almost the same as the peak in chromatogram (b), the other peak at 44.5 nm could be assigned to the Me-α-CD. As shown in Figure 2, chromatogram (c) showed no signal assignable to free Me-α-CD. Chromatogram (c) showed no peak around 44.5 nm, indicating the removal of the free Me-α-CD to obtain the pure inclusion complex **4e**. When we tried to form the inclusion complex by a direct reaction of photodimer **2** with PEG-BA in the presence of Me-α-CD, the ^{1}H NMR spectrum of the resulting polymer showed a negligibly low signal for Me-α-CD. This result suggests that the accidental rotaxanation in DMAc barely occurred, and the very low rotaxanation degree ranging from 1.0-1.8 % shown in Table 1 means that the speed of CD dissociation from the PEG was much faster than the capping rate of **3** with **2**. As a consequence, these results indicated that the inclusion complex of Me-α-CD with the polyamide chain was successfully formed during the polymerization of **2** with **3**, and that the pure product could be isolated by the present method.

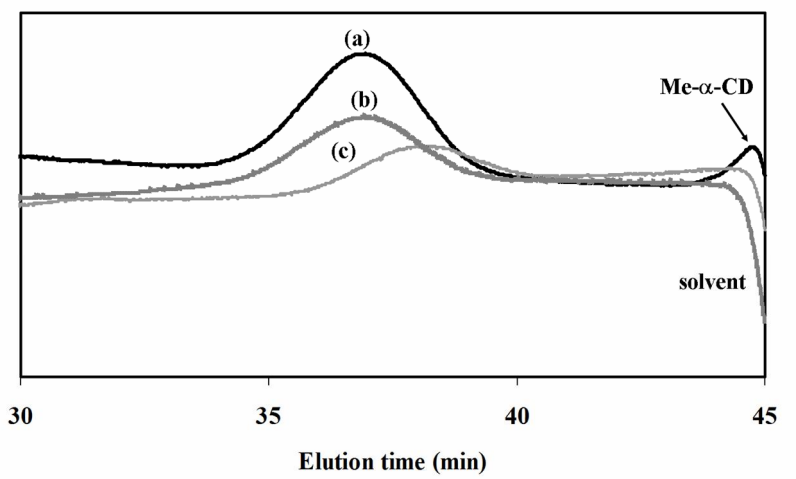

Figure 2. Representative GPC chromatograms of (a) a mixture of **4a** and Me-α-CD, (b) **4a**, and (c) **4e** (DMF, 0.5 mL/min, 40℃)

4-3-2. Thermal properties of 4

The thermo-mechanical performance of **4** was measured by DSC (Figure 3) and TGA (Figure 4) analyses. As depicted in Figure 3, the DSC curves of **4a** - **4e** displayed a similar curve pattern. The T_g of each polyamide was almost the same (-54℃). The T_m also showed no outstanding changes, although the T_c showed a slight increase and decrease (Table 2). Upon the increased amount of Me-α-CD threaded onto the back bone chain, the intensity of both the exothermic peak of crystallization and the endothermic peak of melting decreased with an increasing CD amount. This phenomenon means that the presence of CD made polymer

crystallization more difficult, presumably due to the location indeterminacy of the movable CD around the polyamide backbone.

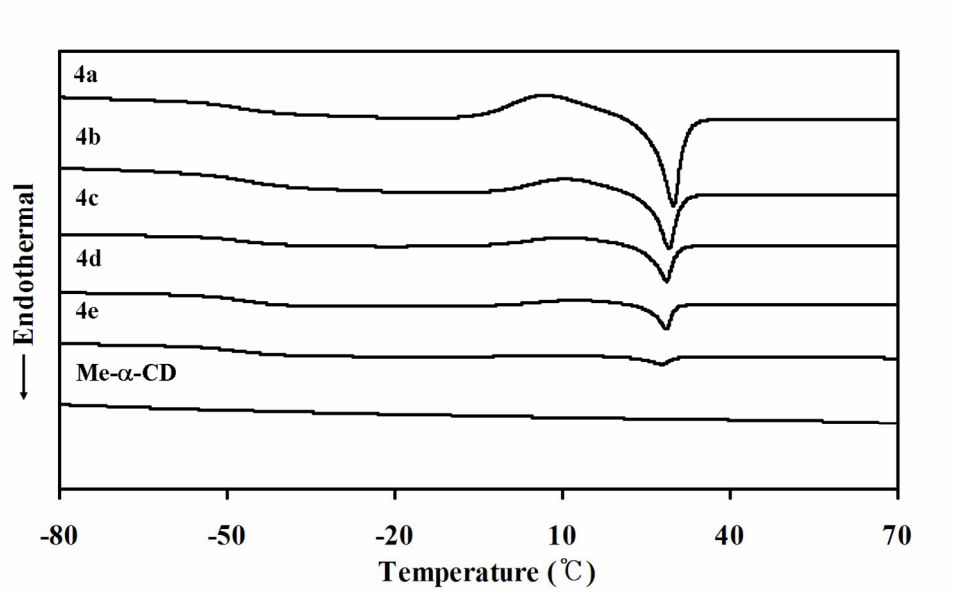

Figure 3. DSC curves of **4a** - **4e** and Me-α-CD

According to the literature[10,24], polyrotaxanes with a high threading ratio of α-CD underwent a two-step thermal decomposition process; the higher temperature ones corresponding to the axle chain as a central block and stopper, versus the lower temperature ones with the α-CDs threaded. However, polyamide **4** showed only a one-step thermal decomposition process as seen in the TGA curves of **4a** - **4e** (Figure 4), presumably due to the very low threading ratio of Me-α-CD in **4**. On the other hand, the T_{10} of **4a** - **4c** increased

gradually with an increase in the amount of CD in **4**, whereas the T_{10} of **4d** and **4e** decreased and approached the T_{10} of Me-α-CD. The T_{50} also showed a similar trend with the T_{10} (Table 2). As a result, the T_{10} of the polymer increased after the threading of a very small amount of CD (0.018 and 0.030) to the chain backbone, owing to the chains being rendered rigid by rotaxanation.

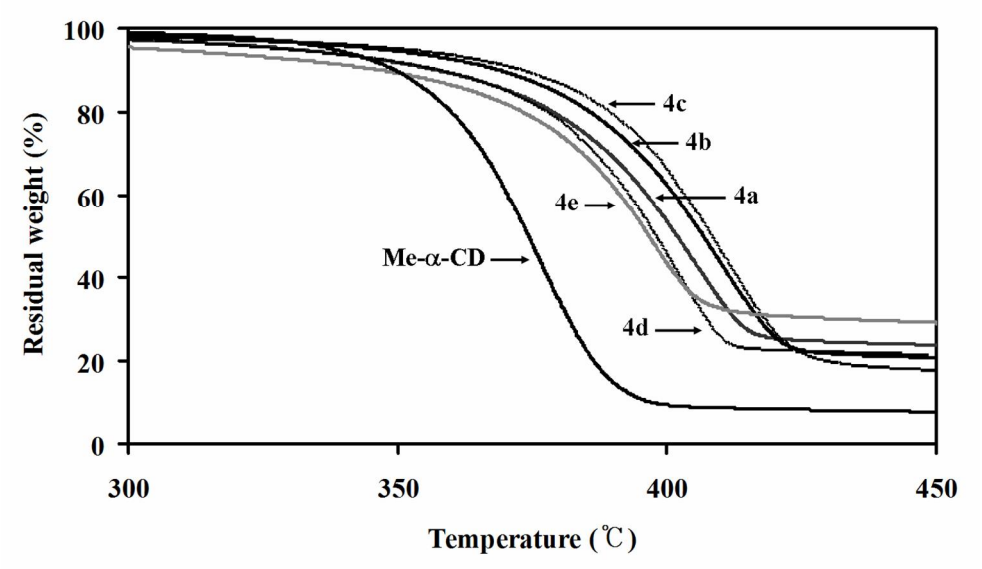

Figure 4. TGA curves of **4a** - **4e** and Me-α-CD

Table 2. DSC / TGA analysis of polyamides and Me-α-CD

Name	T_{10} /℃	T_{50} /℃	T_g /℃	T_c /℃ ($\triangle H_c$ /Jg^{-1})	T_m /℃ ($\triangle H_m$ /Jg^{-1})
4a	357	401	-54	7 (-20.2)	30 (19.2)
4b	367	406	-54	11 (-14.6)	29 (17.1)
4c	373	408	-54	12 (-10.8)	28 (10.1)
4d	356	398	-53	14 (-5.31)	26 (6.6)
4e	346	396	-54	9 (-1.92)	27 (2.18)
Me-α-CD	346	373	70	127	218

4-3-3. UV-degradation

Figure 5 depicts the changes of the ^{1}H NMR spectra of **4e** before and after UV irradiation. Yang et al. reported that the cyclobutane structure of α-truxillic acid dimethyl ester, which was formed by [2+2] cycloaddition with UV irradiation (λ > 260 nm), was photocleaved into two cinnamic acids by means of UV irradiation (λ < 260 nm).[19] We performed a photocleavage test of **4e** using a xenon-lamp (2.5 mW / cm^2) (Scheme 2). After illumination to the **4e** solution in DMSO (20 mg / mL) for 6 days, ^{1}H NMR and GPC analysis were carried

out to confirm the cleavage of **4e**. From the NMR analysis (Figure 5 (b)), two peaks at 6.50 and 7.35 ppm appeared after UV-irradiation for 6 days. The two peaks corresponded with those of the vinylene groups of 4-acetoamidocinnamamide conjugated with PEG-BA (Figure 5 (a)). At the same time, the integration intensity of the cyclobutane peak at 4.16 ppm decreased obviously. These results support the photocleavage of the cyclobutane ring of **4e** by UV-irradiation. The photocleavage of polyamide **4e** was also confirmed by GPC analysis (Figure 6). With an increasing time of UV exposure, the peak of **4e** was shifted to a higher elution time, and the molecular weight of **4e** also decreased from 1.74×10^4 to 5.28×10^3 g / mol.

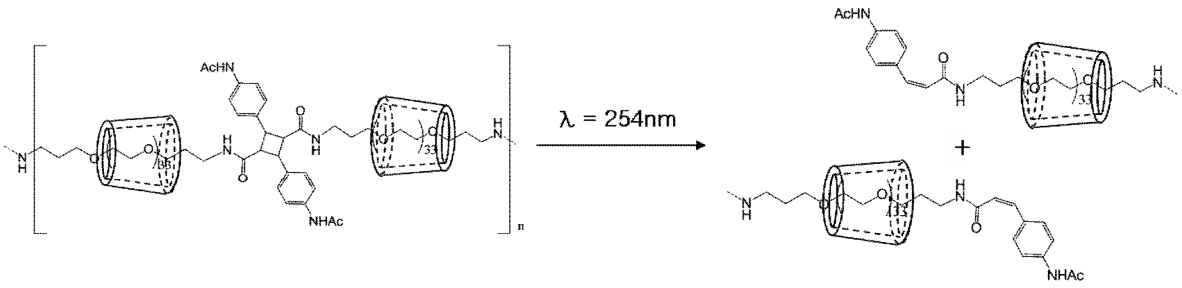

Scheme 2. Degradation of **4e** with UV exposure

4. ***Synthesis of Photo-degradable Polyamide Rotaxanes from Cinnamate Photodimer and α-Cyclodextrin***

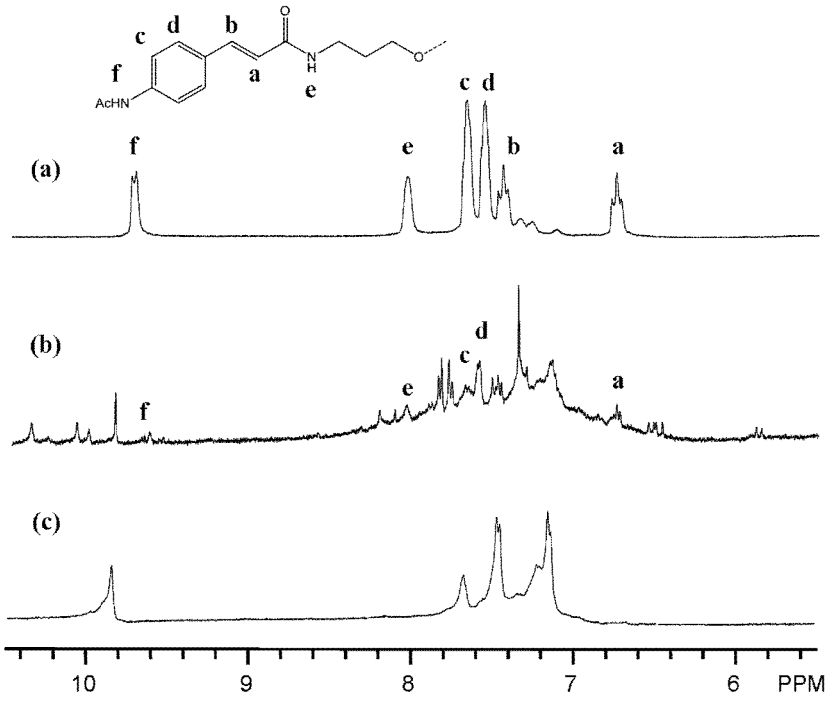

Figure 5. ^{1}H NMR spectra of: (a) 4-acetoamidocinnamamide conjugated with PEG-BA, (b) 4e after UV exposure for 6 days, and (c) **4e** (400 MHz, DMDO-d_6)

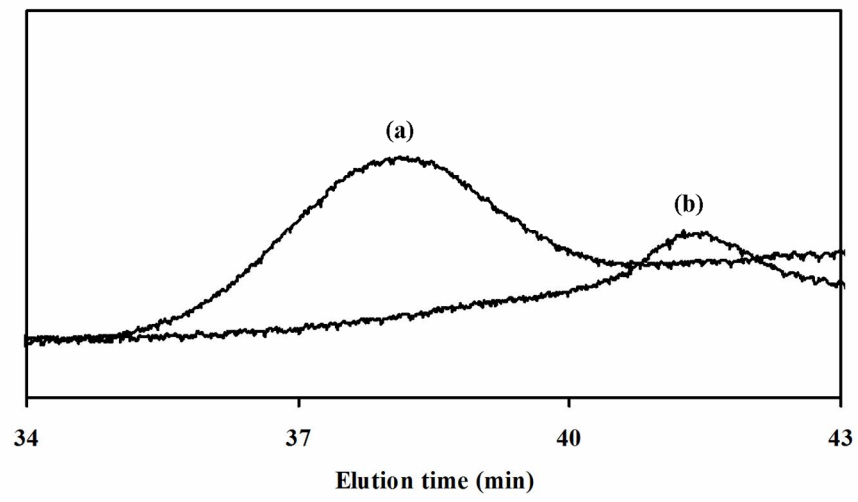

Figure 6. GPC chromatograms of **4e** (a) before and (b) after UV exposure for 6 days (DMF, 0.5 mL/min, 40℃)

4-4. Conclusion

Polyamide rotaxanes were prepared by a polycondensation of 4,4'-acetoamido-α-truxillic acid with diaminated pseudorotaxanes from an inclusion complex of polyethyleneglycol bisamine with methylated-α-cyclodextrin. The thermal degradation temperature of the polyamides was enhanced by inclusion complex formation with methylated-α-cyclodextrin, even when a very small amount of methylated-α-cyclodextrin was threaded into the polymer backbone. The polyamide polyrotaxane with methylated-α-cyclodextrin was degraded by UV-irradiation (λ < 260 nm) via the photocleavage of the cyclobutane ring in 4,4ô-diacetoamido-α-truxillic acid to 4-aminocinnamic acid.

Acknowledgement: The researches were financially supported by ALCA project (5100270) of JST.

4. ***Synthesis of Photo-degradable Polyamide Rotaxanes from Cinnamate Photodimer and α-Cyclodextrin***

Reference

1. Kaneko, T.; Tran, H.T.; Matsusaki, M.; Akashi, M. *Chem. Mater.*, 2006, **18**, 6220.

2. Harada, A.; Kamachi, M. *J. Chem. Soc. Chem. Commun.,* 1990, **19**, 1322.

3. Harada, A.; Li, J.; Kamachi, M. *Nature,* 1992, **356**, 325.

4. Wenz, G.; Han, B.H.; Müller, A. *Chem. Rev*., 2006, **106**, 782.

5. Ooya, T.; Eguchi, M.; Yui, N. *J. Am. Chem. Soc*., 2003, **125**, 13016.

6. Okumura, Y.; Ito, K. *Adv. Mater*., 2001, **13**, 485.

7. Lee, W.K.; Ichi, T.; Ooya, T.; Yamamoto, T.; Katoh, M.; Yui, N. *J. Biomed. Mater. Res. A*, 2003, **67**, 1087.

8. Yamashita, A.; Yui, N.; Ooya, T.; Kano, A.; Maruyama, A.; Akita, A.; Kogure, K.; Harashima, H. *Nat. Protoc.*, 2007, **1**, 2861.

9. Ooya, T.; Yui, *N. J. Control. Release*, 1999, **58**, 251.

10. Yamaguchi, I,; Miya, K.; Osakada, K.; Yamamoto, T. *Polym. Bull*., 2000, **44**, 247.

11. Tong, X.; Hou, D.; Zhang, X.; Ye, L.; Zhang, A.; Feng, Z. *Chinese J. Polym. Sci*., 2008, **26,** 723.

12. Lendlein, A.; Jiang, H.; Jünger, O.; Langer, R. *Nature*, 2005, **434**, 879.

13. Yasaki, K.; Suzuki, T.; Yazawa, K.; Kaneko, D.; Kaneko, T. *J. Polym. Sci. A1*, 2011, **48**,

1112.

14. Pattabiraman, M.; Kaanumalle, L.S.; Natarajan, A.; Ramamurthy, V. *Langmuir*, 2006, **22**, 7605.

15. Kaneko, T.; Thi, T.H.; Shi, D.J.; Akashi, M. *Nat. Mater*., 2006, **5**, 966.

16. Kaneko, T.; Kaneko, D.; Wang, S. *Plant Biotechnol*., 2010, **27**, 243.

17. Wang, S.; Tateyama, S.; Kaneko, D.; Ohki, S.; Kaneko, T. *Polym. Degrad. Stab.,* 2011, **96**, 2048.

18. Shi, D.J.; Matsuaski, M.; Kaneko, T.; Akashi, M. *Macromolecules,* 2008, **41**, 8167.

19. Yang, H.; Jia, L.; Wang, Z.; Di-Cicco, A.; Levy, D.; Keller, P. *Macromolecules*, 2011, **44**, 159.

20. Guieu, S.; Sollogoub, M. *J. Org. Chem*., 2008, **73**, 2819.

21. Takeo, K.; Mitoh, H.; Uemura, K. *Carbohydr. Res*., 1989, **187**, 203.

22. Arai, T.; Hayashi, M.; Takagi, N.; Takata, T. *Macromolecules*, 2009, **42**, 1881.

23. Yamashita, Y.; Chujo, Y.; Kobayashi, H.; Kawakami, Y. *Polym. Bull*., 1981, **5**, 361.

24. Tong, X.; Zhang, X.; Ye, L.; Zhang, A.; Feng, Z. *Soft Matter*., 2009, **5**, 1848.

General Conclusion

5 General Conclusion

Every chapter was summarized by described below.

In chapter 2, we demonstrated the design and preparation of the hydrolyzable polyrotaxane composed of an ester-containing PEG chain and α-CDs. The hydrolysis of polyrotaxane into its water-soluble components under aqueous conditions adjusted to both a basic and almost neutral pH was confirmed by monitoring continuous changes in transmittance and by GPC measurements of clear upper portions collected from suspensions.

In chapter 3, we prepared series of polyrotaxanes containing ester linkages in the main chain to trigger the supramolecular dissociation in water by means of hydrolysis of the esters. Crosslinking of the hydrolyzable polyrotaxanes was carried out in two ways, one was a crosslinking between intermolecular cyclic components (*internal* crosslink) and the other was a crosslinking between the terminals of the polyrotaxanes (*terminal* crosslink). Hydrogel **I**-**IV** showed high water content and hydrophilic surface. The *internally*-crosslinked gels had higher compressive stress and initial modulus, while the *terminally*-crosslinked gels showed higher ultimate strain. Viscoelastic behavior of *internally*-crosslinked hydrogels was very

different from that of *terminally*-crosslinked hydrogels and similar to that of topological gel. The *terminally*-crosslinked hydrogels were more stable during degradation than the *internally*-crosslinked hydrogels in PBS. These degradations accompanied decrease in the storage modulus, and showed various degradation profiles, which were modulated by the crosslinking manners and molecular weights of the polyrotaxanes. A preliminary cell adhesion test using NIH3T3 cells onto the *terminally*-crosslinked hydrogels demonstrated cellular responses by means of decrease in storage modulus and change of surface chemical characteristics of hydrogels. These results could provide a possibility to develop polyrotaxane-based hydrogel systems as biodegradable materials for tissue engineering, such as implantable scaffold and drug delivery system, since polyrotaxanes are allowed to be designed uniquely by modulating lots of structural parameters, such as various crosslinking methods, combinations of polyrotaxane component, and molecular weight of the back bone polymer.

In chapter 4, polyamide rotaxanes were prepared by a polycondensation of 4,4ô-acetoamido-α-truxillic acid with diaminated pseudorotaxanes from an inclusion complex of polyethyleneglycol bisamine with methylated-α-cyclodextrin. The thermal degradation temperature of the polyamides was enhanced by inclusion complex formation with methylated-α-cyclodextrin, even when a very small amount of methylated-α-cyclodextrin

was threaded into the polymer backbone. The polyamide polyrotaxane with methylated-α-cyclodextrin was degraded by UV-irradiation (ə < 260 nm) via the photocleavage of the cyclobutane ring in 4,4ô- diacetoamido-α-truxillic acid to 4-aminocinnamic acid.

ACHIEVEMENT

Articles

1. Hojoon SHIN, Seiji TATEYAMA, and Tatsuo KANEKO ; Synthesis of Photo-degradable Polyamide Rotaxanes with Cinnamate Photodimer and Cyclodextrin. Journal of Materials Life Society, *Accepted*.

2. Ryo KATOONO, Shin-ichiroh FUKUDA, Hojoon SHIN, and Nobuhiko YUI ; Preparation of hydrolyzable polyrotaxane containing ester linkages and its degradation behavior. Chemistry Letters. Vol. 37 (2008), No. 9, pp.988-989

Presentations

1. Hojoon SHIN, Seiji TATEYAMA, and Tatsuo KANEKO, Synthesis of bio-based aliphatic-aromatic polyamides containing cyclodextrin via solid inclusion complexes. ICBP, Seoul, 2013.

2. 辛昊俊, 上遠野亮, Jung-woog SHIN, 由井伸彦, エステル含有ポリロタキサン架橋ヒドロゲルの加水分解過程における特性の解析. 第39回医用高分子シンポジウム, Tokyo, 2010.

3. Hojoon SHIN, Ryo KATOONO and Nobuhiko YUI ; Preparation of polyrotaxane hydrogels based on water-soluble hydrolyzable polyrotaxane. 2nd AMBC, Singapore, 2009.

4. Hojoon SHIN, Ryo KATOONO, and Nobuhiko YUI ; Preparation of supramolecular hydrogels composed of hydrolyzable polyrotaxanes and their mechanical properties and degradation behavior. 第58回高分子学会年次大会, Kobe, 2009.
5. Hojoon SHIN, Shin-ichiroh FUKUDA, Ryo KATOONO and Nobuhiko YUI ; Preparation of hydrogels based on hydrolyzable polyrotaxane. MACRO 2008, Taipai, 2008.
6. Hojoon SHIN, Ryo KATOONO and Nobuhiko YUI ; Preparation of supramolecular hydrogels based on biodegradable polyrotaxanes cross-linked by multi-armed PEG. 第57回高分子学会年次大会, Yokohama, 2008.
7. Hojoon SHIN, Shin-ichiroh FUKUDA, Ryo KATOONO and Nobuhiko YUI ; Preparation of supramolecular hydrogels composed of hydrolyzable polyrotaxane and their mechanical properties. 第57回高分子討論会, Osaka, 2008.

ACKNOWLEDGMENT

The authorôs supreme appreciation is owed on Prof. Tatsuo Kaneko who is my supervisor, for his guidance, dedicated support and continuous motivation during research and the writing of this dissertation. When I suffered from serious mental pain, his advice gave me metal vitality and courage to overcome every trouble.

The advice and support of the other member of his committee, namely, Prof. Ebitani, Prof. Matsumi, Prof. Miura, and Prof. Yamaguchi also gratefully acknowledged.

I would like to express my gratitude to Research Assistant Dr. Seiji Tateyama for his supports laid a smooth way for my research. Through rewarding discussions, I have gained much more knowledge in experimental technique. At the same time, I would like to express my appreciation to Kaneko Lab members. They supported my experiment and living truly in JAIST for a long time.

When I came to Japan for the first time in order to challenge doctor degree, Prof. Yui gave me good chance of studying abroad and to challenge new research filed. He supported my early school life and taught seriousness of scientific research filed. Also, Assistant Prof. Katoono, he taught many things to me about chemical experiment and basic attitude as chemist. I would like to thank two Professors and all Yui Lab members.

For my Minor-research theme and advice on technique of cellular experiment, I thank Prof. Jung-woog Shin (Inje University) and Prof. Masayuki Yamaguchi. I also would like to thank many Lab members in Prof. Shin and Prof. Yamaguchi Lab.

I would like to thank Dr. Yamaoka, Dr. Kakinoki, and Dr. Yamashita in Department of Bio medical Engineering, National Cerebral and Cardiovascular Center. They supported and advised my cellular experiment using hydrogels truly. Thanks to their help, I was able to endure and finish hard experiment in Osaka for a long time.

Finally, I would like to express my thanks to Korean society members in JAIST.

Hojoon Shin

March, 2014

Minor-Research Theme

Quantitative Measurement of Cell Adhesive Force between Cell and PLGA Surface

HOJOON SHIN

Supervised by Professor Jung-Woog Shin, Ph.D, [1]
and Professor Masayuki Yamaguchi, Ph.D [2]

[1]Collage of Biomedical Science & Engineering, Inje University (Korea)
[2]School of Materials Science, Japan Advanced Institute of Science & Technology (Japan)

School of Materials Science

Japan Advanced Institute of Science and Technology

March 2009

ABSTRACT

Adhesion of an anchorage dependent cell to extracellular matrix is a fundamental and important process in physiological cell behavior such as survival, proliferation, differentiation, activation and movement. Qualitative and quantitative measurements have been adopted to measure adhesive force. In this study, we utilized a micropipette as a cantilever beam to measure quantitative cell adhesive force. The adhesive force was calculated by using the relationship between the deflection and force experienced by the pipette when detaching a cell from polymer surface. BMSC was seeded on PLGA-coated glass surface and cultured for 4hrs and 12hrs. The shape and dimension of pipette was measured by using image analysis software and the pipette was reconstructed with finite element analysis program and the amount of deflection measured was imposed in the program. The average attachment forces of the cells on PLGA at 4 hrs and 12 hrs were 0. 13 ± 0.015 nN and 0.42±0.035 nN, respectively. Evaluating cell attachment more precisely by measuring the detachment force quantitatively could allow finding of optimal condition of parameters related to surface condition.

Keywords : Quantitative measurements, Adhesive force, BMSC, PLGA, Cell adhesive force